

COMPUTATIONS OF AIR FILMS BETWEEN MOVING WEBS  
AND SUPPORT ROLLERS FOR STEADY/UNSTEADY  
OPERATING CONDITIONS

By

KANDASAMY SATHEESH

Bachelor of Technology

Indian Institute of Technology


Bombay, India

1996

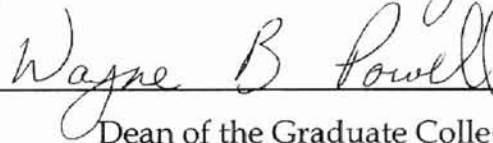
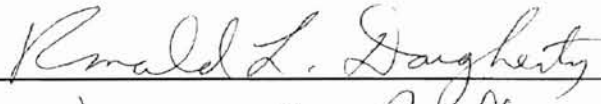
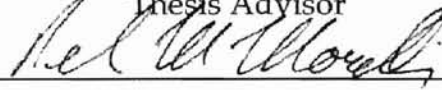
Submitted to the Faculty of the  
Graduate College of the  
Oklahoma State University  
in partial fulfillment of  
the requirements for  
the degree of  
MASTER OF SCIENCE  
May 1998

COMPUTATIONS OF AIR FILMS BETWEEN MOVING WEBS  
AND SUPPORT ROLLERS FOR STEADY/UNSTEADY  
OPERATING CONDITIONS

Thesis Approved:



Thesis Advisor



Dean of the Graduate College

## ACKNOWLEDGEMENTS

I wish to express my sincere appreciation and gratitude to Prof. F.W. Chambers for his intelligent supervision, patience and enthusiasm he showed during the course of this research work and during my career at Oklahoma State University. I am also indebted to Dr. Y.B. Chang for his suggestions on the expression for the frequency of sinusoidal oscillation of a web. I would also like to thank other committee members for their suggestions and help.

I am greatly indebted to my parents Dr. P. Kandasamy and Dr.(Ms).G. Kandasamy and my sister Kuhayini for their prayers and support they provided during my stay with them and also when I was away from them.

Moreover, I wish to express my sincere thanks to those who provided suggestions and help to make this research work a great success. I would also like to thank my friends, Dheenoth, Hari, Madhav, Rajeeve, Thirumal and Vijay for giving me a great company which made my life at Oklahoma State University a memorable one.

I would like to express my sincere thanks to OSU's Web Handling Research Center for providing financial support during the course of this research.

Kandasamy Satheesh

## TABLE OF CONTENTS

Chapter	Page
CHAPTER 1 INTRODUCTION.....	1
1.1 BACKGROUND.....	1
1.2 FOIL BEARING THEORY.....	7
1.3 OBJECTIVES.....	10
CHAPTER 2 LITERATURE REVIEW.....	13
CHAPTER 3 MATHEMATICAL FORMULATION.....	20
3.1 DERIVATION OF GOVERNING EQUATION.....	20
3.2 GOVERNING EQUATIONS.....	26
3.2.1 Tangency Point Location.....	31
3.2.2 Boundary Conditions.....	31
3.3 FINITE DIFFERENCE SOLUTION TECHNIQUE.....	34
CHAPTER 4 RESULTS.....	40
4.1 EFFECT OF TENSION TRANSIENTS AND AIR FILM THICKNESS PERTURBATIONS IN AIR FILM THICKNESS DISTRIBUTION.....	42
4.1.1 Impermeable Web.....	42
4.1.1.1 Constant tension case.....	42
4.1.1.2 Effect of Step Change in Tension case.....	48
4.1.1.3 Effect Sinusoidal Fluctuation in Tension case.....	53
4.1.1.4 Effect of Perturbation on Air Film Thickness.....	59
4.1.2 Permeable Web.....	63
4.1.2.1 Constant Tension Case.....	62
4.1.2.2 Step Change in Tension Case.....	64
4.1.2.3 Sinusoidal Fluctuation in Tension Case.....	66
4.2 COMPARISON BETWEEN FINITE STIFFNESS AND ZERO STIFFNESS MODELS.....	68
4.2.1 Impermeable Web.....	68
4.2.2 Permeable Web.....	71
4.3 COMPARISON OF TENSION TRANSIENTS - STEP VARIATION.....	73
CHAPTER 5 CONCLUSIONS AND RECOMMENDATIONS.....	79
REFERENCES.....	82
APPENDIX A DERIVATION OF GOVERNING EQUATIONS.....	88
APPENDIX B DERIVATION OF DIFFERENCE EQUATIONS.....	94
APPENDIX C COMPUTER PROGRAM FOR COMPUTATION OF AIR FILM AND PRESSURE DISTRIBUTIONS.....	98



## LIST OF FIGURES

FIGURE 1.1: SCHEMATIC OF CONTINUOUS LOOP FOR WEB HANDLING APPLICATION.....	3
FIGURE 1.2 : SCHEMATIC OF WEB PASSING OVER A ROLLER .....	5
FIGURE 1.3: SCHEMATIC OF THREE-DIMENSIONAL FOIL BEARING .....	9
FIGURE 1.4: SCHEMATIC OF THREE REGIONS IN A FOIL BEARING .....	12
FIGURE 3.1: DIFFERENTIAL FLUID ELEMENT FOR DYNAMIC EQUILIBRIUM ANALYSIS .....	22
FIGURE 3.2: DIFFERENTIAL ELEMENT FOR CONSERVATION OF MASS ANALYSIS FOR A IMPERMEABLE WEB .....	27
FIGURE 3.3: DIFFERENTIAL ELEMENT FOR CONSERVATION OF MASS ANALYSIS FOR A PERMEABLE WEB .....	28
FIGURE 3.4: DIFFERENTIAL WEB ELEMENT .....	29
FIGURE 3.5: SCHEMATIC INDICATING TANGENCY POINTS FOR INITIAL CONDITIONS .....	32
FIGURE 4.1: COMPARISON BETWEEN PRESENT RESULTS AND PUBLISHED RESULTS ( $V_w=2.54$ M/S, $T_{INT}/W=273$ N/M, $M=0.0207$ KG/M <sup>2</sup> ).....	45
FIGURE 4.2: COMPARISON BETWEEN PRESENT RESULTS AND PUBLISHED RESULTS ( $V_w=2.54$ M/S, $T_{INT}/W=273$ N/M, $M=0.0207$ KG/M <sup>2</sup> ).....	45
FIGURE 4.3: TRANSIENT AIR-FILM THICKNESS PROFILES ( $V_w=10.16$ M/S, $T_{INT}/W=273$ N/M, $M=0.0922$ KG/M <sup>2</sup> ).....	46
FIGURE 4.4: 20% STEP CHANGE IN TENSION ( $V_w=15.24$ M/S, $T_{INT}/W=87.66$ N/M, $M=0.0254$ KG/M <sup>2</sup> ) .....	50
FIGURE 4.5: 50% STEP CHANGE IN TENSION ( $V_w=15.24$ M/S, $T_{INT}/W=87.66$ N/M, $M=0.0254$ KG/M <sup>2</sup> ).....	50
FIGURE 4.6: 20% STEP CHANGE IN TENSION ( $V_w=15.24$ M/S, $T_{INT}/W=263$ N/M, $M=0.0254$ KG/M <sup>2</sup> ) .....	52
FIGURE 4.7: 50% STEP CHANGE IN TENSION ( $V_w=15.24$ M/S, $T_{INT}/W=263$ N/M, $M=0.0254$ KG/M <sup>2</sup> ). .....	51

FIGURE 4.8: 20% STEP CHANGE IN TENSION ( $V_w=15.24$ M/S, $T_{INT}/w=263$ N/M, $M=0.0922$ KG/M <sup>2</sup> ) .....	53
FIGURE 4.9: 50% STEP CHANGE IN TENSION ( $V_w=15.24$ M/S, $T_{INT}/w=263$ N/M, $M=0.0922$ KG/M <sup>2</sup> ) .....	53
FIGURE 4.10: SINUSOIDAL FLUCTUATION IN TENSION ( $V_w=15.24$ M/S, $T_{INT}/w=87.66$ N/M, $M=0.0254$ KG/M <sup>2</sup> , $A=0.5T, \omega=\omega_N$ ).....	56
FIGURE 4.11: SINUSOIDAL FLUCTUATION IN TENSION ( $V_w=15.24$ M/S, $T_{INT}/w=87.66$ N/M, $M=0.0254$ KG/M <sup>2</sup> , $A=0.5T, \omega=2\omega_N$ ) .....	57
FIGURE 4.12 SINUSOIDAL FLUCTUATION IN TENSION ( $V_w=15.24$ M/S, $T_{INT}/w=263$ N/M, $M=0.0254$ KG/M <sup>2</sup> , $A=0.5T, \omega=\omega_N$ ).....	57
FIGURE 4.13: SINUSOIDAL FLUCTUATION IN TENSION ( $V_w=15.24$ M/S, $T_{INT}/w=263$ N/M, $M=0.0922$ KG/M <sup>2</sup> , $A=0.5T, \omega=\omega_N$ ).....	58
FIGURE 4.14 30% PERTURBATION IN AIR FILM DISTRIBUTION BETWEEN $\xi=0.23-0.31, (V_w=15.24$ M/S, $T_{INT}/w=175.3$ N/M, $M=0.0922$ KG/M <sup>2</sup> ) .....	60
FIGURE 4.15: 30% PERTURBATION IN AIR FILM DISTRIBUTION BETWEEN $\xi=0.23-0.39(V_w=2.54$ M/S, $T_{INT}/w=175.3$ N/M, $M=0.0922$ KG/M <sup>2</sup> ) .....	60
FIGURE 4.16: 30% PERTURBATION IN AIR FILM DISTRIBUTION BETWEEN $\xi=0.23-0.39(V_w=5.08$ M/S, $T_{INT}/w=175.3$ N/M, $M=0.0922$ KG/M <sup>2</sup> ) .....	61
FIGURE 4.17: 20% PERTURBATION IN AIR FILM DISTRIBUTION BETWEEN $\xi=0.23-0.39(V_w=5.08$ M/S, $T_{INT}/w=175.3$ N/M, $M=0.0922$ KG/M <sup>2</sup> ) .....	61
FIGURE 4.18: TRANSIENT AIR FILM THICKNESS PROFILES-POROUS WEB ( $V=10.16$ M/S, $T_{INT}/w=87.66$ N/M, $M=0.0922$ KG/M <sup>2</sup> , $K=3E-6$ (M <sup>3</sup> S <sup>-1</sup> /M <sup>2</sup> -PA) .....	63
FIGURE 4.19: 20% STEP CHANGE IN TENSION ( $V_w=15.24$ M/S, $T_{INT}/w=87.66$ N/M, $M=0.0254$ KG/M <sup>2</sup> , $K=3E-6$ (M <sup>3</sup> /S)/(M <sup>2</sup> -PA) .....	65
FIGURE 4.20: 50% STEP CHANGE IN TENSION TENSION ( $V_w=15.24$ M/S, $T_{INT}/w=87.66$ N/M, $M=0.0922$ KG/M <sup>2</sup> , $K=3E-6$ (M <sup>3</sup> /S)/(M <sup>2</sup> -PA) .....	65
FIGURE 4.21: SINUSOIDAL OSCILLATION IN TENSION, ( $V_w=15.24$ M/S, $T_{INT}/w=87.66$ N/M, $M=0.0254$ KG/M <sup>2</sup> , $K=3E-6$ (M <sup>3</sup> /S)/M <sup>2</sup> - PA, $A=0.2T, \omega=\omega_N$ ).....	67

FIGURE 4.22: SINUSOIDAL OSCILLATION IN TENSION ( $V_w=15.24$ M/S, $T_{INT}/W=87.66$ N/M, $M=0.0254$ KG/M <sup>2</sup> , $K=3E-6$ (M <sup>3</sup> /S)/M <sup>2</sup> -PA, $A=0.5T$ , $\omega=\omega_N$ ).....	67
FIGURE 4.23: COMPARISON BETWEEN WEBS WITH DIFFERENT WEB STIFFNESS VALUES ( $V_w=10.16$ M/S, $T_{INT}/W=87.6$ N/M, $M=0.0922$ KG/M <sup>2</sup> , $EI/W=0.0$ , $1.5E-5$ N-M, $5.0E-5$ N-M)70	70
FIGURE 4.24: COMPARISON BETWEEN WEBS WITH DIFFERENT WEB STIFFNESS VALUES ( $V_w=10.16$ M/S, $T_{INT}=87.6$ N/M, $M=0.0922$ KG/M <sup>2</sup> , $EI/W=0.0$ , $1.5E-5$ N-M, $5.0E-5$ N-M).....	70
FIGURE 4.25 : COMPARISON BETWEEN FINITE STIFFNESS AND ZERO STIFFNESS MODELS FOR PERMEABLE WEBS ( $V_w=10.16$ M/S, $T_{INT}/W=165.33$ N/M, $M=0.0922$ KG/M <sup>2</sup> , $K=5E-6$ (M <sup>3</sup> /S)/(M <sup>2</sup> -PA).....	72
FIGURE 4.26 : COMPARISON BETWEEN FINITE STIFFNESS AND ZERO STIFFNESS MODELS FOR PERMEABLE S WEB( $V_w=10.16$ M/S, $T_{INT}/W=165.33$ N/M, $M=0.0922$ KG/M <sup>2</sup> , $K=3E-6$ (M <sup>3</sup> /S)/(M <sup>2</sup> -PA).....	72
FIGURE 4.27: STEP CHANGE IN TENSION FOR PERFECTLY FLEXIBLE WEB ( $V_w=15.24$ M/S, $T_{INT}/W=87.66$ N/M, $M=0.0254$ KG/M <sup>2</sup> , WITH 50% STEP CHANGE).....	74
FIGURE 4.28: STEP CHANGE IN TENSION FOR A WEB WITH $EI/W=1.52E-5$ N-M ( $V_w=15.24$ M/S, $T_{INT}/W=87.66$ N/M, $M=0.0254$ KG/M <sup>2</sup> , WITH 50% STEP CHANGE).....	74

## LIST OF TABLES

TABLE 4.1: CASES CONSIDERED WITH CONSTANT TENSION .....	75
TABLE 4.2: CASES CONSIDERED WITH PERTURBATION IN AIR FILM THICKNESS.....	75
TABLE 4.3: CASES CONSIDERED WITH STEP CHANGE IN TENSION .....	76
TABLE 4.4: CASES CONSIDERED WITH SINUSOIDAL OSCILLATION IN TENSION .....	77

## NOMENCLATURE

A	Amplitude of oscillation
$A_1$	Constant Coefficient of Finite Difference Equation
$A_2$	Constant Coefficient of Finite Difference Equation
$A_3$	Constant Coefficient of Finite Difference Equation
a	Acceleration of a differential fluid element
b	Web thickness (m)
$B_1$	Constant Coefficient of Finite Difference Equation
$B_2$	Constant Coefficient of Finite Difference Equation
$B_3$	Constant Coefficient of Finite Difference Equation
$C_1, C_2$	Constants of integration
$C_3$	Constant Coefficient of Finite Difference Equation
$D_1$	Constant Coefficient of Finite Difference Equation
$D_2$	Constant Coefficient of Finite Difference Equation
$D_3$	Constant Coefficient of Finite Difference Equation
E	Modulus of elasticity ( $\text{N}/\text{m}^2$ )
$E_1$	Constant Coefficient of Finite Difference Equation
F	Force (N)
$F_s$	Shear force (N)

$F_3$	Constant Coefficient of Finite Difference Equation
$h$	Air film thickness (m)
$h_o$	Constant central region air film thickness (m)
$i$	Subscript indicating the position in x direction(along roller)
$I$	Moment of inertia of web cross section ( $m^4$ )
$k$	Permeability coefficient of porous web ( $m^2$ )
$K$	Permeability of web ( $m^3s^{-1}/m^2\text{-Pa}$ )
$L$	Distance between the two end supports (m)
$L_h$	Distance between the support roller and the tangency point (m).
$L_1, L_2$	Location(x coordinates) of points on the roller within which tangency points are located
$m$	Mass of the web per unit area ( $kg/m^2$ )
$M$	Moment (N-m)
$n$	Subscript indicating time step
$p$	Pressure ( $N/m^2$ )
$p_a$	Ambient Pressure ( $N/m^2$ )
$p_o$	Initial pressure in air bearing region ( $N/m^2$ )
$Q$	Mass flow rate ( $m^3/s$ )
$R$	Roller radius (m)

$S$	Shear Force acting on the cross section of the tape (N)
$T$	Web tension (N)
$t$	Time (s)
$t'$	Non-dimensional time
$V$	Velocity in $x$ direction (m/s)
$V_R$	Roller surface velocity (m/s)
$V_W$	Web velocity (m/s)
$V_t$	Velocity of the air escaping through the porous web (m/s)
$w$	Width of the web (m)
$x$	Spatial coordinate along the direction of web velocity
$X_0$	X Location of the Tangent Point
$Y_0$	Y Location of the Tangent Point
$y$	Spatial coordinate along radial direction
$y_i^n$	Denotes the Value of $y$ at $i$ th location and $n$ th time step
$z$	Spatial coordinate along the width of the web
$\delta(x)$	Function Describing Roller Surface Geometry
$\delta_{\max}$	Maximum height of the Roller Surface
$\lambda$	Mean free path length (m)
$\lambda_a$	Mean free path length at atmospheric pressure (m)

$\mu$	Dynamic viscosity of air (Pa-s)
$\nu$	Kinematic viscosity of air (m <sup>2</sup> /s)
$\rho$	Web density (kg/m <sup>3</sup> )
$\tau$	Viscous shear stress (N/m <sup>2</sup> )
$\omega_n$	Natural frequency of oscillation (rad/s)
$\omega$	Frequency of oscillation (rad/s)



# CHAPTER 1

## INTRODUCTION

### 1.1 Background

Web Handling has become an important process in the fields of the textile industry, the magnetic/polymeric film industry and the computer industry. Hence it has become a major area of interest for both the industries and researchers. The term "effective web handling" means that the web must be handled at near optimum conditions so that the quality of web would not be jeopardized. This has to be taken care from the time it is manufactured until it goes for storage. There are several stages where these processes should be given close attention and the parameters should be controlled.

In the industries webs fly at very high speeds over guide and control rollers. When webs run over rollers at very high speeds, there exists an air film gap between the roller and the web. This happens due to the air entrained by the high speed pulling of the web over the roller. This air film acts as a cushion between the roller and web. It reduces rubbing of the two solid surfaces in motion. Hence it is important that the air film be thick enough to prevent abrasion and by that prevent damage to the web and also be thin enough to maintain traction and by that prevent lateral wandering of the web over the roller. Hence this air film thickness should be controlled for a particular application. This can be done by controlling the operating condition for that particular application. There are certain parameters which play a major role in this process of controlling the air film thickness.

Foil bearings have received growing attention in recent years. So far their application has been mainly confined to the transport of thin foils such as magnetic tapes, papers or plastics over stationary spindles. They may however, have some potential use in bearings for the support of rotating spindles.

A flexible foil pulled around a cylindrical guide, roller or magnetic head is a situation which commonly occurs in drives for magnetic tapes, papers and other such materials (shown in Figure 1.1). When a flexible web passes over a spindle, a thin air layer is formed between the two surfaces. This is typically the foil bearing configuration. This ultra thin layer separates two solid surfaces. Mastering the conditions under which this layer is formed is fundamental to avoid (or reduce) problems such as wear degradation or demagnetization phenomena in similar situations.

Figure 1.2 illustrates the sort of problem which is to be analyzed. The basic configuration is that of a foil bearing. A web approaches a spindle of radius  $R$  at a velocity  $V$ . The wrap angle  $\theta$  is considered to be known. As the web passes over the spindle, it entrains air and a pressure field is generated in the contacting zone. The problem consists of finding the air film profile as a function of the following parameters.

- 1) Roller diameter
- 2) Web/Roller speed
- 3) Mass of web



- 4) Roughness of web
- 5) Moisture content of air
- 6) Thickness of the web
- 7) Stiffness of web
- 8) Static electricity
- 9) Web tension

When the roller/web speed is very high, there is more air entrained, consequently, the higher the air film thickness. With increase in roller diameter, the air film thickness increases. With increase in mass of the web, the air film thickness would increase (for the higher speed case) when all other parameters are kept constant. Porous webs tend to have a smaller air film thickness compared to their impermeable counterparts as there would be air leakage through the porosities.

Another major concern in the process of web handling is the problem concerned with the propagation of disturbances while the web is in motion. This has become a major concern as this might even damage the web or make it lose traction depending on the magnitudes and frequencies of its occurrence. Hence the study of different modes of disturbance might be fruitful to the industry. As there are many moving parts involved in web handling processes, the occurrence of disturbances is inevitable. Hence it has become an important area

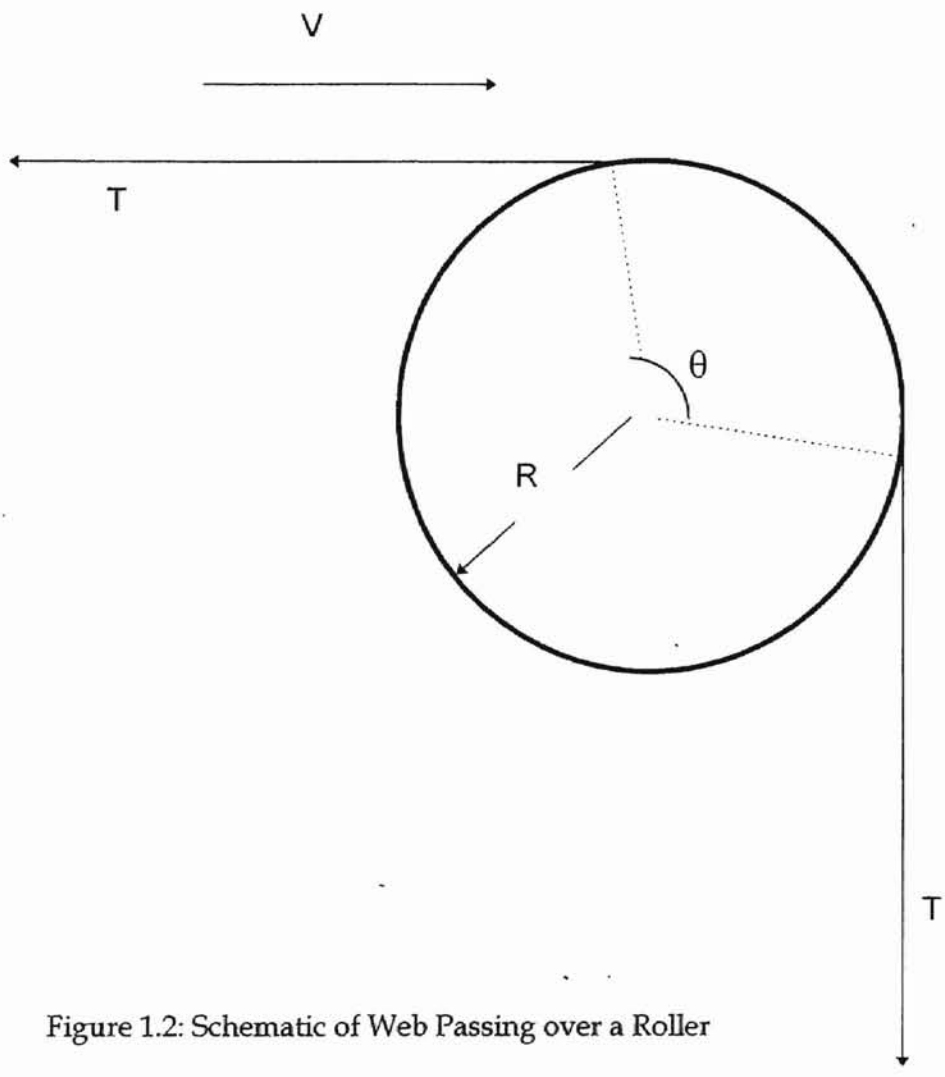


Figure 1.2: Schematic of Web Passing over a Roller

of concern in web handling. These disturbances can be classified into two major subdivisions. They are,

- 1) Disturbance due to perturbation in the air film thickness
- 2) Disturbance due to fluctuation in tension

Here in this research two types of tension variations have been considered,

- 1) Step increase in tension
- 2) Sinusoidal fluctuation in tension

For the air film perturbation case, only a step perturbation in the wrap region of the air film thickness was considered.

Sudden change in tension can cause tightening of the web over the roller, and it can lead to breakage of the web, or the increase in air film can lead to loss of traction. Hence the air film thickness variation after the increased tension is applied must be given close attention. Numerical simulation is the most convenient way of doing this as it is cost effective and faster than an experiment. The results from the numerical computations can also be used to fine tune an experiment. Results obtained from the numerical modeling can be used to improve the design. The modes of tension transients we consider are as follows. For a case with a step change in tension, once the steady state is reached, a step change in tension is applied. The magnitude of the tension is kept constant after the time of its application, and the response of air film thickness and pressure is observed until the second steady state for the changed state is obtained. There can be a range of magnitudes studied. For the sinusoidal variation case, the

fluctuation is a function of time and changes for each time step. Here the tension is a function of both amplitude of oscillation and frequency of oscillation. Fluctuation is applied once a steady state solution is reached for the initial tension.

From the above explanation the importance of web-air-roller interaction can be easily understood. Hence we should find the means for modeling the above process. Researchers who worked on similar problems suggest that the problem of a foil bearing is physically very similar to the web handling process. Researchers have come up with various forms of governing equations in different coordinate systems. For simplicity we confine ourselves with the Cartesian coordinate system.

## **1.2 Foil Bearing Theory**

The term “foil bearing” was first coined by Blok and Van Rossum (1953). That was the first paper published on foil bearings. A foil bearing consists of a rotating spindle and stationary foil (as shown in Figure 1.3). Alternatively the spindle can be stationary and the foil can move. The film developed between these two surfaces is due to the motion of one surface or both of them.

In this problem, Reynolds equation relates the pressure in the fluid film and the air film thickness to the parameters such as speed of the web/roller and the kinematic viscosity of air. The foil equilibrium equation relates the elastic properties of the foil to the tension and pressure applied to the foil. The Reynolds equation in the Cartesian coordinate system can be cast as the one given below.

$$\frac{\partial \left( h^3 p \frac{\partial p}{\partial x} \right)}{\partial x} + 6\lambda_a p_a \frac{\partial \left( h^2 \frac{\partial p}{\partial x} \right)}{\partial x} = 6\mu V \frac{\partial p h}{\partial x} + 12\mu \frac{\partial p h}{\partial x} \quad (1.1)$$

We can simplify the above equation by invoking some assumptions such as incompressibility of air, infinite width of web and steady state in time. Hence the Reynolds equation reduces to the one given below.

$$\frac{\partial \left( h^3 \frac{\partial p}{\partial x} \right)}{\partial x} = 6\mu V \frac{\partial h}{\partial x} \quad (1.2)$$

The equilibrium equation for a foil can be derived by setting up the stress, strain and bending moment resultants. The equilibrium equation is,

$$\frac{Et^3}{12(1-\nu^2)} \nabla^2 \nabla^2 h + \frac{Et(h-h_o)}{R^2} = p - p_o - \frac{T}{R} \left( 1 - R \frac{\partial^2 h}{\partial x^2} \right) \quad (1.3)$$

where t- thickness of the web.

In the entrance region, pressure increases from atmospheric pressure to the film pressure, p, and an exponential decrease in the air film thickness occurs in this region. In the central region, air film thickness is almost a constant, and the pressure profile exhibits a plateau. In the exit region, the pressure decreases from the film pressure p to the atmospheric pressure while the air film gap increases to infinity (refer to Figure 1.4). Many researchers have presented relationships for air film thickness as a function of the speed of the web, kinematic viscosity of air and the tension applied. It can be given by the following form.



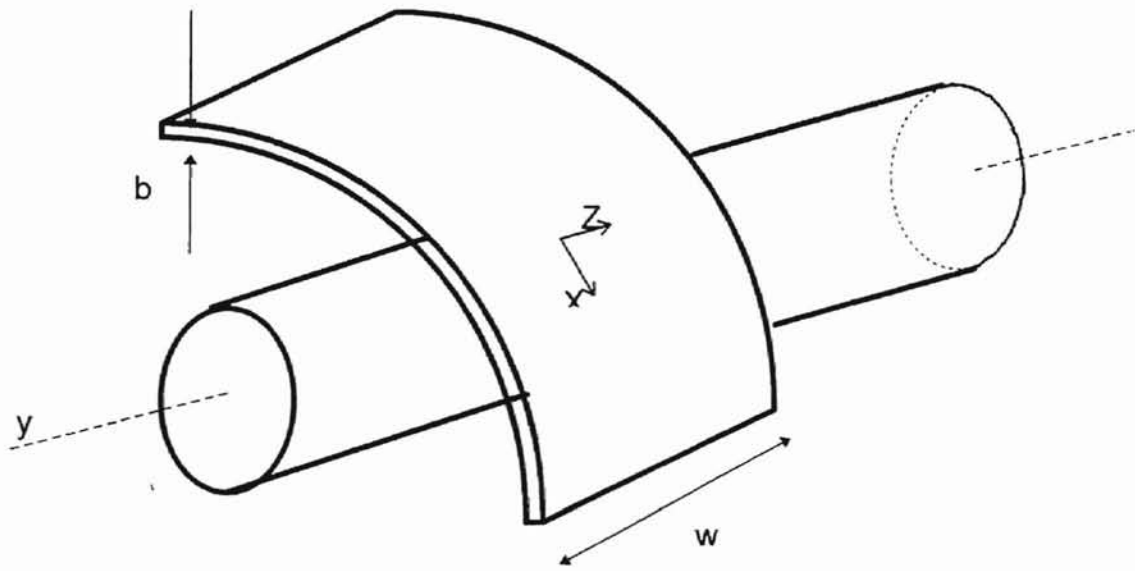


Figure 1. 3: Schematic of Three-Dimensional Foil Bearing

$$h_o = KR \left( \frac{6\mu V}{T} \right)^{2/3} \quad (1.4)$$

The researchers have suggested different values for K. Most of the researchers agree to a value very close to K=0.643. Knox and Sweeney (1971) suggested an equation for the case where both the web and roller are in motion.

It is,

$$h_o = 0.643R \left[ \frac{6\mu(V_{web} + V_{roller})}{T} \right]^{2/3} \quad (1.5)$$

The relationship for the air film gap in the central region is based on the assumption that the web is infinite in width and there is no air leakage in the span-wise direction. It also suggests that the pressure remains constant along the width of the web. This constant pressure might not be true in actual practice, as the pressure must reduce to the atmospheric pressure at the edge.

### 1.3 Objectives

From the foregoing discussion it can be concluded that predicting air film thickness in web handling applications is vital for controlling and manipulating the air film thickness. It is becoming important for design considerations and to ensure the quality of the materials manufactured by web handling processes. Hence the primary objectives of this study are:

- 1) Numerically study progressive development of air film thickness between a web and a roller

- 2) Numerically study the effects of the following parameters on the air film thickness
  - a) Web tension
  - b) Web/Roller velocity
  - c) Web porosity
  - d) Web mass
  - e) Roller radius
  - f) Effect of slip flow
- 3) Determine the effect of tension transients on air film thickness
- 4) Determine the effect of disturbance propagation on air film thickness
- 5) Determine the effect of web stiffness on air film thickness

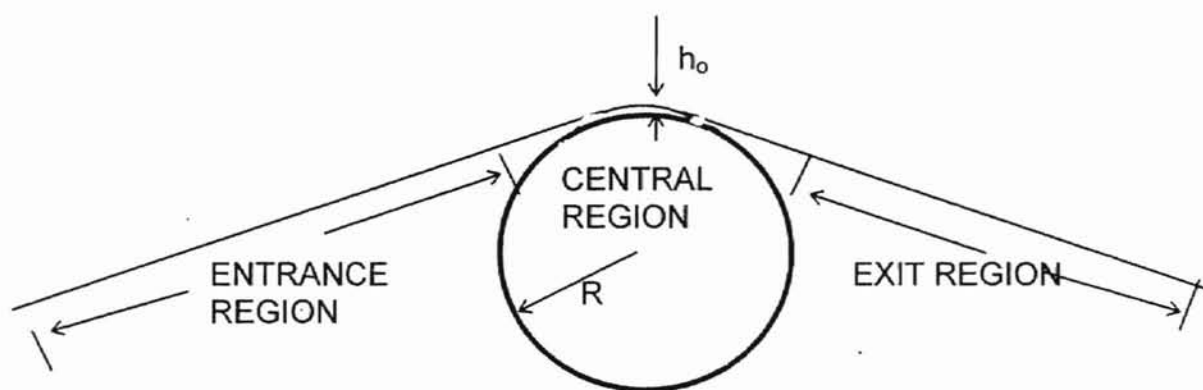


Figure 1.4: Schematic of Three Regions in a Foil Bearing

## CHAPTER 2 LITERATURE REVIEW

Any numerical model that is to be solved using numerical techniques demands a good mathematical model comprising almost all of the physics of the problem concerned. An extensive literature review reveals that the problem for which we seek a solution can be modeled using the analogous problem of interaction between a magnetic tape and a recording head. Here the effective data transfer requires a very thin air film gap and high speed motion of the web (tape) over the head. So the parameters affecting the air film gap should be controlled well. Hence in this review we are concerned only with the problems dealing with magnetic tape/heads and similar foil bearing problems. It has already been mentioned that the web handling process is governed by the coupled Reynolds lubrication equation and the foil equation of motion for a finite length of web.

The first literature published on foil bearings was by Blok and Van Rossum (1953). These authors conducted an experiment with a cellophane foil using oil as the lubricant. They developed a theory based on the assumption that the tape remains straight until such time as it becomes a perfect circle separated from the spindle over an angle of wrap by a constant film thickness. Using the assumed film shape, they were able to derive an expression for the film thickness in the region of uniformity (central constant thickness region).

Baumeister (1963) presented a set of six different foil differential equations. The nominal foil clearances were obtained for each of these equations. However the numerical techniques employed and the boundary conditions used were not stated in his paper. In a paper by Eshel and Elrod (1965), it was shown that the film thickness shape for both the entrance and exit regions can be determined more easily in terms of an extended independent coordinate system. Barlow (1967) developed a foil bearing problem incorporating the effects of bending stiffness and compressibility of lubricant. The equations were nonlinear and the boundary conditions were divided equally between the two ends of the tape. Linearized solutions were derived for large wrap angles neglecting the bending stiffness of the tape. He suggested that while a membrane assumption is assumed, air, the lubricant cannot be considered as incompressible. On the other hand, when the foil has a finite stiffness, the incompressibility assumption can be made.

Eshel and Wildmann (1968) analyzed the dynamic behavior, in which they derived general equations for an infinitely wide foil, but they only give a solution for the problem with an initial disturbance to a foil in the uniformity zone. Eshel (1969) considered a foil with finite stiffness and solved numerically several cases of a bearing with an initial disturbance. He used a linearized treatment of the differential equation which is limited by the fact that the excursions of disturbances must be small compared to the steady state air film gap. But applications where shaft excursions are of the order of film thickness or

more make the linearized approach insufficient for stability studies. His results showed that, for typical disturbances that were introduced into the bearing, the disturbances were swept out at half the speed of the web. He has also showed that the effect of higher film stiffness on this phenomenon was small. Eshel (1970) investigated the effect of some parameters useful in overcoming excessive air gaps. Since the air gaps involved were very small, the foil bearing equations were modified to include the effect of molecular mean free path. It was shown that near small corners in the solid walls one can reduce the air film thickness considerably. Barnum and Elrod (1971) published a paper concerning the problem of a foil bearing subjected to small variations in tape tension. Eshel and Lowe (1973) developed a modified model of a foil bearing taking into account some details of the particular geometry of magnetic tape heads to predict separation and compared it to the experimental results. Stahl et al. (1974) developed a new approach for the analysis of wide foil bearings. Here the equation of motion for a finite length of tape is coupled to the transient lubrication equation for the air film between the tape and the recording head. Compressibility and slip flow were retained in the fluid mechanics equation. Flexural rigidity and high speed dynamic effects were retained in the foil equation of motion. The steady state solution to the coupled equations is obtained as the limiting case of the transient initial value problem. As the differential equations were written relative to the undeflected tape, it was possible to investigate the effect of noncircular head geometries. In addition,

wave propagation effects in the tape and the interaction of waves in the tape with the air bearing region were studied. Knox and Sweeney (1971) presented equations for the separation between a web and a roller near the curved surface of the roller. These equations relate the separation to the curved surface radius, taking into account the fluid viscosity, speed of the web and the tension applied to the web. They gave separate equations for rotating and a non-rotating cylinders. For the non-rotating cylinder,

$$\frac{h_o}{R} = 0.65 \left| \left( \frac{6\mu V}{T} \right) \right|^{2/3} \quad (2.1)$$

and for a rotating cylinder,

$$\frac{h_o}{R} = 0.65 \left| \left( \frac{12\mu V}{T} \right) \right|^{2/3} \quad (2.2)$$

These equations were shown to be acceptable by an indirect method, which involved measuring the coefficient of friction of film surfaces of known roughness moving across smooth cylinders under various conditions of speed, tension and radius. They have also presented a relationship for the boundary layer thickness. It is given as ,

$$\delta(x) = 6.37(\mu x / \rho V)^{2/3} \quad (2.3)$$

where x is the distance from the starting point of the boundary layer. In a non-dimensional form it can be cast as,

$$\frac{\delta}{h_o} = 9.82 \left( \frac{T}{6\mu V} \right)^{1/6} \left( \frac{T}{6\mu R V^2} \right)^{1/2} \left( \frac{x}{R} \right)^{1/2} \quad (2.4)$$



For a typical condition with  $V=6.038$  m/s,  $\mu=2.63 \times 10^{-3}$  Pa-s,  $R=0.038$  m,  $T=136.63$  N/m,  $x=0.3$  m, and  $\rho=221$  kg/m<sup>3</sup>,  $\delta/h_0$  was found to be 479. Hence it can be seen that the boundary layer is much thicker than the air gap when the boundary layer is allowed to develop for 0.3 m. Gross (1980) reviewed the differential equation for a tape transport with air as a lubricant and discussed ways in which the equations may be linearized and the coordinates stretched.

Hardie and McEttles (1988) worked on flexible foil slider bearings used in direct access storage devices. The steady state analysis revealed the effects of various values of stiffness on air film and pressure profile. Three-dimensional analyses of foil bearings were performed by Rongen (1989) in which he incorporated bending stiffness and the effect of the finite width of the tape. He used the Gauss-Siedel algorithm to solve the problem. Similar analysis was done by Heinrich and Connolly (1992) in which they used finite element analysis to solve the problem for recording head geometries. Connolly et al. (1995) worked on designing non-contact bi-directional magnetic tape recording heads with transverse slots. They used slots with sharp corners to skive the air film produced as the tape engages the magnetic head in high speed tape drives. These slots produce intimate contact between the tape and the head. Their model accounted for slip flow. They validated the results with experimental results.

Baugh and Talke (1996) developed both numerical and experimental techniques for the head/tape interface. They used an asperity compliance curve to calculate the contact pressure between the head and tape resulting from

compression of surface asperities. Experimental measurements were taken using monochromatic interferometry. They described the need for multi-wavelength interferometry to improve measurement resolution at extremely close spacings. Kothari (1996) developed a detailed two-dimensional transient model that can predict the effect of parameters such as tension, web mass, web permeability, slip, and web velocity on the air film and pressure distributions. Satheesh et al.(1997) continued his work to determine the effect of tension transients on air film thickness. They studied the effect of step, sinusoidal variation in tension on the air film and pressure distributions. Hashimoto (1997) derived equations for the finite width compressible foil bearing problem. In the derivation of the air film thickness formula, the two dimensional Reynolds equation and the foil equilibrium equation were discretized by the finite difference method and solved iteratively to obtain the pressure and air film thickness distributions for various parameters. Based on the numerical results he obtained a convenient formula which estimated the air film thickness between a web and a roller. He also performed some experimental validation using optical sensors and compared the results with the calculated results and showed that his predictions agree well with the experimental results.

Now let us look at permeable webs which behave differently from the impermeable web. Riddiford (1969a) studied the air entrainment phenomenon between a permeable paper web and a dryer surface of infinite width. Reducing

the air gap is supposed to increase drying as the air layer is a good insulator. Yamauchi et al. (1976) solved this problem for a permeable web. According to them air leakage velocity through the web is proportional to the pressure difference across the web, where the constant of proportionality is the permeability coefficient of the permeable media. Watanabe and Sueoka (1990) indicate a linearly decreasing central air gap region for a permeable web and a constant air gap region for an impermeable web. Entrance and exit regions exhibit more or less the same behavior for both the cases.

From the foregoing literature review, it can be concluded that the foil bearing problem can be modeled using a infinite width assumption of the foil incorporating the stiffness of the web, slip flow, porosity of the web, and compressibility of air to yield a complete model obtained by numerical solution. Hence the approach that is going to be followed can be given by,

- 1) Setting up governing equations.
- 2) Writing the finite difference equivalent of the governing equations.
- 3) Guessing good initial conditions for the first step accounting for the boundary conditions.
- 4) Finding an algorithm to solve the difference equations.
- 5) Developing a computer code to simultaneously solve this problem.
- 6) Comparing the results to published results.

## CHAPTER 3

### MATHEMATICAL FORMULATION

#### 3.1 Derivation of Governing Equation

The problem at hand can be described by two coupled partial differential equations, the Reynolds lubrication equation and the foil equation of motion for a finite length of foil, along with appropriate boundary conditions. The derivation of governing equations follows the approach described previously by Kothari (1996) employing the boundary conditions specified by Granzow and Leebeck (1984).

The Reynolds lubrication equation expresses dynamic equilibrium and mass conservation for an isothermal ideal gas, neglecting the fluid inertia and assuming laminar flow with no variation in pressure or viscosity through the thickness of the fluid film. It can be derived by considering the differential element of fluid shown in Figure 3.1. It should be noted that the forces shown are for a unit width of foil into the page.

Applying Newton's second law for the fluid element,

$$\sum F = ma \Rightarrow \frac{\partial \tau}{\partial y} - \frac{\partial p}{\partial x} = \rho \frac{DV}{Dt} \quad (3.1)$$

By virtue of Newton's law of viscosity, shear stress can be expressed as,

$$\tau = \mu \frac{\partial V}{\partial y} \quad (3.2)$$

Incorporating the above relationship in the force balance equation yields,

$$\mu \frac{\partial^2 V}{\partial y^2} = \frac{\partial \phi}{\partial x} + \rho \frac{DV}{Dt} \quad (3.3)$$

As mentioned above, by neglecting the fluid inertia, we have,

$$\rho \frac{DV}{Dt} \approx 0 \quad (3.4)$$

Hence equation (3.3) becomes,

$$\mu \frac{\partial^2 y}{\partial y^2} = \frac{\partial \phi}{\partial x} \quad (3.5)$$

Integrating equation (3.5) yields,

$$V = \frac{1}{2\mu} \left( \frac{\partial \phi}{\partial x} \right) y^2 + C_1 y + C_2 \quad (3.6)$$

Constants  $C_1$  and  $C_2$  can be evaluated from the boundary conditions. Using the

“slip flow” boundary conditions (Slip given by  $\lambda \frac{\partial V}{\partial y}$  [Granzow and Lebeck (1984)] ).

$$V \Big|_{y=0} = \lambda \frac{\partial V}{\partial y} \Big|_{y=0} \Rightarrow C_2 = \lambda C_1 \quad (3.7)$$

$$V \Big|_{y=h} = V - \lambda \frac{\partial V}{\partial y} \Big|_{y=h} \Rightarrow C_1 = \frac{V - \frac{1}{2\mu} \frac{\partial \phi}{\partial x} h(h+2\lambda)}{(h+2\lambda)} \quad (3.8)$$

Let us consider mass conservation for the element shown in Figure 3.2. Mass conservation for a permeable web is shown in Figure 3.3.

$$Q_{in} - Q_{out} = \frac{\partial(\rho h \Delta x)}{\partial t} \quad (3.9)$$

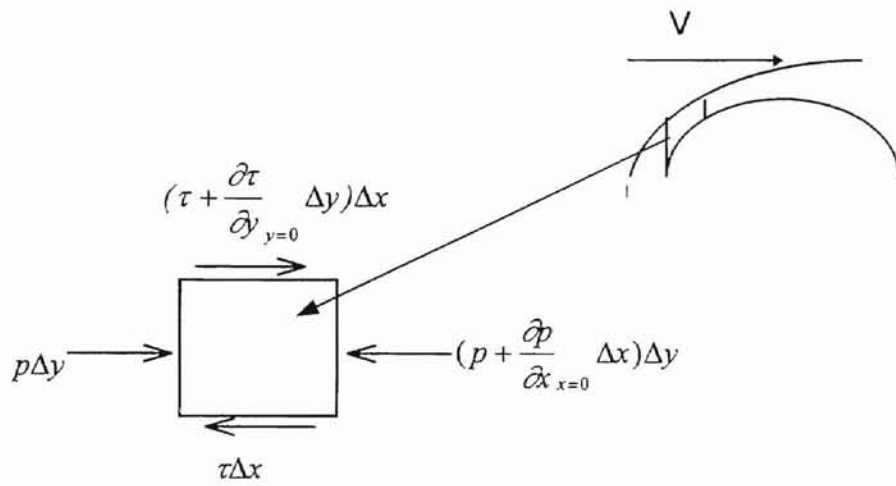


Figure 3.1: Differential fluid element for equilibrium analysis.

Dividing both sides of the equation by  $\Delta x$  and taking the limit as  $\Delta x$  approaches zero yields,

$$\frac{\partial Q}{\partial x} = -\frac{\partial(\rho h)}{\partial t} \quad (3.10)$$

Mass flow rate (per unit width) is obtained by integrating over the velocity profile given by equation (3.6) yielding,

$$\begin{aligned} Q &= \int_0^h \rho V dy = \rho \int_0^h \left( \frac{1}{2\mu} \frac{\partial p}{\partial x} y^2 + C_1 y + C_2 \right) dy \\ &= \rho \left( \frac{1}{6\mu} \frac{\partial p}{\partial x} h^3 + \frac{C_1}{2} h^2 + C_2 h \right) \end{aligned} \quad (3.11)$$

Substituting the expressions for  $C_1$  and  $C_2$  yields,

$$Q = \rho \left( \frac{V}{2} h - \frac{1}{12\mu} \frac{\partial p}{\partial x} h^3 - \frac{1}{2\mu} \frac{\partial p}{\partial x} h^2 \lambda \right) \quad (3.12)$$

Substituting this expression into the mass conservation equation yields,

$$\frac{\partial \left[ \rho \left( \frac{V}{2} h - \frac{1}{12\mu} \frac{\partial p}{\partial x} h^3 - \frac{1}{2\mu} \frac{\partial p}{\partial x} h^2 \lambda \right) \right]}{\partial x} = -\frac{\partial(\rho h)}{\partial t} \quad (3.13)$$

Introducing The expression for the density of an ideal gas is given by the following equation,

$$\rho = \frac{p}{RT} \quad (3.14)$$

After introducing this expression in equation (3.13) and rearranging yields,

$$\frac{\partial \left( h^3 p \frac{\partial \phi}{\partial x} \right)}{\partial x} + 6 \frac{\partial \left( \lambda h^2 p \frac{\partial \phi}{\partial x} \right)}{\partial x} = 6\mu V \frac{\partial (ph)}{\partial x} + 12\mu \frac{\partial (ph)}{\partial t} \quad (3.15)$$

The mean free path length of an ideal gas is proportional to the inverse of the density. Therefore for an isothermal ideal gas, the mean free path length is proportional to the inverse of the pressure. This implies that the  $\lambda p$  product in the second term of equation (3.15) can be replaced by  $\lambda_a p_a$  (the product at atmospheric conditions). Hence the equation can be given as,

$$\lambda \alpha \frac{1}{\rho} \propto \frac{1}{p}$$

$$\lambda p = \lambda_a p_a \quad (3.16)$$

This yields the following **Reynolds lubrication equation**.

$$\frac{\partial \left( h^3 p \frac{\partial \phi}{\partial x} \right)}{\partial x} + 6\lambda_a p_a \frac{\partial \left( h^2 \frac{\partial \phi}{\partial x} \right)}{\partial x} = 6\mu V \frac{\partial \phi h}{\partial x} + 12\mu \frac{\partial \phi h}{\partial t} \quad (3.17)$$

Now let us look at the methodology to derive the foil equation of motion. It can be derived by considering the differential element of foil shown in Figure 3.4. Let us consider the force balance in y direction.

$$\sum F_y = (\rho w b \Delta x) \frac{D^2 y}{Dt^2} = w \Delta x (p - p_a) - \frac{\partial \mathcal{S}}{\partial x} \Delta x + T \frac{\partial y}{\partial x} \Big|_{x+\Delta x} - T \frac{\partial y}{\partial x} \Big|_x \quad (3.18)$$

Where w- Width of tape

b - Thickness of the tape

S - Shear force acting on the cross section of the tape

T- Tension applied to the tape



The relationship between shear force and deflection can be given by,

$$S = EI \frac{\partial^3 y}{\partial x^3} \quad (3.19)$$

Substituting into equation (3.18) and taking the limit as  $\Delta x \longrightarrow 0$ ,

$$w(p - p_a) - EI \frac{\partial^4 y}{\partial x^4} + T \frac{\partial^2 y}{\partial x^2} = \rho w b \frac{D^2 y}{Dt^2} \quad (3.20)$$

Expanding the "total" second derivative  $\frac{D^2 y}{Dt^2}$ ,

$$y = y(x, t)$$

$$\frac{Dy}{Dt} = \frac{\partial y}{\partial x} \frac{\partial x}{\partial t} + \frac{\partial y}{\partial t} = \frac{\partial y}{\partial x} V + \frac{\partial y}{\partial t}$$

$$\frac{D^2 y}{Dt^2} = \frac{\partial \left( \frac{\partial y}{\partial x} V + \frac{\partial y}{\partial t} \right)}{\partial x} \frac{\partial x}{\partial t} + \frac{\partial \left( \frac{\partial y}{\partial x} V + \frac{\partial y}{\partial t} \right)}{\partial t}$$

$$= \frac{\partial^2 y}{\partial x^2} V^2 + 2V \frac{\partial^2 y}{\partial x \partial t} + \frac{\partial^2 y}{\partial t^2} \quad (3.21)$$

Substituting equation (3.21) into equation (3.20) and rearranging yields the following **foil equation of motion**.

$$\rho b \left( \frac{\partial^2 y}{\partial t^2} + 2V \frac{\partial^2 y}{\partial x \partial t} + V^2 \frac{\partial^2 y}{\partial x^2} \right) + \frac{EI}{w} \frac{\partial^4 y}{\partial x^4} - \frac{T}{w} \frac{\partial^2 y}{\partial x^2} = p - p_a \quad (3.22)$$

The Reynolds equation of motion and the foil equation are coupled through the pressure (p) and through the following relationship between the film thickness (h) and the tape displacement (y),

$$h(x, t) = y(x, t) - \delta(x) \quad (3.23)$$

where  $\delta(x)$  is a function describing the roller surface geometry. It is assumed that the foil is simply supported at the guides and the pressure is ambient at the ends of the roller.

### 3.2 Governing Equations

Consider a finite length of a web moving at a constant velocity  $V_w$  over a roller or support between two other support rollers as shown in Figure 3.5. Deflection of the web from the equilibrium position is denoted by  $y(x,t)$ , and the air film thickness between the roller and web is denoted by  $h(x,t)$ . The pressure developed between the roller and the web is coupled to the film thickness,  $h$ , and the web tension,  $T$ , as well as to the other operating variables.

The system can be described using two PDE's,

(1) The web equation of motion

$$\rho b \left( \frac{\partial^2 y}{\partial t^2} + 2V \frac{\partial^2 y}{\partial x \partial t} + V^2 \frac{\partial^2 y}{\partial x^2} \right) + \frac{EI}{w} \frac{\partial^4 y}{\partial x^4} - \frac{T}{w} \frac{\partial^2 y}{\partial x^2} = p - P_a \quad (3.24)$$

and

(2) Reynolds transient lubrication equation

$$\frac{\partial \left( h^3 p \frac{\partial \phi}{\partial x} \right)}{\partial x} + 6\lambda_a P_a \frac{\partial \left( h^2 \frac{\partial \phi}{\partial x} \right)}{\partial x} = 6\mu V \frac{\partial \phi h}{\partial x} + 12\mu \frac{\partial \phi h}{\partial t} \quad (3.25)$$

The two governing equations are coupled through the pressure ( $p$ ) and through the following relationship between the film thickness ( $h$ ) and the foil displacement ( $y$ ),

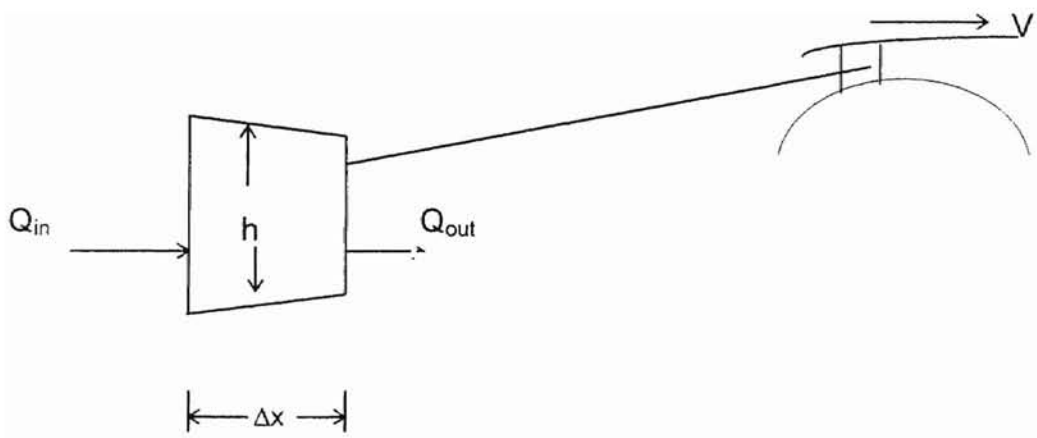


Figure 3.2: Differential Element for Conservation of Mass Analysis for an Impermeable Web

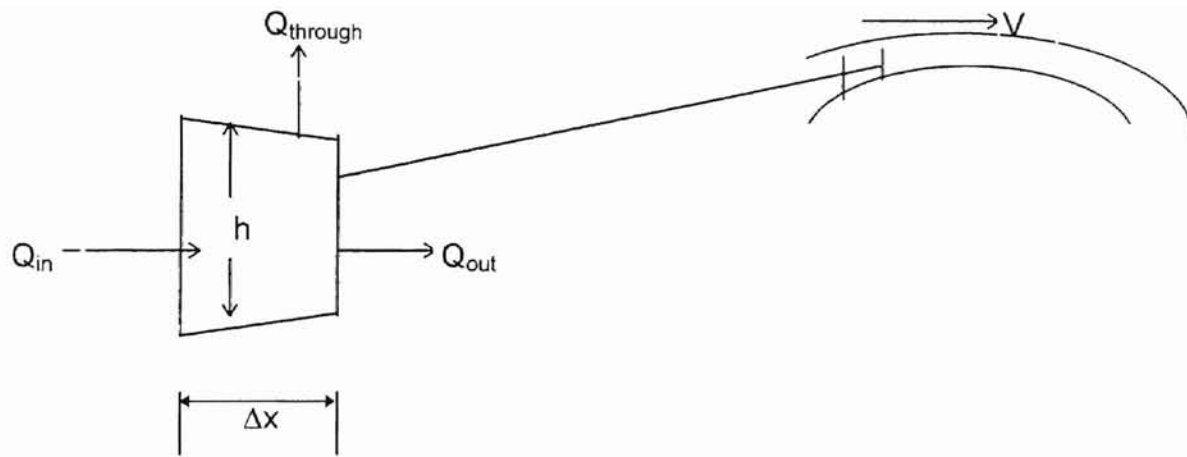


Figure 3.3: Differential Element for Conservation of Mass Analysis for a Permeable Web

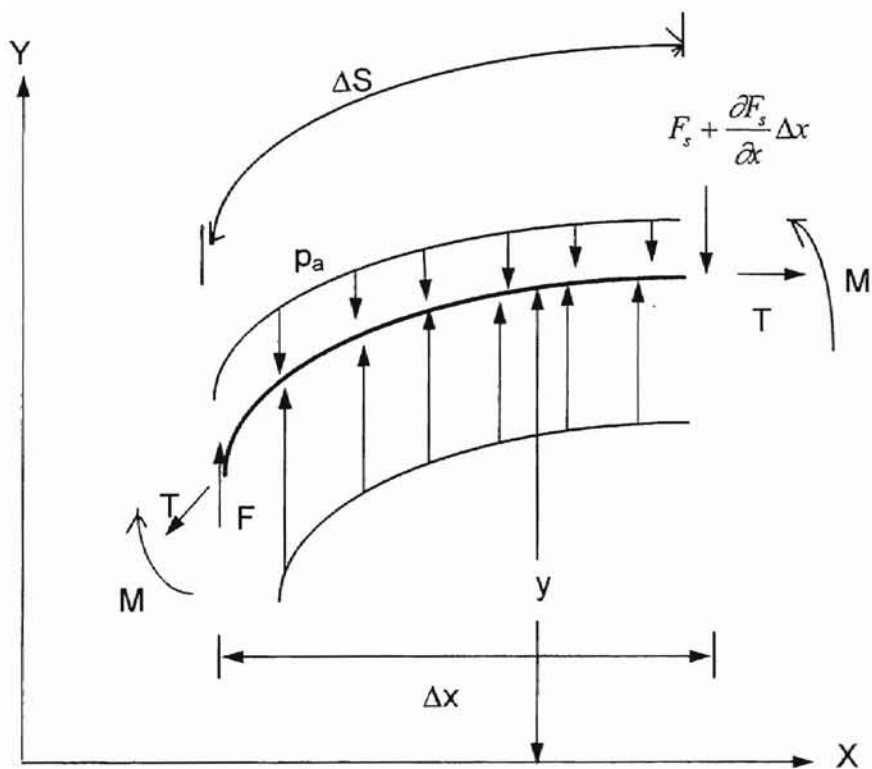


Figure3.4: Differential Web Element

$$h(x,t) = y(x,t) - \delta(x) \quad (3.26)$$

The Reynolds lubrication equation needs to be modified for the case of a rotating roller and permeable webs (eg. textile, paper). If  $V_R$ ,  $V_w$ ,  $V_t$  are the roller surface velocity, web velocity and velocity of air through (in the direction perpendicular to the web velocity) of the permeable web respectively, then the Reynolds lubrication equation is modified as follows.

$$\frac{\partial \left( h^3 p \frac{\partial \phi}{\partial x} \right)}{\partial x} + 6\lambda_a p_a \frac{\partial \left( h^2 \frac{\partial \phi}{\partial x} \right)}{\partial x} = 6\mu(V_R + V_w) \frac{\partial \phi h}{\partial x} + 12\mu \frac{\partial \phi h}{\partial t} + 12\mu K p (p - p_a)$$

or

$$\frac{\partial \left( h^3 p \frac{\partial \phi}{\partial x} \right)}{\partial x} + 6\lambda_a p_a \frac{\partial \left( h^2 \frac{\partial \phi}{\partial x} \right)}{\partial x} = 6\mu(V_R + V_w) \frac{\partial \phi h}{\partial x} + 12\mu \frac{\partial \phi h}{\partial t} + 12 \frac{k}{b} p (p - p_a) \quad (3.27)$$

Here the air velocity through the permeable web is as given by Murakama and Inamura (1976),

$$V_t \propto (p - p_a)$$

$$V_t = K (p - p_a) \quad (3.28)$$

was used.

where  $k$ = permeability coefficient of permeable web ( $m^2$ )

$$K = \text{permeability of permeable web } \{ (m^3/\text{sec}) / (m^2 \cdot \text{Pa}) \}$$

$$b = \text{thickness of the web (m)}$$

$(p-p_a)$ =pressure drop across the permeable web ( $N/m^2$ )

### **3.2.1 Tangency Point Location**

As the initial conditions were described for the region within the tangency points, the determination of tangency points(i.e. the locations on the roller surface where the web is tangent to the roller) is required. Referring to Figure 3.5 one can geometrically obtain expressions for  $X_o$  and  $Y_o$

$$X_o = 0.5L - (R+h_o)\sin\theta \quad (3.29)$$

$$Y_o = (\delta_{max} - R) + (R+h_o)\cos\theta \quad (3.30)$$

where,  $X_o$  is the X-axis coordinate for the tangent point,

$Y_o$  is the Y-axis coordinate for the tangent point, and

$\theta$  is the angle included between the web and the reference line.

### **3.2.2 Boundary Conditions**

Referring to Figure 3.5 the boundary conditions for the problem are,

$$y(L_1,t) = y(L_1,0) = \text{constant} \quad (3.31)$$

$$y(L_2,t) = y(L_2,0) = \text{constant} \quad (3.32)$$

$$y_x(L_1,t) = y_x(L_1,0) = \text{constant, and} \quad (3.33)$$

$$y_x(L_2,t) = y_x(L_2,0) = \text{constant} \quad (3.34)$$

Where  $y_x$  represents derivative of  $y$  with respect to  $x$ . The  $y$ 's at two ends  $L_1$  and  $L_2$  are calculated directly based upon the roller geometry. The pressure is taken to be ambient at the ends of the roller.

$$p(L_1,t) = p(L_2,t) = p_a \quad (3.35)$$

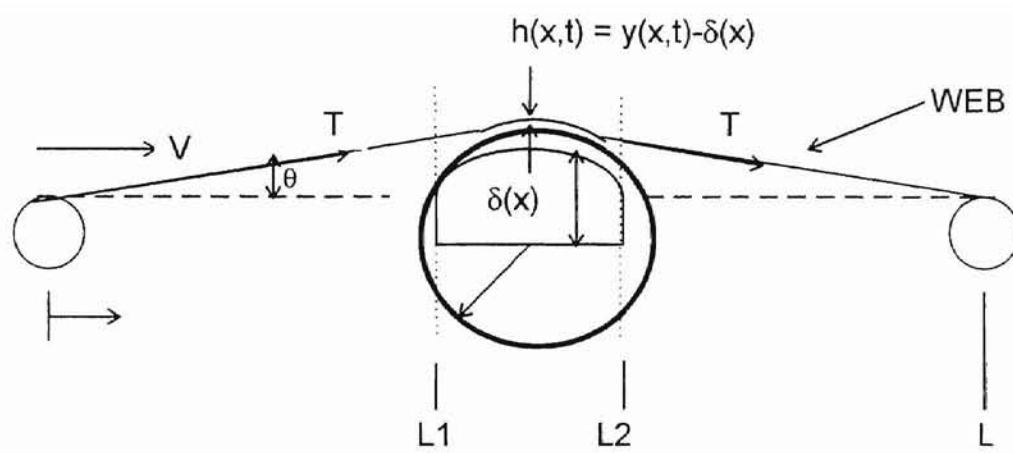


Figure3.5: Schematic Indicating Tangency Points for Initial Conditions



### 3.2.3 Initial Conditions

Referring to Figure 3.5, the initial conditions for the air film gap and pressure for the domain within the tangency points are,

$$h=h_o=0.643R(6\mu V/T)^{2/3}=\text{constant, and} \quad (3.36)$$

$$p=p_o=p_a+T/w=\text{constant} \quad (3.37)$$

For the region outside the tangency point, the displacement is taken to be linear and pressure to be atmospheric.

Work carried out by the researchers in web handling can be subdivided into two groups. One with a perfectly flexible web and the other with a web with finite stiffness. Current work involves computations for both kinds of webs. Computations have been performed with the following kinds of webs:

- 1) with a perfectly flexible web (with zero stiffness)
- 2) with a web with finite stiffness

All of the other operating conditions were kept the same for the sake of comparison. Each of the problems concerned was solved using different numerical techniques. Let us see the way the equations can be solved. Both of the techniques use the finite difference approach to approximate the derivatives in the equations.

### 3.3 Finite Difference Solution Technique

The finite difference operators used to approximate the terms in the differential equations are given below:

$$y_{xx} = \frac{\partial^2 y}{\partial x^2} = (y_{i+1}^{n+1} - 2y_i^{n+1} + y_{i-1}^{n+1}) / \Delta x^2 \quad (3.38a)$$

$$y_{tt} = \frac{\partial^2 y}{\partial t^2} = (y_i^{n+1} - 2y_i^n + y_i^{n-1}) / \Delta t^2 \quad (3.38b)$$

$$y_{xt} = \frac{\partial^2 y}{\partial x \partial t} = (y_{i+1}^{n+1} - y_{i+1}^{n-1} - y_{i-1}^{n+1} + y_{i-1}^{n-1}) / 4\Delta x \Delta t \quad (3.38c)$$

$$p_x = \frac{\partial p}{\partial x} = (p_{i+1}^{n+1} - p_{i-1}^{n+1}) / 2\Delta x \quad (3.38d)$$

$$p_t = \frac{\partial p}{\partial t} = (p_i^{n+1} - p_i^n) / \Delta t \quad (3.38e)$$

$$p_{xx} = \frac{\partial^2 p}{\partial x^2} = (p_{i+1}^{n+1} - 2p_i^{n+1} + p_{i-1}^{n+1}) / \Delta x^2 \quad (3.38f)$$

$$h_x = \frac{\partial h}{\partial x} = (h_{i+1}^{n+1} - h_{i-1}^{n+1}) / 2\Delta x \quad (3.38g)$$

$$h_t = \frac{\partial h}{\partial t} = (h_i^{n+1} - h_i^n) / \Delta t \quad (3.38h)$$

where  $y_{xx}$  represents the second derivative of  $y$  with respect to  $x$  and  $y_i^n$  represents the value of  $y$  at node  $i$  and time step  $n$ .

#### 3.3.1 Zero Stiffness model

In this case, we consider the stiffness of the foil to be negligible and simplify the PDE by dropping the contribution of the stiffness term. Hence the equation of motion of the web reduces to the following,

$$\rho b \left( \frac{\partial^2 y}{\partial t^2} + 2V \frac{\partial^2 y}{\partial x \partial t} + V^2 \frac{\partial^2 y}{\partial x^2} \right) - \frac{T}{w} \frac{\partial^2 y}{\partial x^2} = p - p_a \quad (3.39)$$

which can be written in the following form,

$$\rho (y_{tt} + 2V_w y_{xt} + V_w^2 y_{xx}) - \frac{T}{w} y_{xx} = p - p_a \quad (3.40)$$

and the Reynolds lubrication equation is,

$$\frac{\partial \left( h^3 p \frac{\partial p}{\partial x} \right)}{\partial x} + 6\lambda_a p_a \frac{\partial \left( h^2 \frac{\partial p}{\partial x} \right)}{\partial x} = 6\mu(V_R + V_w) \frac{\partial (ph)}{\partial x} + 12\mu \frac{\partial (ph)}{\partial t} + 12\mu \frac{k}{b} p(p - p_a) \quad (3.41)$$

which can be expressed in the following form,

$$\begin{aligned} (h^3 pp_{xx} + h^3 p_x^2 + 3h^2 pp_x h_x) + 6\lambda_a p_a (h^2 p_{xx} + 2hp_x h_x) = [12\mu(ph_t + hp_t) + \\ 6(V_R + V_w)\mu(p_x h + h_x p) + 12\frac{k}{b} p(p - p_a)] \end{aligned} \quad (3.42)$$

The two governing equations are coupled through the pressure,  $p$ , and the following relationship between the air film thickness,  $h(x,t)$ , between the roller and web and the web displacement  $y(x,t)$ , with respect to the equilibrium position:

$$h(x,t) = y(x,t) - \delta(x) \quad (3.43)$$

The above system of equations can be solved by substituting the proper finite difference operators for the derivatives and solving the resultant finite difference equations simultaneously using the boundary conditions and initial conditions discussed in the previous section. Substituting the equivalent finite difference operators into the governing equations yields the following set of finite difference equations:

### Web equation of motion

$$B_1 y_{i-1}^{n+1} + D_1 y_i^{n+1} + A_1 y_{i+1}^{n+1} = E_1 \quad (3.44)$$

where  $B_1$ ,  $D_1$ ,  $A_1$  are constants containing the coefficients from the equation of motion of web and  $E_1$  contains the values of foil displacement,  $y(x,t)$ , at time step  $n$  and  $(n-1)$  and pressure,  $p$  at time step  $n$ .

### Reynolds Lubrication equation

$$B_2 p_{i-1}^{n+1} + D_2 p_i^{n+1} + A_2 p_{i+1}^{n+1} = E_2 \quad (3.45)$$

where  $B_2$ ,  $D_2$ ,  $A_2$  are constants containing the values of pressure,  $p$ , at time step,  $n$ , and values of air film gap,  $h(x,t)$ , at time step,  $n$ , and  $(n+1)$  obtained by solving the equation of motion of the web. The finite difference form of the Reynolds lubrication equation is nonlinear. This is inconvenient to solve if the above finite difference operators are used. The equation is linearized as given by Stahl et al. (1974) using an approximation at the old time step  $n$  instead of the new time step  $(n+1)$  in those terms involving products of  $p$  and its derivatives. To understand how this is done, consider the first term in the Reynolds lubrication equation. The result after carrying out the differentiation is  $h^3 p p_{xx} + h^3 p_x^2 + 3h^2 p p_x h_x$ . If  $p_i^n$  is used for  $p$  instead of  $p_i^{n+1}$  and a difference approximation involving  $n$  instead of  $(n+1)$  is used for  $p_x$ , then the result is linear in those values of  $p$  at time step  $n+1$ .

### **3.3.2 Finite Stiffness Model**

Here we assume the stiffness of the foil to be non-zero and the governing equations are,

$$\rho b \left( \frac{\partial^2 y}{\partial t^2} + 2V \frac{\partial^2 y}{\partial x \partial t} + V^2 \frac{\partial^2 y}{\partial x^2} \right) + \frac{EI}{w} \frac{\partial^4 y}{\partial x^4} - \frac{T}{w} \frac{\partial^2 y}{\partial x^2} = p - p_a \quad (3.46)$$

which can be expressed as

$$\rho b (y_{tt} + 2V_w y_{xt} + V_w^2 y_{xx}) + \frac{EI}{w} y_{xxxx} - \frac{T}{w} y_{xx} = p - p_a \quad (3.47)$$

and the Reynolds equation remains the same as for the case with zero stiffness model. Now let us look at the finite difference equivalents of the above equations.

#### **Web equation of motion**

$$C_3 y_{i-2}^{n+1} + B_3 y_{i-1}^{n+1} + A_3 y_i^{n+1} + D_3 y_{i+1}^{n+1} + F_3 y_{i+2}^{n+1} = E_3 \quad (3.48)$$

where  $C_3, B_3, A_3, D_3, F_3$  are constants containing the coefficients from the equation of motion of web and  $E_3$  contains the values of foil displacement,  $y(x,t)$  at time step  $n$  and  $(n-1)$  and pressure,  $p$  at time step  $n$ .

#### **Reynolds lubrication equation**

It is as same as the one given for the zero stiffness model, equation 3.45.

### 3.4 Some other parameters that are used in obtaining the solution

A grid mesh  $\Delta x$  is chosen and the time step  $\Delta t$  is chosen small enough to maintain the numerical stability of the solution. To determine a suitable value of  $\Delta t$  for a chosen  $\Delta x$ , a "steady state" solution was calculated using a relatively large value for  $\Delta t$ . If the solution obtained after a few iterations changed considerably, the solution was continued for smaller  $\Delta t$ . For stability in this numerical solution technique, a time step of  $1 \times 10^{-7}$  seconds was used. For larger time step it was found that the solution diverges. The **Zero stiffness model** was solved using the tri-diagonal matrix algorithm for both the equations. The **Finite stiffness model** was solved using the LU decomposition method for the web equation of motion and the Tridiagonal matrix algorithm for the Reynolds equation. Here LU decomposition means that the coefficient matrix was decomposed into Lower and Upper triangular matrices before inverting them to get the solution of the equations.

Here, for both zero stiffness and finite stiffness models, solutions were obtained at 125 grid points uniformly distributed between  $L_1$  and  $L_2$ . It was decided to use 125 grid points after a finer grid could not make a significant difference in the air film and pressure distributions.  $\Delta x$  and  $\Delta t$  were chosen such that the numerical stability was assured. For all of the cases considered, time steps of  $1 \times 10^{-7}$ s or smaller were chosen based on the stability criteria.

Convergence criteria for the steady state computations were applied to the air film thickness. Convergence was judged to occur when the sum of the 125

non-dimensional changes in air film thickness between iterations was less than  $10^{-4}$ . The same convergence criterion was applied for the two steady states obtained for the step variation in tension case and for the step variation in air film thickness case, but the comparisons were made for points  $2\pi$  apart in angle; at the same phase point in the steady state oscillation case.

## CHAPTER 4

### RESULTS

Numerical computations have been performed to predict the transient behavior of the air film thickness subjected to tension transients and to perturbation in the air film thickness distribution outside the wrap region. The stiffness of the web also has been incorporated in some of the computations. In these two-dimensional computations, the infinitely wide web moves over a roller in the longitudinal direction with two end supports as shown in Figure 3.5

A computer code was written in FORTRAN to solve the finite difference equations (equations 3.44 and 3.45 or 3.45 and 3.48) given in Chapter 3. The code simultaneously solves the two finite difference equations yielding the spacing and pressure distribution between the moving web and the roller as a function of both time and distance along the roller. Steady state is assumed when the sum of the non-dimensional difference in the air film distributions between iterations decreases to a value of  $1 \times 10^{-4}$ .

The roller profile is defined with the distance of the roller surface from a reference line joining the two end supports. All of the distances in the direction perpendicular to the motion of the web are measured with respect to this line (refer to Figure 3.5) joining the two end supports. The air film thickness above the roller surface is obtained by subtracting the roller profile from the displacement of the web with respect to the reference line. The foil is assumed to



be infinitely wide. For the tension/air film transient cases, the foil was assumed to be perfectly flexible.

Sample simulation parameters for film thickness computation for web roller interface

Web Parameters:

$m(\rho b) = 0.0922 \text{ kg/m}^2$ , web mass per unit area

$T/w = 263 \text{ N/m}$ , web tension per unit width

$EI/w = 1.52 \times 10^{-5} \text{ N-m}$ , flexural rigidity

$V_w = 15.24 \text{ m/s}$ , web velocity

Lubrication Parameters:

$\mu = 1.81 \times 10^{-5} \text{ Pa-s}$ , dynamic viscosity of air

$P_a = 1.01325 \times 10^5 \text{ Pa}$ , ambient pressure

$\lambda_a = 0.0$ , it has been assumed to be a no slip condition

Roller and Web Geometry(see Figure 3.5):

$L = 0.85 \text{ m}$ , distance between two end supports

$L_1 = 0.35 \text{ m}$ , location of the left reference point on the roller

$L_2 = 0.50 \text{ m}$ , location of the right reference point on the roller

$R = 20.4 \text{ cm}$ , roller radius

$\xi = (x-L_1)/(L_2-L_1)$ , non-dimensional distance along the roller

$\xi_{L1} = 0.0$

$\xi_{L2} = 1.0$

Finite Difference Parameters:

$\Delta t = 1 \times 10^{-7}$  s, time step for numerical solution

$\Delta x = 1.23 \times 10^{-3}$  m, grid size for numerical solution

The results section has been subdivided into two subdivisions. They are:

1) Transients of air film thickness due to variation in tension and disturbance in the air film thickness

This has been subdivided into following subsections,

- a) Constant tension case
- b) Step variation in tension case
- c) Sinusoidal fluctuation in tension case
- d) Step variation in air film thickness case.

2) Comparison between finite stiffness model and zero stiffness model

## **4.1 Effect of Tension Transients and Perturbation in Air Film**

### **Distribution Near the Entrance Region on Air Film Thickness**

#### **Distribution**

##### **4.1.1 Impermeable Web**

###### **4.1.1.1 Constant tension case**

Let us look at the constant tension case where the steady state solution was obtained via a transient approach. Here the initial values, described in section 3.2.3 for the air film thickness and the pressure distributions were

assumed and the solution was allowed to develop as the time progressed, reaching a final steady state.

Air film thickness distribution development and the pressure distribution developments are compared with a published result in Figures 4.1 and 4.2. The operating conditions considered for this case were taken to be  $V=2.54$  m/s,  $T/w=273$  N/m,  $m=0.0207$  kg/m<sup>2</sup>. We can observe that the results obtained using the present study and the results obtained by Bhushan (1990) are in good agreement. We can observe some difference in the air film distribution and the pressure distribution because of the number of grid points that were chosen to plot the published results. If we compare the central region air film thickness for this case we can see that the present method predicts a value of  $1.145 \times 10^{-6}$  m, on the other hand Bhushan et al. (1990) predicts a value of  $1.15 \times 10^{-6}$  m. This is a very good agreement for engineering purposes. As far as the pressure profile is concerned the present method predicts a lower value at the exit region where the pressure falls below atmospheric pressure. Nevertheless we can say that the code developed for this present study predicts the air film and pressure distributions well. A higher velocity case with  $V = 10.16$  m/s,  $T/w = 263$  N/m and  $m = 0.0922$  kg/m<sup>2</sup> is shown in Figure 4.3. From the transient air film profile given in Figure 4.3 we can say that the initial oscillations are sinusoidal in nature, but they achieve steady state very fast in 3 ms. For all of the computations performed, the angle of wrap between L1 and L2 was taken to be 20 degrees.

If we look at the pressure profile given in Figure 4.2 we can conclude the following. In the entrance region pressure increases from ambient pressure to film pressure,  $P$ , and then a constant pressure prevails in the constant air film thickness region. Near the exit region the pressure gradient is negative which leads to a drop in the air film thickness from the central region air film value, but in the exit region pressure decreases from film pressure to  $P$  to ambient pressure whereas the air film thickness increases to infinity from  $h_0$ . The above result can also be inferred from the Reynolds equation. It is obvious that a negative pressure gradient can exist only if the air gap at the exit is less than  $h_0$ , which is incompatible with an increasing air gap. The increase in air gap is therefore preceded by a region where the air film gap is less than  $h_0$  in which pressure decreases to below ambient followed by a region of increasing gap and increasing pressure.

After establishing confidence in the model developed by the comparison of results with the published results, it was decided to determine the effect of tension/air film thickness transients in the distribution of air film and pressure.

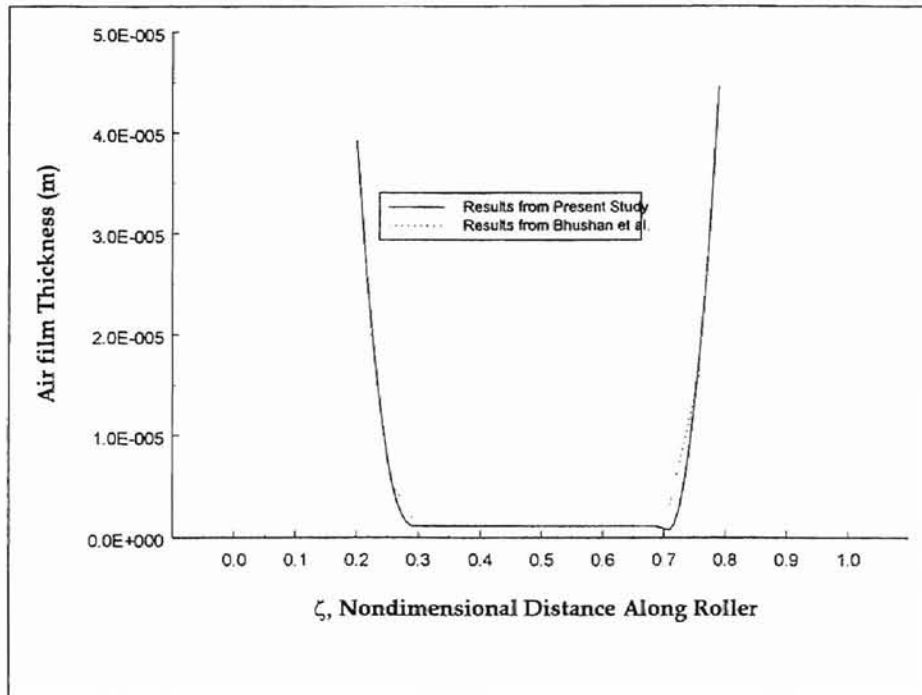


Figure 4.1 :Comparison between the present results and the published results ( $V_w=2.54$  m/s,  $T=273$ N/m,  $m=0.0207$  kg/m<sup>2</sup>)

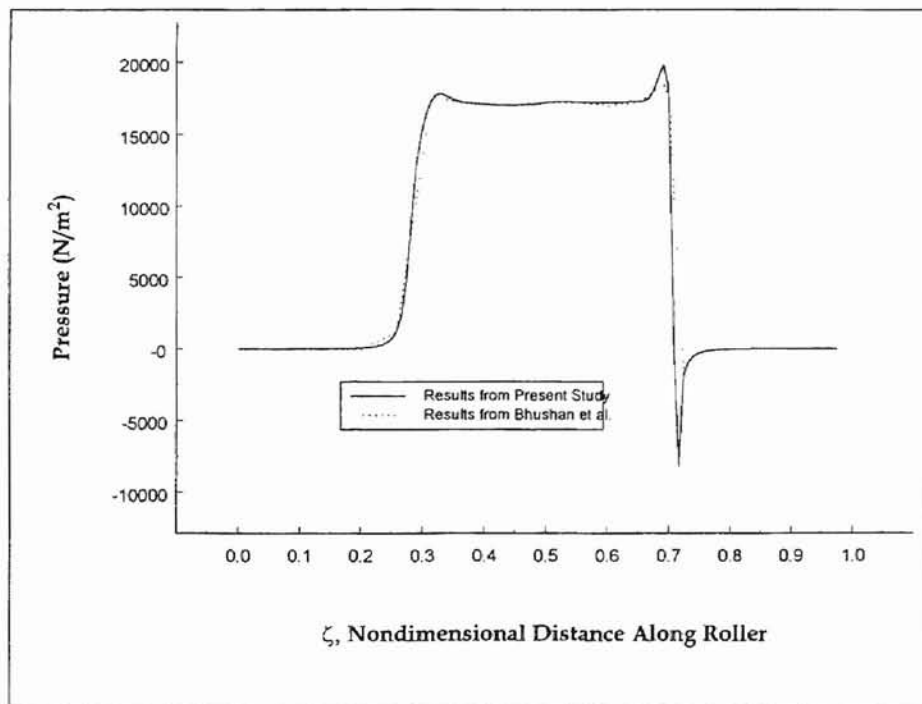


Figure 4.2 : Comparison between the present results and the published results ( $V_w=2.54$  m/s,  $T=273$ N/m,  $m=0.0207$  kg/m<sup>2</sup>)

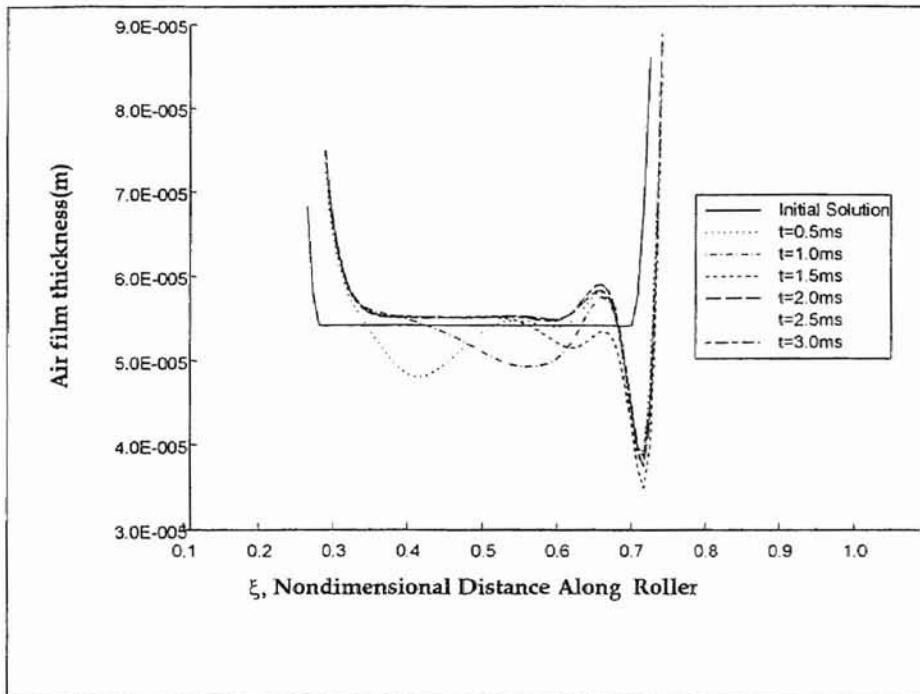


Figure 4.3 : Transient Air-film thickness profiles  
 ( $V_w=10.16$  m/s,  $T=273$ N/m,  $m=0.0922$  kg/m<sup>2</sup>)

#### 4.1.1.2 Effect of Step Change in Tension Case

Computations were performed for the same size of rotating roller. Here a step variation in tension was applied once the steady state solution was obtained for the initial tension. Hence we seek a steady state solution for the increased tension. Our concern in this case was to see the transient response of the air film thickness after the increased tension is applied. Computations were halted once the convergence criterion was satisfied for the second time (i.e., first time for the initial tension and the second time for the increased tension). Developing profiles were presented as a function of non-dimensional time defined by  $t^* = V_w * t / 2\pi R$ , where  $t$  is the time in seconds, and  $R$  is the roller radius. Two different magnitudes of step changes were applied.

- 1) 20% step increase in tension
- 2) 50% step increase in tension

Solutions were obtained for  $T/w = 87.6$  N/m and  $T/w = 263$  N/m in order to verify the effect of initial tension in the transient response of the air films. In the computations, the following operating conditions were kept constant unless otherwise specified. Velocity of the web and roller were taken to be 15.24 m/s and two different web masses were used.

Results for a step variation in tension with  $V = 15.24$  m/s,  $T/w = 87.6$  N/m, and  $m = 0.0254$  kg/m<sup>2</sup> are presented in Figure 4.4. The figure clearly depicts the case for a 20% step increase in tension applied after the initial steady

state solution is obtained. It can be seen that traveling wave-like air film profiles exist and eventually reaches a second steady state. For the case with a 50% step change (Figure 4.5) in tension, it takes a longer time to reach the steady state and the magnitude of oscillation is also higher compared to a lower step change in tension. It is reasonable to have longer time for a higher step as this would disturb the air film thickness distribution more as compared to a lower step. It also can be seen in the developing air film profiles that a lower air film thickness exists near the entrance region. We also can observe an increase in air film thickness at the exit region above the initial steady state solution. In the above cases the 20% step exhibits an 11% reduction in the central region air film thickness and the other case shows a 21% reduction in the air film thickness. The length of the central region is more for the 50% step case as compared to the 20% step case.

If we consider a case with higher initial tension ( $T/w = 263 \text{ N/m}$ ) with other parameters kept constant, from Figures 4.6 and 4.7 it can be observed that the range of oscillation is small as compared to a lower tension case. In this case a 20% step causes an 11% reduction in the air film thickness and the 50% case shows a 26.7% reduction in the central region of the air film thickness. For all of the cases considered, we can observe an increase in the length of the central constant thickness region.

If we look at the case with higher web mass with  $m = 0.0922 \text{ kg/m}^2$  and  $T/w = 263 \text{ N/m}$  (refer to Figure 4.8) we can observe that there are



comparatively fewer oscillations for the same time intervals and settles down faster as compared to the lower mass case and there could not be any increase in the air film thickness observed at the exit region. This trend has been observed for the case with a 50% step also (refer to Figure 4.9). Again a higher step takes more time to reach the steady state solution. Hence it suggests that a higher web mass does not let the web fly off for this set of operating conditions. Oscillations are significant and a higher step change in tension case shows a higher range of oscillation. For this case a 20% step change in tension leads to a 12.8% reduction in air film thickness and the 50% step leads to a 25.6% reduction in the air film thickness.

For all the cases considered above we can observe an increase in the air film thickness at the exit region, which might not be expected for an increase in tension. It is normally expected to have a lower air film thickness when the tension is increased. This can be explained as follows: when the tension is increased, suddenly it pulls the web towards the roller, as we deal with an infinitely wide web there is no air leakage to the side. Hence to satisfy continuity, a reduction in air film thickness at the entrance region must be supported by an increase in the air film thickness at the exit region. This can be a possible reason for the air film thickness to increase above the initial steady state distribution. The initial oscillation after the step change is applied is sinusoidal in shape, and the maxima's and minima's occur almost at the same location at a particular time. The oscillations eventually die out to yield the second steady state.

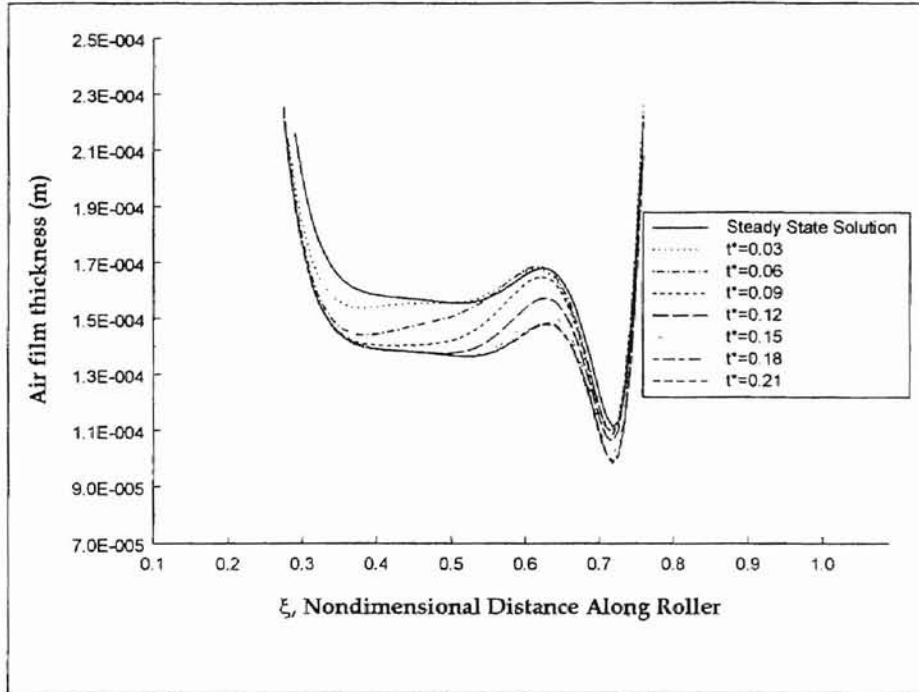


Figure 4.4: 20% Step Change in Tension  
 ( $V_w=15.24$  m/s,  $T_{init}/w=87.66$  N/m,  $m=0.0254$  kg/m<sup>2</sup>)

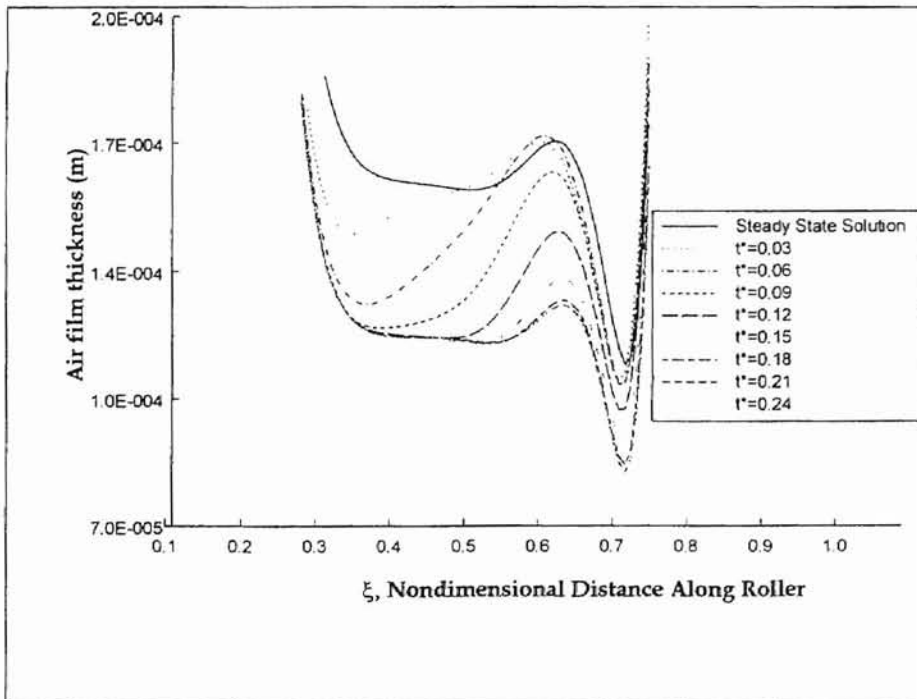


Figure 4.5: 50% Step Change in Tension  
 ( $V_w=15.24$  m/s,  $T_{init}/w=87.66$  N/m,  $m=0.0254$  kg/m<sup>2</sup>)

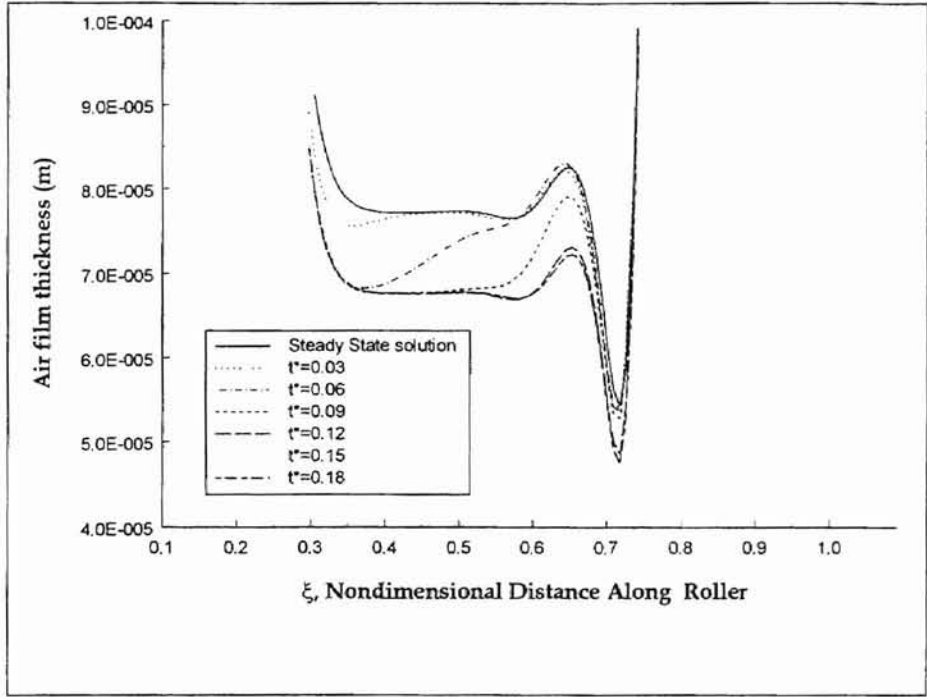


Figure 4.6: 20% Step Change in Tension  
 ( $V_w=15.24$  m/s,  $T_{init}/w=263$  N/m,  $m=0.0254$  kg/m<sup>2</sup>)

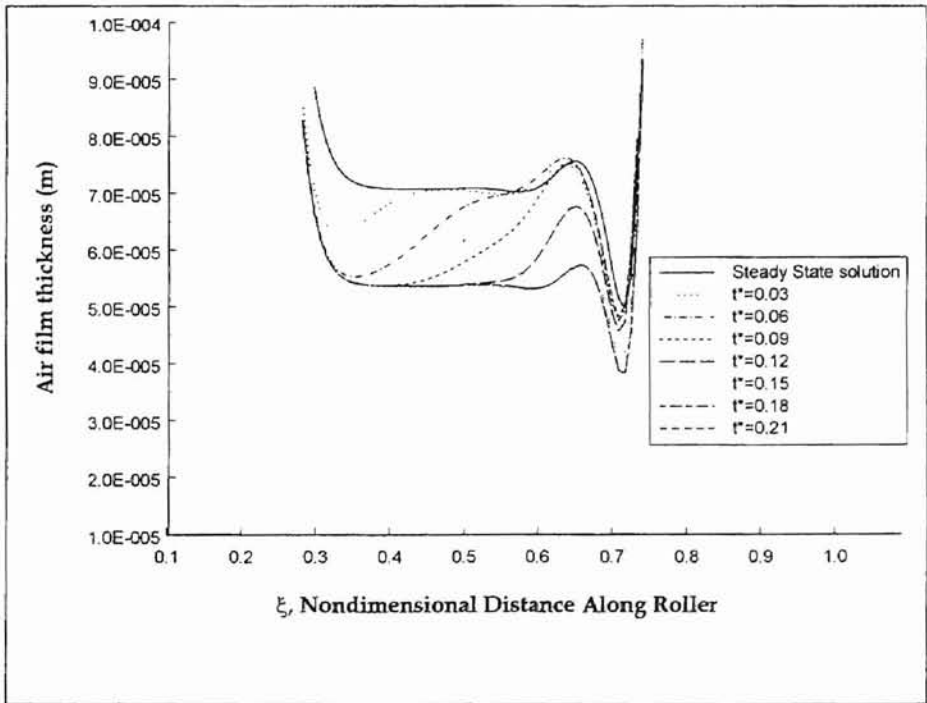


Figure 4.7: 50% Step Change in Tension  
 ( $V_w=15.24$  m/s,  $T_{init}/w=263$  N/m,  $m=0.0254$  kg/m<sup>2</sup>)

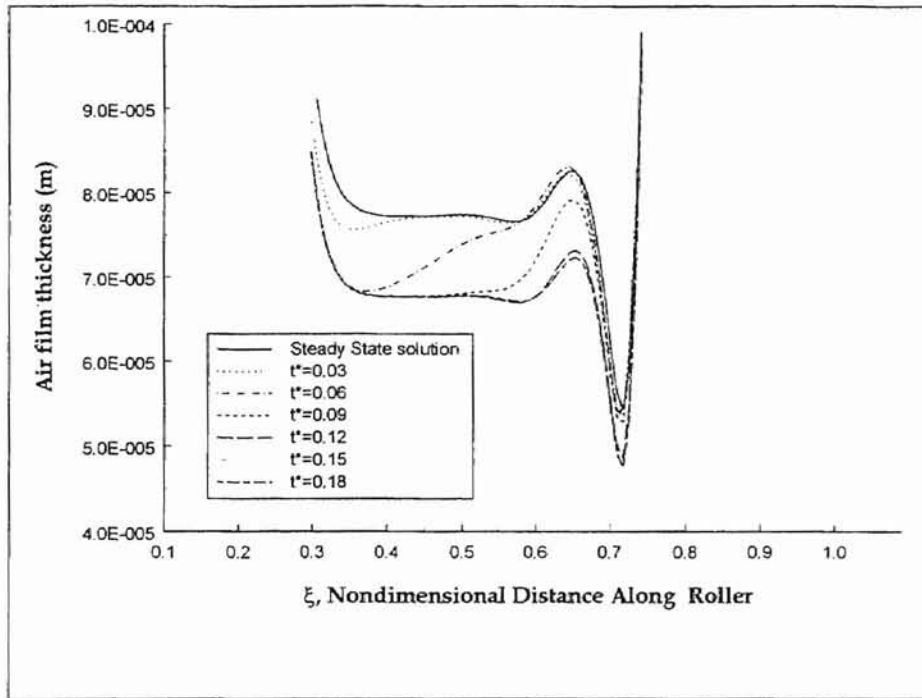


Figure 4.8: 20% Step Change in Tension  
 ( $V_w=15.24$  m/s,  $T_{init}/w=263$  N/m,  $m=0.0922$  kg/m<sup>2</sup>)

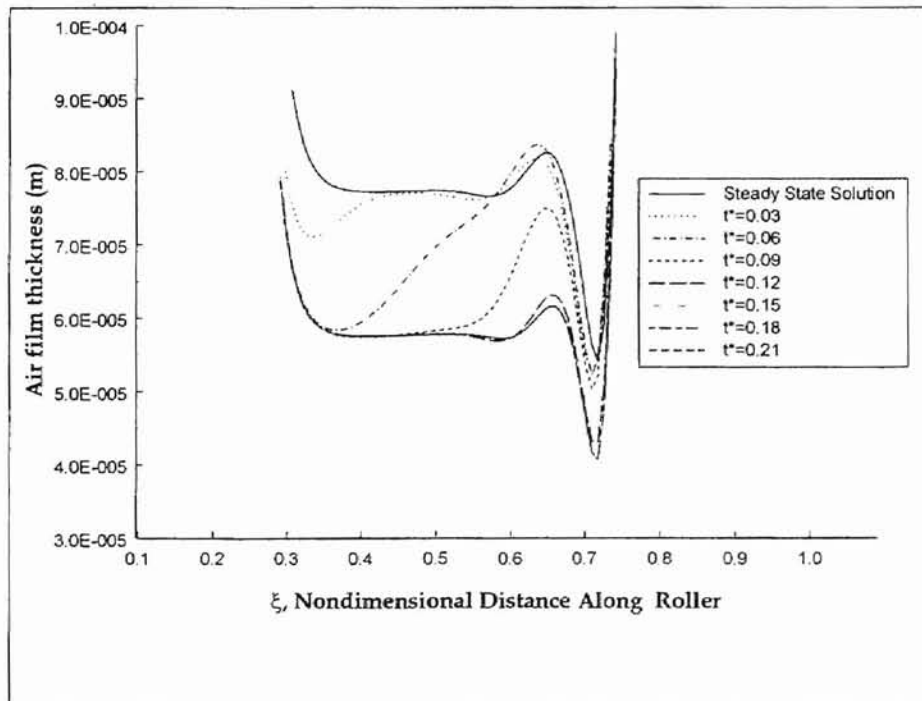


Figure 4.9: 50% Step Change in tension  
 ( $V_w=15.24$  m/s,  $T_{init}/w=263$  N/m,  $m=0.0922$  kg/m<sup>2</sup>)

#### 4.1.1.3 Effect of Sinusoidal Fluctuation in Tension Case

Sinusoidal Oscillations in tension were studied for two different cases.

- 1) Changing the Amplitude (A) of Oscillation.
- 2) Changing the Frequency ( $\omega$ ) of Oscillation.

Once the steady state solution is achieved tension applied is changed as follows,

$$T = T_{\text{initial}} + A * T_{\text{initial}} * \sin \omega t$$

A natural frequency ( $\omega_n$ ) of the web's oscillations for the problem at hand can be given by the following relationship [Chang(1990)],

$$\omega_n = \left( \frac{\pi}{L_h} \right) \left( \frac{T}{\left( m + \frac{\pi \rho w}{4} \right)} \right)^{1/2}, \quad (4.1)$$

where as  $\omega$  is an integer multiple of  $\omega_n$ . Developing profiles were given as a function of angle of rotation of the roller given by, alpha ( $\alpha$ )= $\omega t$ , where t is time in seconds.

Here the frequency employed was chosen as an integer multiple of the natural frequency given by the above relationship. For simplicity and comparison, web velocity and roller velocity were taken to be  $V = 15.24$  m/s. Computations were performed for two different web masses and two different initial tensions. In Figure 4.10, the air film distribution is given for  $T/w = 87.6$  N/m,  $m = 0.0254$  kg/m<sup>2</sup>,  $A = 0.5T$ ,  $\omega = \omega_n$ . Here we can observe that the cycle of oscillation repeats after 360 degrees. In this case the air film thickness distribution oscillates within an amplitude range of  $2 \times 10^{-5}$  m. It can also be seen

that the air film thickness distribution near the exit region increases above the steady state distribution at that point. However it eventually comes down (similar to the results for step variation in tension). However there was a significant difference in the amplitude of the excursions for the case with  $\omega = 2\omega_n$  (Figure 4.11). For this case the range of the amplitude magnitude was found to be  $4 \times 10^{-5}$  m. If we look at the case with  $T/w = 263$  N/m, we can observe that for  $A = 0.5T$ ,  $\omega = \omega_n$  (Figure 4.12), the magnitude of the range of excursions is small compared to the previous case with lower tension, but it can also be noticed that with increase in oscillating frequency in tension, air film oscillation also increases.

Now let us look at the case with increased mass ( $m = 0.0922$  kg/m<sup>2</sup>) with  $T = 263$  N/m,  $A = 0.5T$  and  $\omega = \omega_n$  (Figure 4.13) We can see that the oscillations exhibit similar patterns as in the previous case. Even for this case we can observe that near the exit region there is a slight overshoot of the air film thickness and then it settles down with time. It can also be noticed that the air film thickness distribution does not change much beyond a certain angle of rotation until it satisfies the convergence criterion. If we consider the case with  $T/w = 263$  N/m, we can notice that the length of the central region is large compared to the case with  $T/w = 87.6$  N/m. In all the cases observed so far there was not any excess overshoot observed which can lead to loss in traction and might damage the web. For the ranges of computations performed, there were some cases for which a solution could not be obtained for the oscillating tension. Some of these

problems were rectified using a very small time step ( $1 \times 10^{-9}$  s) for the computations. There were some other problems which cropped up while using very small time step. When we use a very small time step the change in the tension is going to be very small and also it was found to be difficult to track the point of complete revolution of the roller as the change in the angle between iteration would be very small. In some situations the non-dimensional difference in the air film thickness between iterations started oscillating beyond a certain time, this kinds of problems can also be taken care with a very small time steps. There can be some situations in which the oscillation in tension leads to a zero thickness air film. These cases might be taken care to avoid such situation in the industry

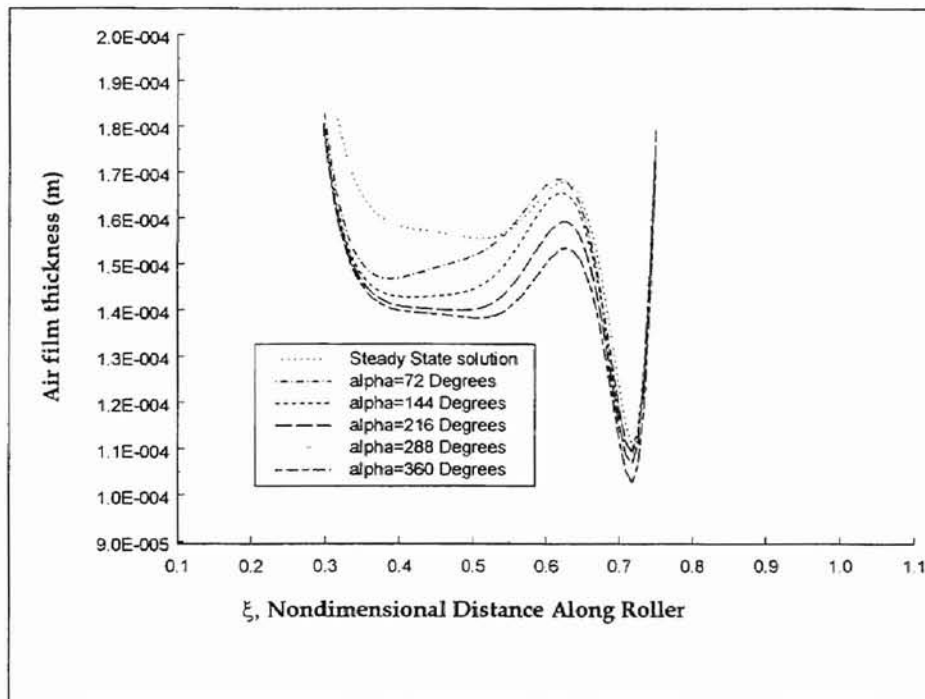


Figure 4.10: Sinusoidal Fluctuation in Tension  
 ( $V_w=15.24$  m/s,  $T_{init}/w=87.66$  N/m,  $m=0.0254$  kg/m<sup>2</sup>,  $A=0.5T$ ,  $\omega=\omega_n$ )

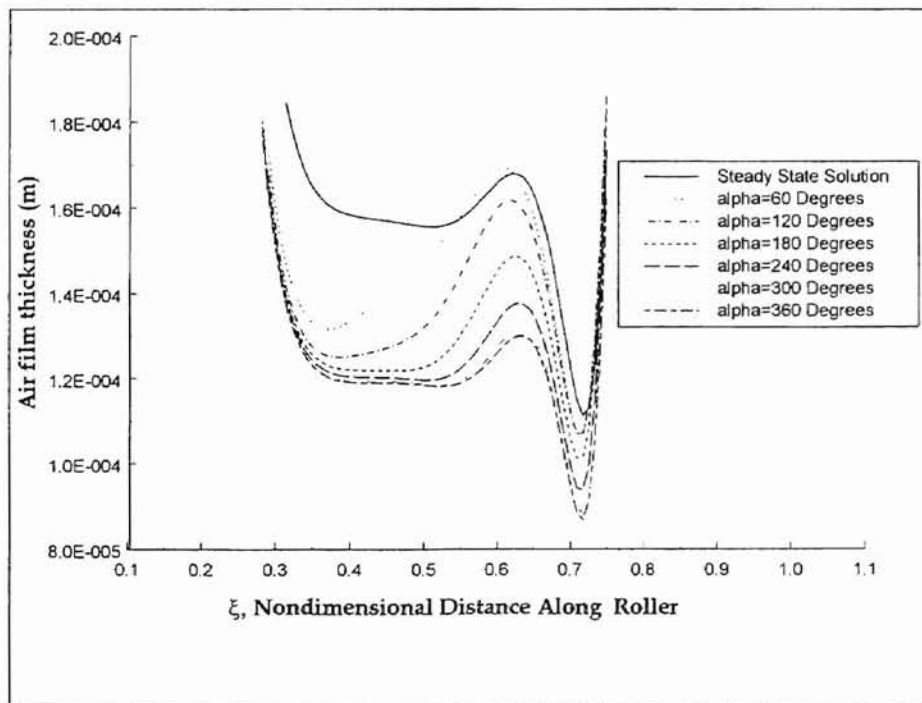


Figure 4.11: Sinusoidal Fluctuation in Tension  
 ( $V_w=15.24$ m/s,  $T_{init}/w=87.66$  N/m,  $m=0.0254$  kg/m<sup>2</sup>,  $A=0.5T$ ,  $\omega= \omega_n$ )



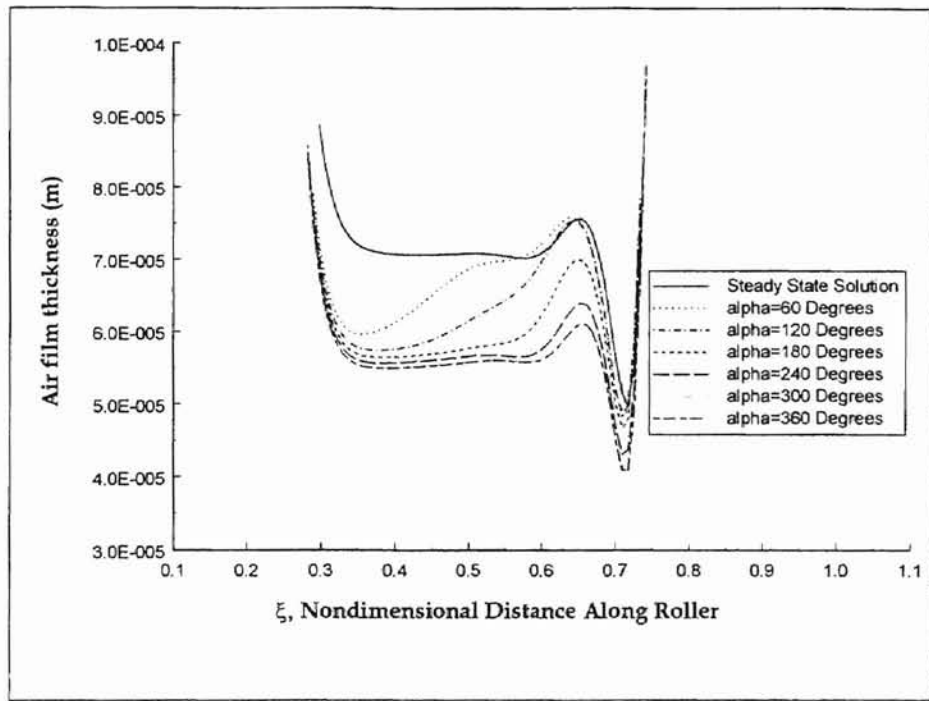


Figure 4.12: Sinusoidal Fluctuation in Tension  
 ( $V_w=15.24$  m/s,  $T_{init}/w=263$  N/m,  $m=0.0254$  kg/m<sup>2</sup>,  $A=0.5T$ ,  $\omega=\omega_n$ )

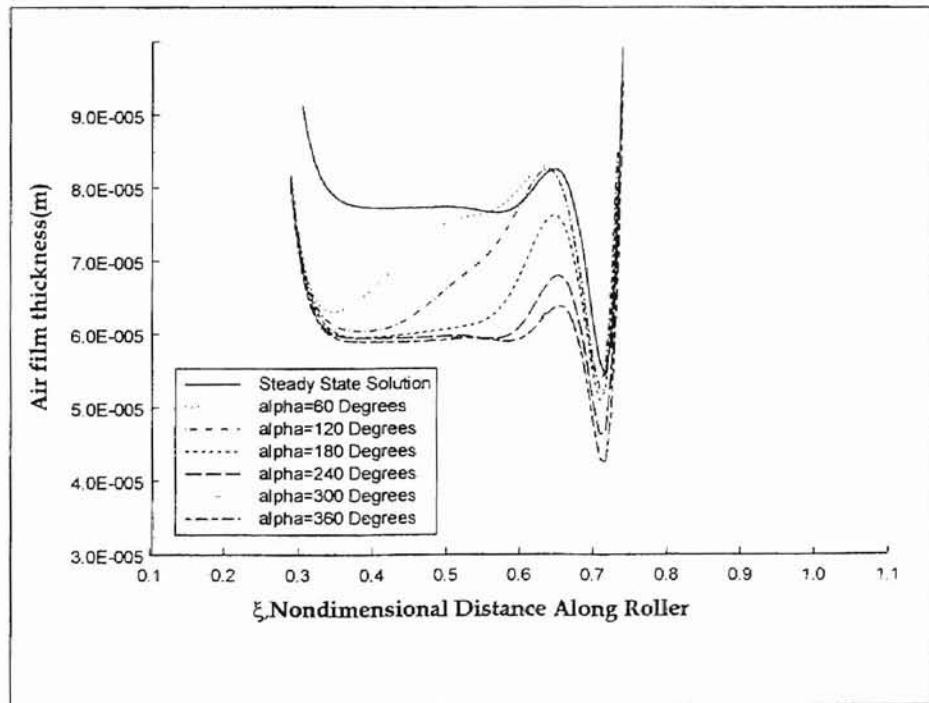


Figure 4.13: Sinusoidal Fluctuation in Tension  
 ( $V_w=15.24$  m/s,  $T_{init}=263$  N/m,  $m=0.0922$  kg/m<sup>2</sup>,  $A=0.5T$ ,  $\omega=\omega_n$ )

#### 4.1.1.4 Effect of Perturbation in Air Film Thickness

For this case the effect of introduced disturbances in the air film thickness was studied. Perturbations were introduced at a non-dimensional distance,  $\xi = 0.23 - 0.31$  for an operating condition with  $V = 15.24 \text{ m/s}$ ,  $T/w = 175.3 \text{ N/m}$  and  $m = 0.0922 \text{ kg/m}^2$  with a 20% increase in the air film thickness as shown in Figure 4.14, and it was observed how the disturbance propagates. In Figure 4.15 (for  $V = 15.24 \text{ m/s}$ ,  $T/w = 175.3 \text{ N/m}$ ,  $m = 0.0922 \text{ kg/m}^2$ ) a perturbation was introduced between  $\xi = 0.23 - 0.39$ . The magnitude of the disturbance was 30% of the mean of the air film thickness between these points. From the graph we can see that the disturbance was swept towards the exit and finally died out and reached its initial steady state. It was found that with higher perturbations the solution tended to diverge. In Figure 4.16 the air film thickness distribution for  $V = 5.08 \text{ m/s}$ ,  $T/w = 175.3 \text{ N/m}$  and a 30% disturbance was introduced from grid points  $\xi = 0.23 - 0.39$ . It is almost sinusoidal in shape and resembles a traveling sinusoid towards the exit. For the same operating conditions ( $V = 5.08 \text{ m/s}$ ,  $T/w = 175.3 \text{ N/m}$ ) a 30% perturbation in the air film thickness case exhibits a higher amplitude of oscillations as compared to the 20% (Figure 4.17) perturbation case. We can also conclude that for a higher magnitude of oscillation, the propagation is faster as compared to the lower magnitude of perturbation case. Even though the response is very much similar to the one given in the step change in tension case, we can observe a significant difference

between these two cases. For the step change in tension case, a new steady state is established, and we can observe a decrease in the air film thickness. On the other hand for the perturbation in air film case the original steady state was re-established. Another difference which can be observed between the step change in tension case and the perturbation case is the nature of the waves. For the perturbation case, it is a moving sinusoid, where the locations of maxima and minima change as time progresses, but for the step change in tension case the location of maxima or minima do not change until the steady state is obtained. Perturbation in the air film case is equivalent to adding an extra amount of air in-between the web and the roller. Hence it appears that the added air would be swept towards the exit region and the initial steady state is re-established.

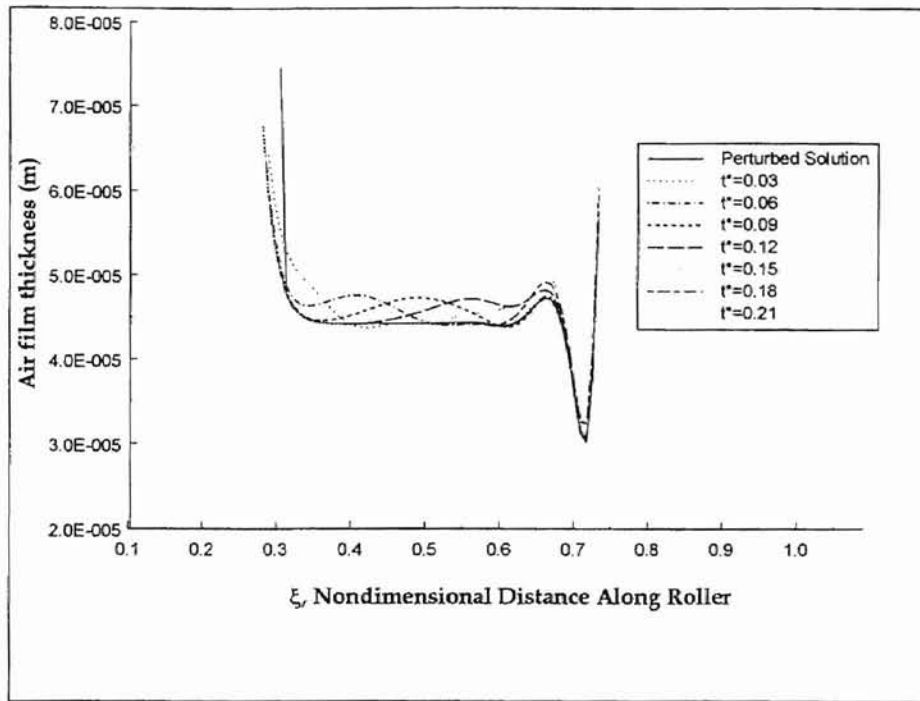


Figure 4.14: 20% Perturbation in Air Film Distribution Between  $\xi=0.23-0.31$   
 ( $V_w=15.24$  m/s,  $T_{init}/w=175.3$  N/m,  $m=0.0922$  kg/m<sup>2</sup>)

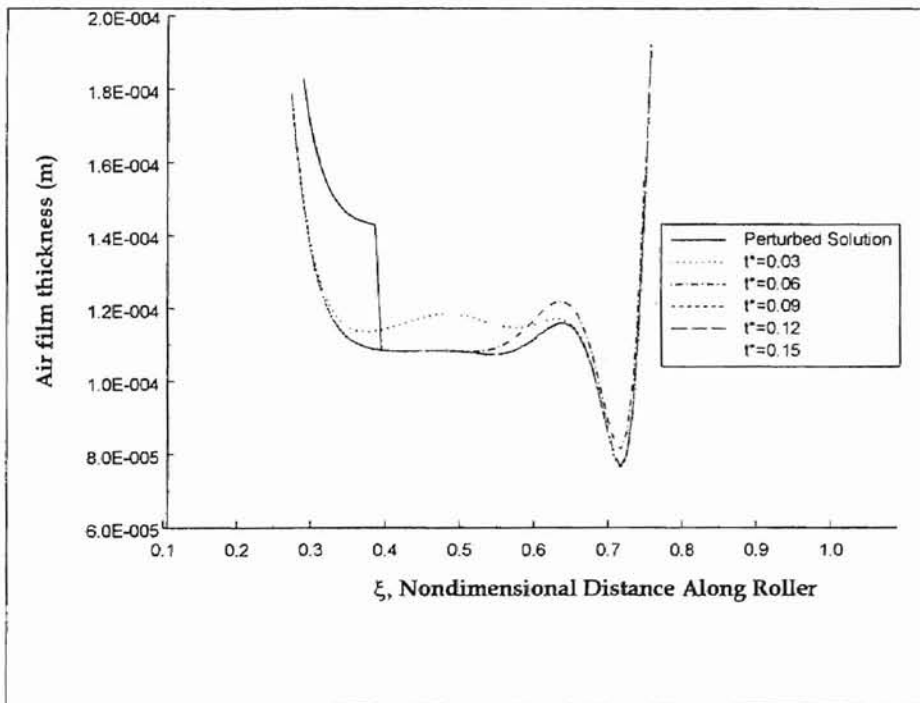


Figure 4.15: 30% Perturbation in Air Film Distribution Between  $\xi=0.23-0.39$   
 ( $V_w=2.54$  m/s,  $T_{init}/w=175.3$  N/m,  $m=0.0922$  kg/m<sup>2</sup>)

UNIVERSITY

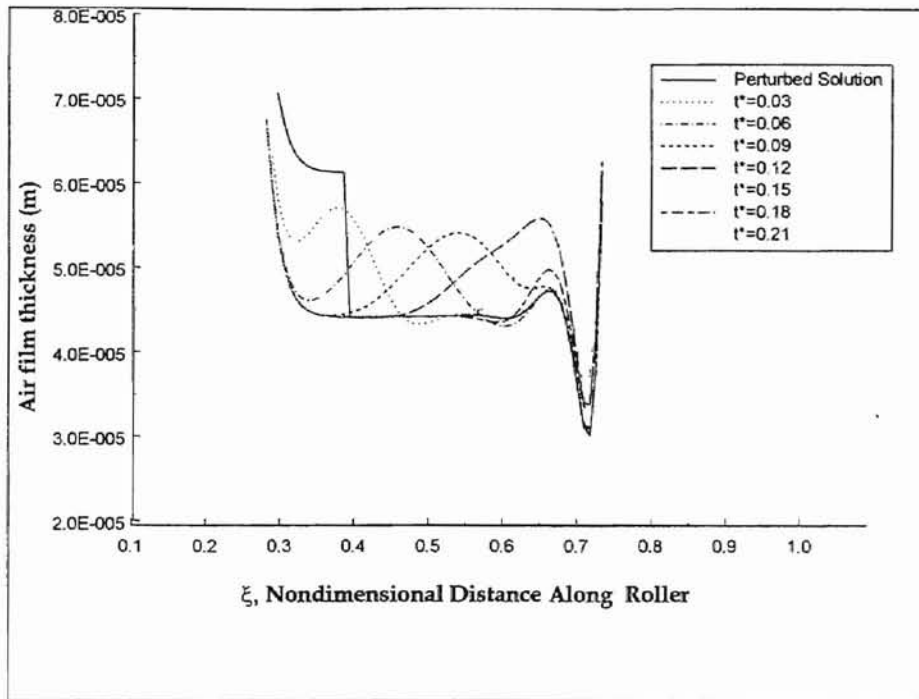


Figure 4.16: 30% Perturbation in Air Film Distribution Between  $\xi=0.23-0.39$   
 ( $V_w=5.08$  m/s,  $T_{init}/w=175.3$  N/m,  $m=0.0922$  kg/m<sup>2</sup>)

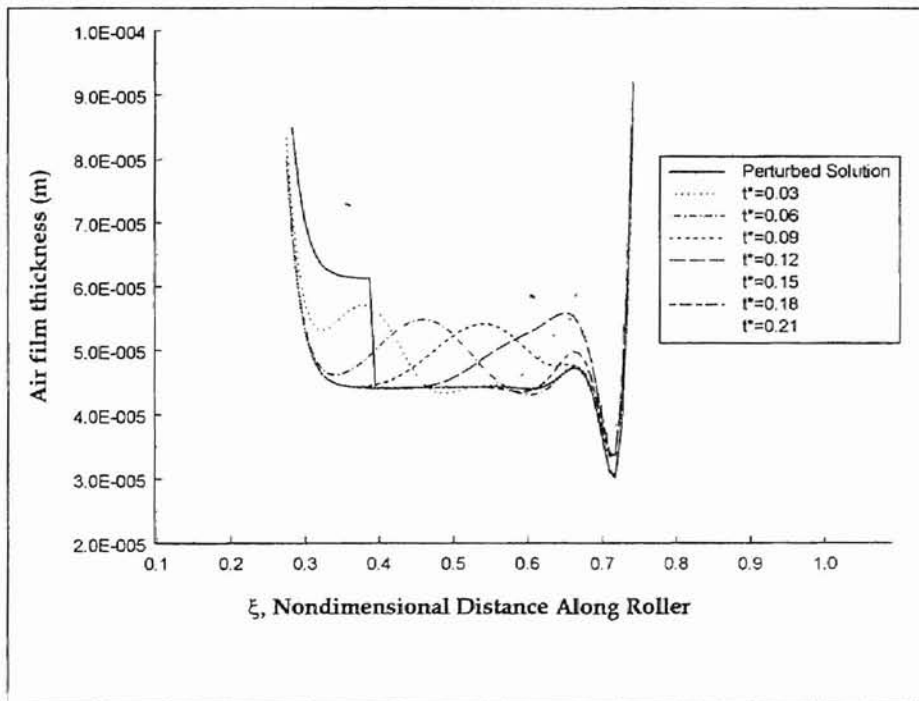


Figure 4.17: 20% Perturbation in Air Film Distribution Between  $\xi=0.23-0.39$   
 ( $V_w=5.08$  m/s,  $T_{init}/w=175.3$  N/m,  $m=0.0922$  kg/m<sup>2</sup>)

## **4.1.2 Permeable Web**

### **4.1.2.1 Constant Tension Case**

Here the solution was allowed to develop from an initial condition to a steady state solution (until it satisfies the convergence criterion). As we can observe from Figure 4.18, the central constant thickness region does not exist for this case, and the air film thickness distribution shows a lower value as compared to the non-porous counterpart with same operating condition. The reason is obviously the porosity through which air can escape. In other words it leads to a lower air film distribution. It can also be observed that the air film thickness decreases almost linearly in the central region. Kothari (1996) performed computations with permeable webs and showed that the slope of the central region increases with increasing permeability coefficient value. He has also showed that for very high permeability cases the central region might show some non-linear behavior. Another significant observation in this case is that the developing profile exhibits some oscillations during the initial stages of development, and entrance and exit regions exhibit almost the same behavior as the results obtained for the impermeable webs.

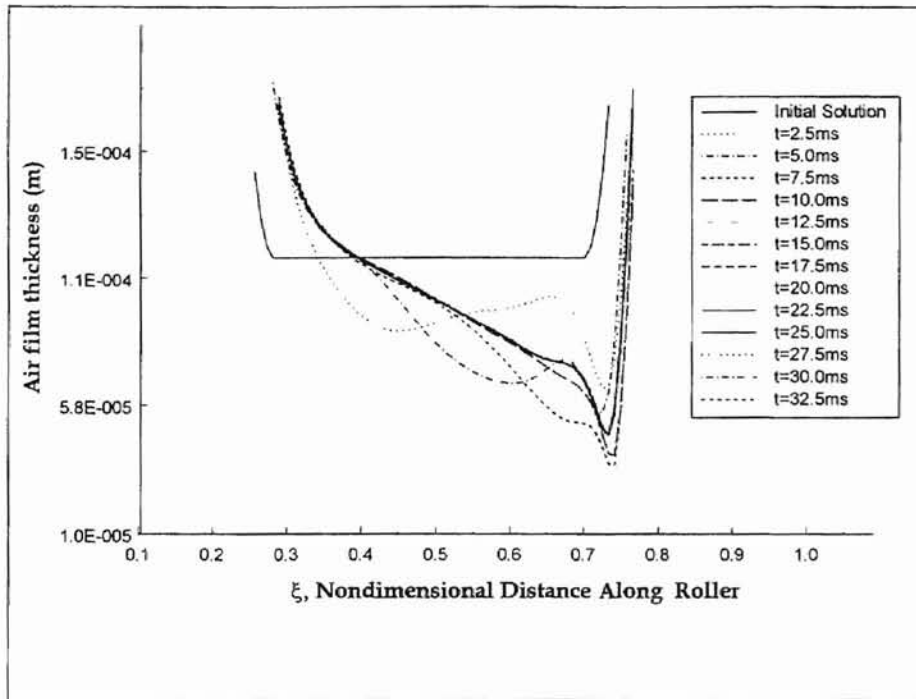


Figure 4.18: Transient Air film Thickness Profiles-Permeable Web  
 ( $V_w = 10.16$  m/s,  $T_{init}/w = 87.66$  N/m,  $m = 0.0922$  kg/m<sup>2</sup>,  $K = 3e-6$  (m<sup>3</sup>/s)/(m<sup>2</sup>-Pa))

#### 4.1.2.2 Effect of Step Change in Tension Case

Results for the step variation in tension for permeable webs are presented in this section. As we can observe from the initial steady state solution, it converges to a second steady state in an orderly manner. In Figure 4.19 (for  $V = 15.24$  m/s,  $T/w = 87.66$  N/m,  $m = 0.0254$  kg/m<sup>2</sup> a with 20% step) we can observe oscillations. The higher step case with a 50% step (Figure 4.20) reaches steady state slower as compared to the lower step case. It can also be observed that the range of oscillation is higher for the 50% step case as compared to that for the 20% step case.

As in the previous cases the oscillations are sinusoidal in nature. As time progressed the sinusoids died out and the solution settled down to new steady state solution. Higher initial tension cases with step increase in tension tended to diverge for the permeable web case. As there would be air leakage through the web, with higher tension, the pressure can collapse to the atmospheric value, which can lead to a zero thickness air film. The reason for this does not seem to be numerical instability and it seems that with increasing tension air film thickness can approach a value of zero. Hence the permeable webs have limitations which should be further explored to alleviate the problem of divergence of solution.



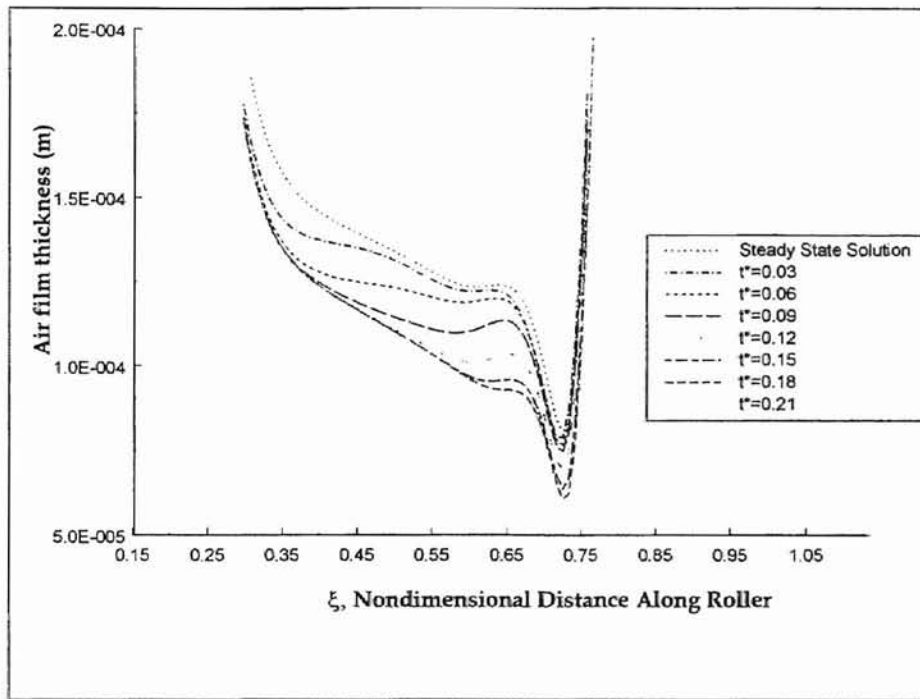


Figure 4.19: 20% Step Change in Tension  
 ( $V_w=15.24$  m/s,  $T_{init}/w=87.66$  N/m,  $m=0.0254$  kg/m<sup>2</sup>,  $K=3e-6$  (m<sup>3</sup>/s)/(m<sup>2</sup>-Pa)

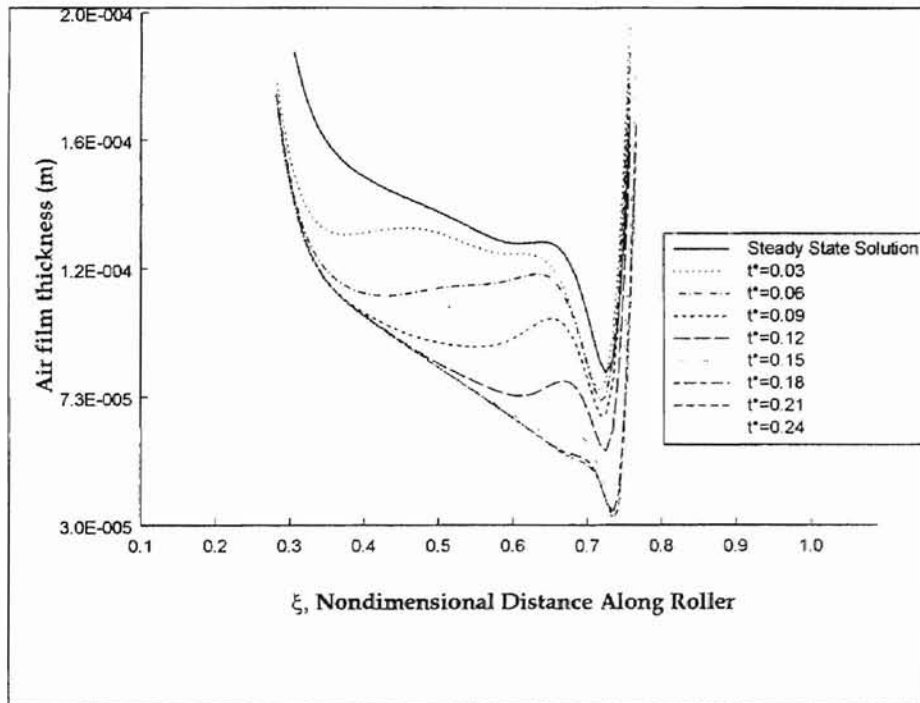


Figure 4.20: 50% Step Change in Tension  
 ( $V_w=15.24$  m/s,  $T_{init}/w=87.66$  N/m,  $m=0.0922$  kg/m<sup>2</sup>,  $K=3e-6$  (m<sup>3</sup>/s)/m<sup>2</sup>-Pa)

#### **4.1.2.3 Effect of Sinusoidal Fluctuation in Tension Case**

Sinusoidal oscillations in tension were applied in the manner described for the impermeable web cases. All of the cases described in impermeable web case could not be repeated for this case, as the convergence criterion could not be satisfied even after a very long time. A possible reason is that when tension is increased suddenly, air leakage through the permeable webs might allow the web to tighten against the roller (with a zero thickness air film). Hence sample results were given to show how it might be controlled. Only a limited number of computations were performed for the permeable webs. In Figure 4.21 with  $A = 0.2T$ , we can observe a lower magnitude of oscillation compared to the higher  $A = 0.5T$  (Figure 4.22). It also can be observed that the oscillations are higher for the higher amplitude ( $A$ ) case. Nevertheless all of the iterations settle down within one revolution of the roller. Even for this case it has been observed that the oscillations are sinusoidal in nature during the initial stages of development.

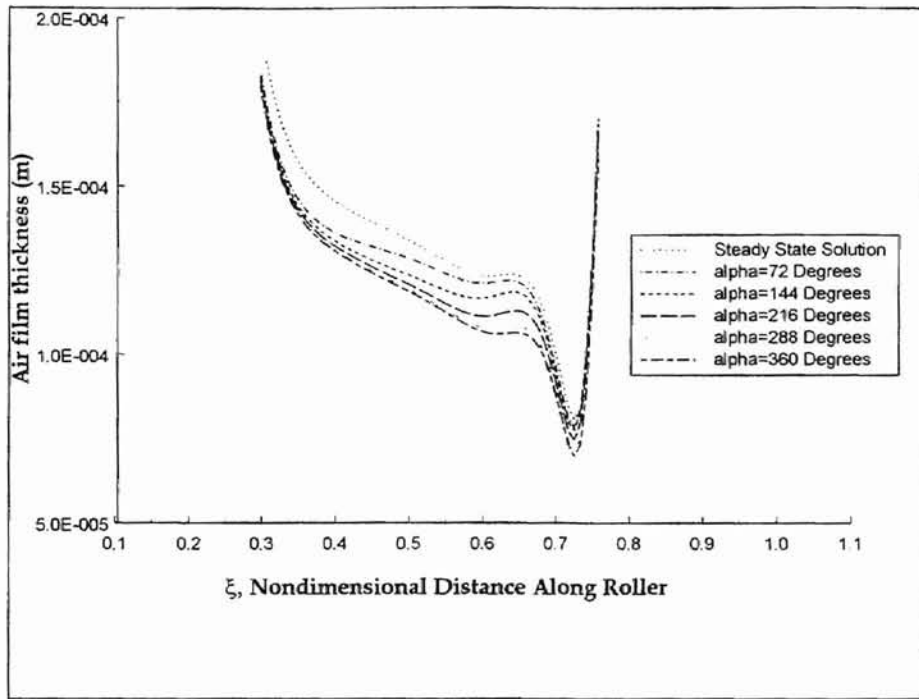


Figure 4.21: Sinusoidal Oscillation in Tension, ( $V_w=15.24$  m/s,  $T_{init}/w=87.66$  N/m,  $m=0.0254$  kg/m<sup>2</sup>,  $K=3e-6$  (m<sup>3</sup>/s)/m<sup>2</sup>-Pa,  $A=0.2T$ ,  $\omega=\omega_n$ )

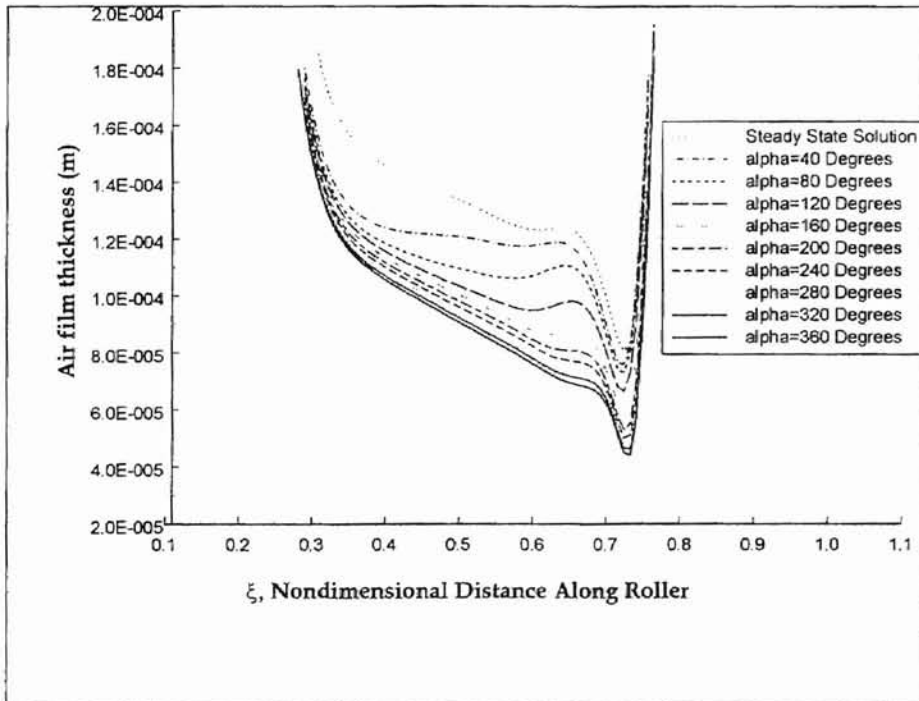


Figure 4.22: Sinusoidal Oscillation in Tension ( $V_w=15.24$  m/s,  $T_{init}/w=87.66$  N/m,  $m=0.0254$  kg/m<sup>2</sup>,  $K=3e-6$  (m<sup>3</sup>/s)/m<sup>2</sup>-Pa,  $A=0.5T$ ,  $\omega=\omega_n$ )

## **4.2 Comparison between Finite Stiffness and Zero Stiffness Models**

### **4.2.1 Impermeable web**

Much of the work which has been carried out in this area assumes perfect flexibility of the foil. This assumption leads to a powerful solution technique and hence the convergence is very fast as compared to a model incorporating stiffness of the web. It has been attempted to see how good the assumption of perfect flexibility is, and to show the difference in air film distribution for different values of web stiffness. Even though there was a significant difference in the air film profiles in some cases, they reach steady state at the same time. As the stiffness incorporated model leads to very time consuming computations, many results were not presented for this case. Hence let us see how the air film distribution look for different values of web stiffness. Figure 4.24 depicts a case with  $V=2.54$  m/s,  $m=0.0922$  kg/m<sup>2</sup>,  $T/w =263$  N/m and with various  $EI/w$  values. It can clearly be seen that with an increase in  $EI/w$  from 0.0 to  $5 \times 10^{-5}$  N-m, there is a significant difference observed in the entrance and exit regions of the air film profile. It can be noticed from the pressure profile that for different values of web stiffness an inlet undulation exists for the non-zero stiffness case, and the amplitude of the undulation increases with increasing rigidity. This inlet wave could not be observed for the zero stiffness case. A similar trend can be observed at the exit region also, but a zero stiffness case also shows an undulation. As a negative pressure gradient exists (Figure 4.25) at the entrance

region for the non-zero stiffness case, there should be an air film thickness which is less than the air film thickness in the central constant thickness region. This is the reason for the inlet wave existing in the region where the pressure gradient is negative. In the paper published by Hardie et al. (1988) a similar trend was shown. In their results it was shown that the magnitude of the inlet undulation increases with increasing stiffness value. They have also showed that the length of the central region decreases with increasing stiffness letting the undulation to grow. As far as the present study is concerned, further refinement is necessary to alleviate the dependency of the results on the time step chosen. In many cases the difference in the air film thickness between iterations converged close to the convergence criterion and then increased suddenly to make the solution diverge. Those situations were made to converge using a very small time step forcing the difference in the air film thickness between iterations to be a small value. Nevertheless, it can be concluded that incorporating stiffness has some significant effects on the air film profile.

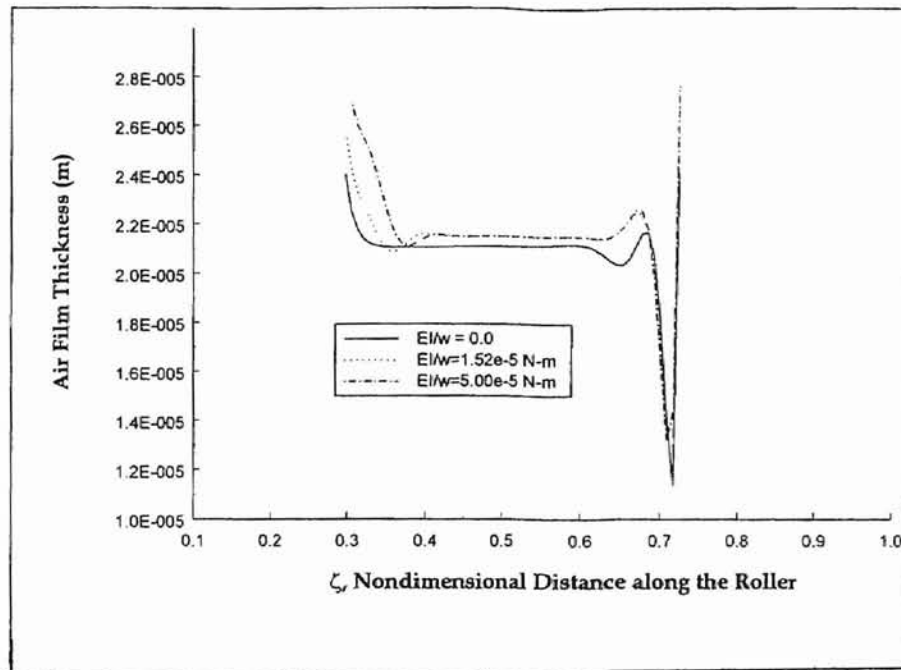


Figure 4.23: Comparison Between Webs with Different Web Stiffness Values  
 ( $V_w=2.54$  m/s,  $T/w=263$  N/m,  $m=0.0922$  kg/m<sup>2</sup>,  $EI/w=0, 1.5e-5$  N-m,  $5e-5$  N-m)

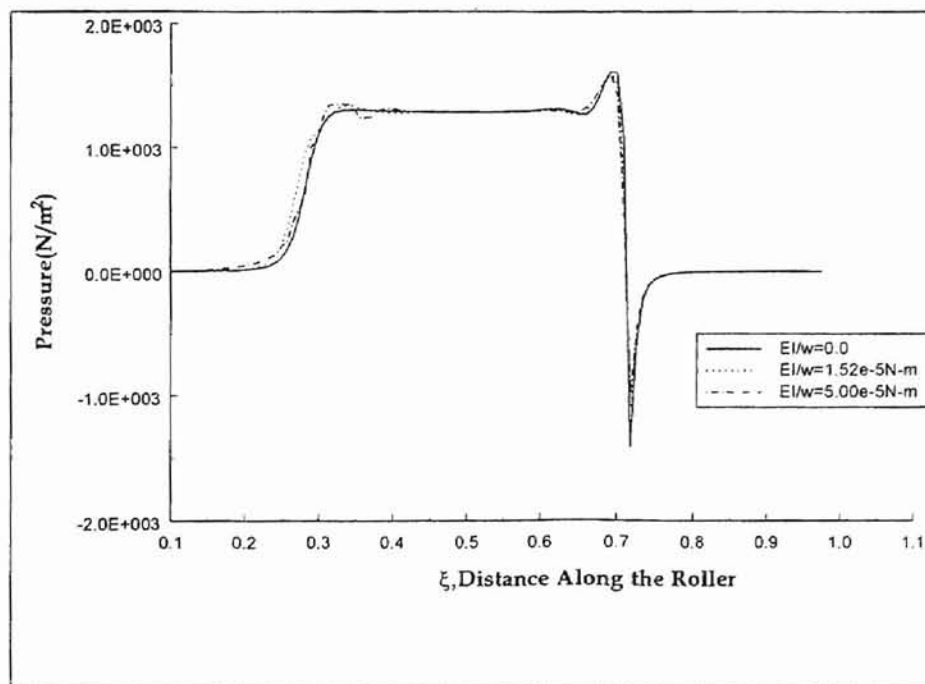


Figure 4.24: Comparison Between Webs with Different Stiffness Values  
 $V_w=10.16$  m/s,  $T/w=87.6$  N/m,  $m=0.0922$  kg/m<sup>2</sup>,  $EI/w=0, 1.5e-5$  N-m,  $5.0e-5$  N-m)

#### 4.4.2 Permeable Web

Computations performed for a permeable webs show significant differences in the entrance, central, exit regions of the air film thickness profile. Results were produced for a permeable webs with porosity values  $K=0.5 \times 10^{-5}$   $(\text{m}^3/\text{s})/(\text{m}^2\text{-Pa})$  (Figure 4.25) and  $K=0.3 \times 10^{-5}$   $(\text{m}^3/\text{s})/(\text{m}^2\text{-Pa})$  (Figure 4.26). We can observe a significant difference in the slope of the central region profiles. The higher permeability case shows a higher slope for the central region profile. Incorporating stiffness has a significant effect on the amplitude of the undulation at the entrance. The explanation for the occurrence of this non-intuitive undulation may be given if further computations are performed in this area. The time taken for the computations with the finite stiffness model was incredibly high, more than twenty fold compared to the perfectly flexible model. Hence it may be proposed that the results produced for the perfectly flexible web are an adequate approximation for design purposes for lower stiffness values of the web. However for very high stiffness values of the web, a significant difference in the air film thickness is expected, and a finite stiffness model would be essential.

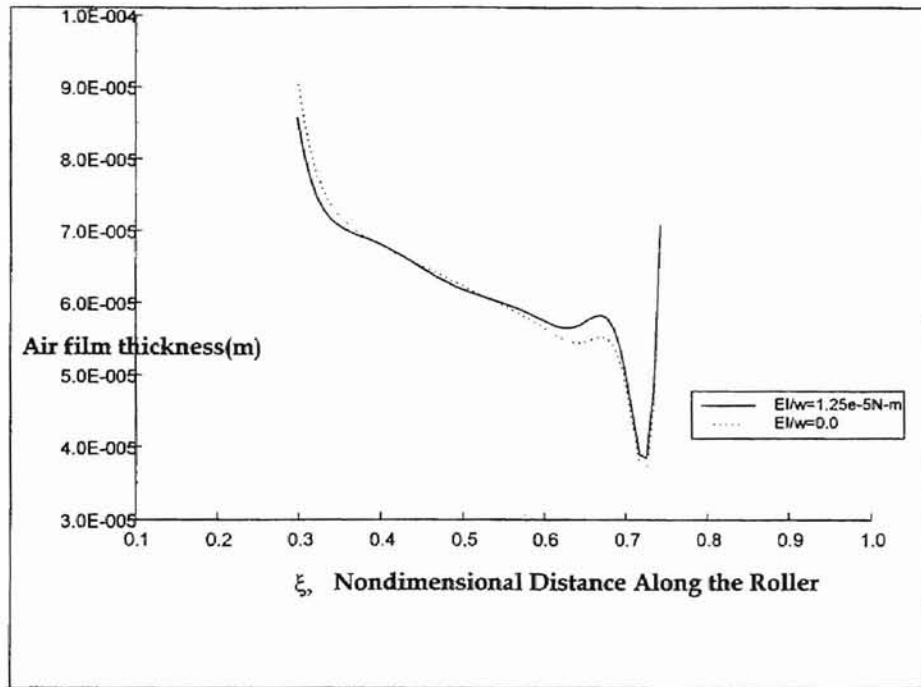


Figure 4.25: Comparison Between Finite Stiffness and Zero Stiffness Models for Permeable Web ( $V_w=10.16$  m/s,  $T=165.33$  N/m,  $m=0.0922$  kg/m<sup>2</sup>,  $K=5e-6$  (m<sup>3</sup>/s)/(m<sup>2</sup>-Pa))

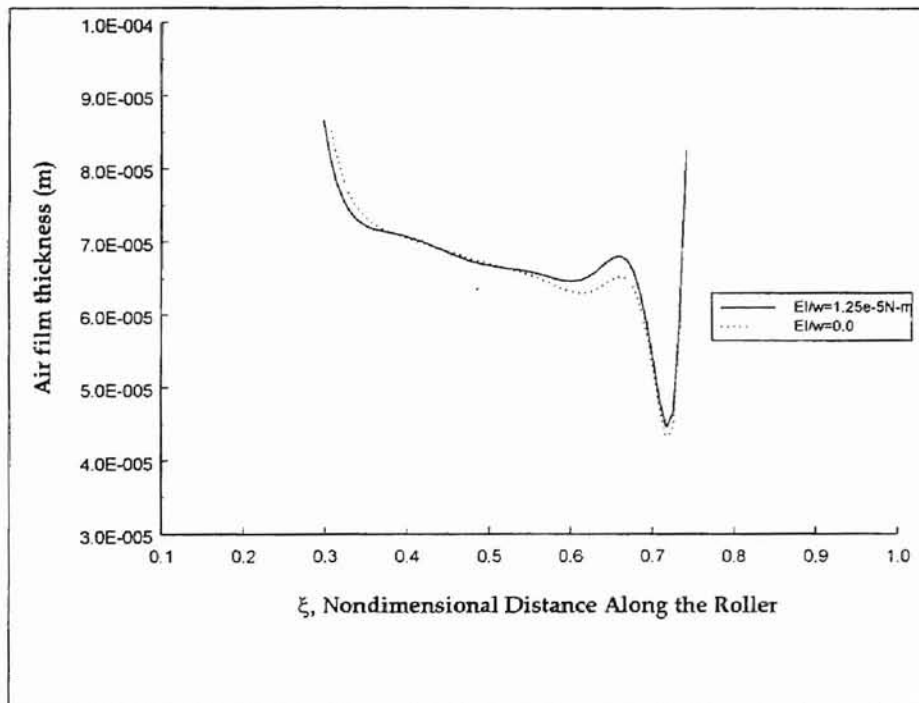


Figure 4.26: Comparison between finite stiffness and Zero Stiffness Models for Permeable Web ( $V_w=10.16$  m/s,  $T=165.33$  N/m,  $m=0.0922$  kg/m<sup>2</sup>,  $K=3e-6$  (m<sup>3</sup>/s)/(m<sup>2</sup>-Pa))



### **4.3 Comparison of Tension Transients - Step Variation**

By comparing Figures 4.27 (without incorporating stiffness) and 4.28 (with stiffness), it can be seen that the difference in air film distribution for the tension transient is not significant after incorporating the stiffness of the web. Hence it has been decided that the effort and time taken for the computations is very high for the difference observed for these cases. It takes approximately 20 minutes for the zero stiffness model to converge for the step change in tension case, and it takes approximately 8 hours for the finite stiffness model to converge. Due to this difference in computational time, it has been decided to suspend the work on tension transients. Here the solution algorithm which was used was developed for a complete matrix with non-zero elements, but in this case as we are seeking solution for a diagonal matrix, it takes a longer time. In some cases first steady state for the initial tension was obtained and the solution diverged once the step increase in tension was applied. Time steps could not be reduced as we wish because, reducing time step would lead to further increase in time to obtain a converged solution. A more efficient solution algorithm is needed to continue study of this topic. Hence only one case of the step change case has been presented here.

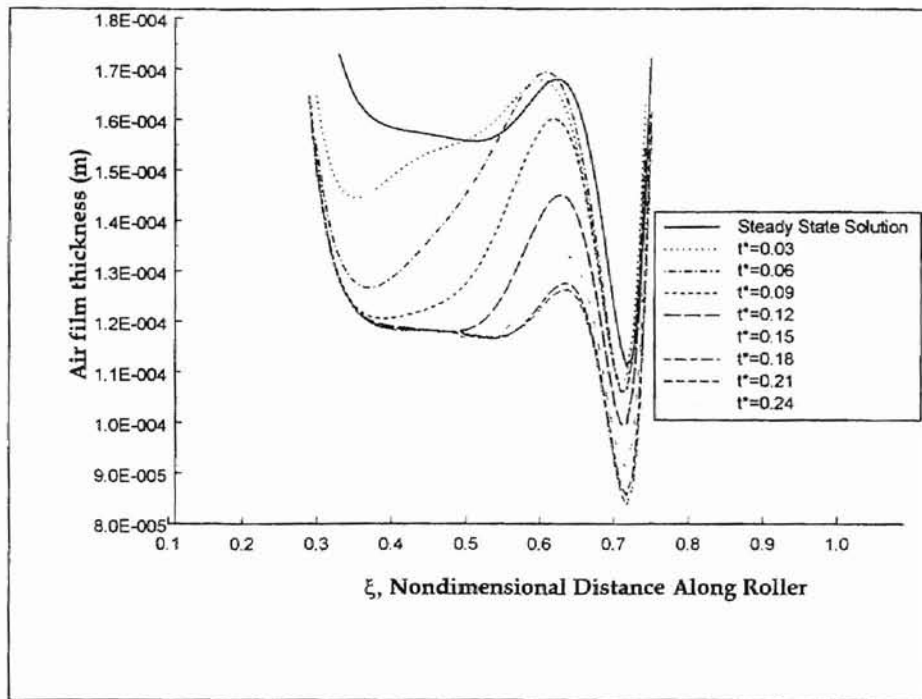


Figure 4. 27: Step change in Tension for Perfectly Flexible Web ( $V_w=15.24$  m/s,  $T_{init}=87.66$  N/m,  $m=0.0254$  kg/m<sup>2</sup>, with 50% Step change)

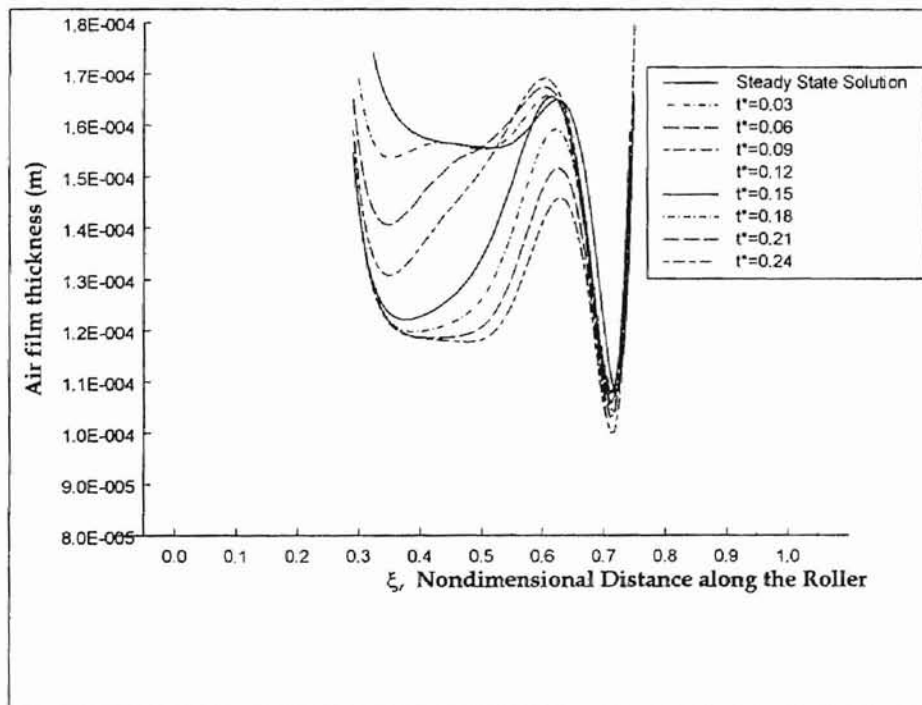


Figure 4. 28: Step Change in Tension for a Web with  $EI/w=1.52e^{-5}$  N-m ( $V_w=15.24$  m/s,  $T_{init}=87.66$  N/m,  $m=0.0254$  kg/m<sup>2</sup>, with 50% Step change)

## SUMMARY OF THE CASES CONSIDERED FOR THE PRESENT STUDY

Speed of the web (m/s)	Tension/width applied (N/m)	Permeability of the web ( $\text{m}^3\text{s}^{-1}/\text{m}^2\text{-Pa}$ )	Stiffness of the Web (N-m)	Mass of the web per unit area ( $\text{kg}/\text{m}^2$ )
2.54	263	0.0	$1.5 \times 10^{-5}$	0.0922
2.54	263	0.0	$5 \times 10^{-5}$	0.0922
10.16	165.3	$3 \times 10^{-6}$	$1.25 \times 10^{-5}$	0.0922
10.16	165.33	$5 \times 10^{-6}$	$1.25 \times 10^{-5}$	0.0922
2.54	273	0.0	0.0	0.0207
10.16	273	0.0	0.0	0.0922
10.16	87.6	$3 \times 10^{-6}$	0.0	0.0922

Table 4.1: Cases Considered with Constant Tension

Speed of the web (m/s)	Tension/width applied (N/m)	Height of the perturbation	Permeability of the web ( $\text{m}^3\text{s}^{-1}/\text{m}^2\text{-Pa}$ )	Stiffness of the Web (N-m)	Mass of the web per unit area ( $\text{kg}/\text{m}^2$ )
15.24	175.3	20%	0.0	0.0	0.0922
2.54	175.3	30%	0.0	0.0	0.0922
5.08	175.3	30%	0.0	0.0	0.0922
5.08	175.3	20%	0.0	0.0	0.0922

Table 4.2: Cases Considered with Perturbation in Air Film Thickness

Speed of the web (m/s)	Tension/width applied (N/m)	Height of the step	Permeability of the web ( $\text{m}^3\text{s}^{-1}/\text{m}^2\text{-Pa}$ )	Stiffness of the Web (N-m)	Mass of the web per unit area ( $\text{kg}/\text{m}^2$ )
15.24	87.6	20%	$3 \times 10^{-6}$	0.0	0.0254
15.24	87.6	50%	$3 \times 10^{-6}$	0.0	0.0254
15.24	87.6	20%	0.0	0.0	0.0254
15.24	87.6	50%	0.0	$1.5 \times 10^{-5}$	0.0254
15.24	87.6	50%	0.0	0.0	0.0254
15.24	263	20%	0.0	0.0	0.0254
15.24	263	50%	0.0	0.0	0.0254
15.24	263	20%	0.0	0.0	0.0922
15.24	263	50%	0.0	0.0	0.0922

Table 4.3: Cases Considered with Step Change in Tension

Speed of the web (m/s)	Tension /width applied (N/m)	Amplitude of Oscillation	Frequency of Oscillation (rad/s)	Permeability of the web ( $\text{m}^3\text{s}^{-1}/\text{m}^2\text{-Pa}$ )	Stiffness of the Web (N-m)	Mass of the web per unit area ( $\text{kg}/\text{m}^2$ )
15.24	87.6	50%	$\omega_n$	0.0	0.0	0.0254
15.24	87.6	50%	$2\omega_n$	0.0	0.0	0.0254
15.24	263	50%	$\omega_n$	0.0	0.0	0.0254
15.24	263	50%	$\omega_n$	0.0	0.0	0.0922
15.24	87.6	20%	$\omega_n$	$3 \times 10^{-6}$	0.0	0.0254
15.24	87.6	50%	$\omega_n$	$3 \times 10^{-6}$	0.0	0.0254

Table 4.4: Cases Considered with Sinusoidal Oscillation in Tension

## CHAPTER 5

### CONCLUSIONS AND RECOMMENDATIONS

The following conclusions can be drawn from the present analysis:

- 1) For the step variation in tension case, there were no overshoots or touch downs observed for the cases considered. Hence it can be said that even with a 50% increase in the tension, the operation would not be affected for the range of conditions studied (i.e. there would not be any harm to the roller or web). We can, however, observe an increase in the air film thickness in the exit region for the developing profile. We can attribute the reason to be mass conservation. When there is a sudden increase in the tension, it tends to reduce the air film. Due to continuity, reduction in one side should be balanced by an increase in the other side (we assume an infinitely wide web hence there is no side leakage). But this trend cannot be observed for a permeable web. As the tension is increased, the air would escape through the porosities. Hence we could not observe any increase in air film thickness for permeable webs.
- 2) For the sinusoidal fluctuation in tension case, we observe similar patterns, but also we can notice that the air film oscillations increase with the oscillation of the tension
- 3) For the case with perturbation in air film thickness introduced outside the wrap region, it can be seen that the pattern is almost the same as that for the

step tension case, but for this case it settles down to the previous steady state solution. It has been noticed that the propagation of the disturbance is a traveling wave which travels to the exit and then dies out.

- 4) It can be observed that incorporating stiffness has a noticeable impact on the air film thickness distribution, especially in the entrance and exit regions. Hence it can be said that preliminary calculations can be performed for initial design purposes, and then the results can be fine tuned with the stiffness incorporated using the steady state solution from the zero stiffness model as the initial guess for the finite stiffness model, enabling faster convergence.
- 5) It was noted that incorporating stiffness of the web for the permeable web does not seem to change the central region air film thickness very much. It definitely changes the entrance and exit regions.
- 6) It was important to note that the step/sinusoidal variation in tension for the permeable webs was not promising as the solution tended to diverge for some cases. For some of the cases converged solution could be obtained with a smaller time step. Perturbation in the air film thickness for impermeable webs shows that the small disturbances that are introduced can be tolerated and the initial steady state solution would be established within one revolution of the roller. Perturbations in the air films could not be tolerated for the permeable webs as even a single solution could not be obtained for this case. The reason can be attributed to occurrence of zero air film thickness which might take place when there is a sudden perturbation is introduced.

Another reason that can be attributed to this problem is the numerical instability of the solution technique that has been adapted.

The following recommendations have been proposed to extend this work beyond the current accomplishments.

- 1) The finite stiffness model takes a very long time to converge, a faster solution technique is needed to have this method used for all of the computations. It can also be seen that how good is the idea of starting the iterations from an initial guess produced by the fast converging zero stiffness model. If this works out very well, this method can be used as a supplement to the zero stiffness model.
- 2) An experimental validation is very much needed for the results produced in this study.
- 3) It is also important to see this results change when a finite width/side leakage assumption is made. It has already been shown that by assuming infinite width of the web, flying-off of the web was observed for an impermeable web. Hence it is important to see the effect of this.
- 4) A better solution methodology can be devised to solve the finite stiffness model. A penta- diagonal solver can be used to solve this problem faster and more effectively.
- 5) Computations can be extended to incorporate rough rollers/rollers-with-grooves to determine the effects of grooved rollers on improving traction.



This might demand a two-dimensional analysis which would be a more detailed and challenging task.

## REFERENCES

1. Adams, G.G., "A Novel Approach to the Foil Bearing Problem," *Tribology and Mechanics of Magnetic Storage Systems, ASLE Special Publication 22*, pp. 1-7, 1987.
2. Blok, H., and Van Rossum, J.J., "The Foil Bearing - A New Departure in Hydrodynamic Lubrication," *Lubrication Engineering*, Vol. 9, pp. 316-320, 1953.
3. Barlow, E.J. "Derivation of Governing Equations for Self-Acting Foil Bearings," *Trans. of ASME, Journal of Lubrication Technology*, Vol. 89, pp. 334-340, 1967.
4. Barnum, T.B., and Elrod, H. G., Jr., "A Theoretical Study of the Dynamic Behavior of Foil Bearing," *Journal of Lubrication Technology, Trans. of the ASME*, pp. 133-142, 1971.
5. Baugh, E., and Talke, F., "The Tape Head Interface a Critical Review and Recent Results," *STLE Tribology Transactions*, Vol. 39, No. 2, pp. 306-313, 1996.
6. Baumeister, H.K., "Nominal Clearances of the Foil Bearing," *IBM J. of Res. and Dev.*, Vol. 7, No. 2, pp. 153-154, April, 1963.
7. Bhushan, B., and Tonder, K., "Roughness-Induced Shear and Squeeze-Film Effects in Magnetic Recording -Part I & II," *Trans. of ASME, Journal of Tribology*, Vol. 111, pp. 220-237, 1989.
8. Bhushan, B., *Tribology and Mechanics of Magnetic Storage Devices*, Springer-Verlag, New York, Chapter 9, 1990.
9. Brewen, A.T., Benson, R.C., and Piarulli, V.J., "A Simple Procedure for Determining Elastohydrodynamic Equilibrium and Stability of a Flexible Tape Flying Over a Recording Head," *Tribology and Magnetic Storage Systems*, Vol. II, *ASLE Special Publication SP-19*, editors, S. Bhushan and N.S. Eiss Jr., pp. 43-51, 1985.
10. Chang, Y. B., "An Experimental and Analytical Study of Web Flutter ", *Ph.D Thesis*, Oklahoma State University, Stillwater, 1990.
14. Connolly, D., and Brock, G.W., "The Design of an In-contact Bi-directional Magnetic Tape Recording Head with Beveled Transverse Slots," *Advances in*

- Information Storage and Processing Systems, ASME, ISPS-Vol. 1, pp. 313-318, 1995.
15. Dais, J.L., and Barnum, T.B., "Geometrically Irregular Foil Bearing," *ASME Journal of Lubrication Technology*, Vol. 96, pp. 224-227, 1974.
  16. Daly, D.A., "Factors Controlling Traction Between Webs and Their Carrying Rolls," *TAPPI Journal*, pp. 88A-90A, Vol. 48, September, 1965.
  17. Ducotey, K.S., and Good, J.K., "The Effect of Web Permeability and Side Leakage on the Air Film Height Between a Roller and Web," *Submitted for Review for Publication in the Journal of Tribology*, January, 1996.
  18. Eshel, A., "Analytical Study of the Self-Acting Foil Bearing," Ph.D. Dissertation, Department of Mechanical Engineering, Columbia University, New York, May, 1966.
  19. Eshel, A., "Compressibility Effects on the Infinitely Wide, Perfectly Flexible Foil Bearing," *ASME Journal of Lubrication Technology*, Vol. 90, pp. 221-225, 1968.
  20. Eshel, A., "The Propagation of Disturbances in the Infinitely Wide, Perfectly Flexible Foil Bearing," *ASME Journal of Lubrication Technology*, Vol. 91, pp. 120-125, 1969.
  21. Eshel, A., "On Controlling the Film Thickness in Self-Acting Foil Bearings," *ASME Journal of Lubrication Technology*, Vol. 92, pp. 359-362, 1970.
  22. Eshel, A., "On Fluid Inertia Effects in Infinitely Wide Foil Bearings," *ASME Journal of Lubrication Technology*, Vol. 92, pp. 490-494, 1970.
  23. Eshel, A., "Reduction of Air Films in Magnetic Recording by External Air Pressure," *ASME Journal of Lubrication Technology*, Vol. 96, pp. 247-249, 1974.
  24. Eshel, A., and Elrod, H.G., Jr., "The Theory of the Infinitely Wide, Perfectly Flexible, Self-Acting Foil Bearing," *ASME Journal of Basic Engineering*, Vol. 87, No. 4, pp. 831-836, 1965.
  25. Eshel, A., and Lowe, A.R., "Experimental and Theoretical Investigation of Head to Tape Separation in Magnetic Recording," *IEEE Trans. on Magnetics*, Vol. MAG-9, No. 4, pp. 683-688, 1973.

26. Eshel, A., and Wildmann, M., "Dynamic Behavior of a Foil in the Presence of a Lubricating Film," *ASME Journal of Applied Mechanics*, Vol. 35, pp. 242-247, 1968.
27. Forsythe, G.E., and Wasow, W.R., *Finite Difference Methods for Partial Differential Equations*, John Wiley & Sons, Inc., New York, pp. 103-105, 1960.
28. Granzow, G.D., "An Improved Foil Bearing Solution," *M.S. Thesis*, Department of Mechanical Engineering, University of New Mexico, 1980.
29. Granzow, G.D., and Leebeck, A.O., "An Improved One-Dimensional Foil Bearing Solution," *Tribology and Mechanics of Magnetic Storage Systems, ASLE Special Publication 16*, pp. 54-58, 1984.
30. Gross, W.A., Matsch, L.A., Castelli, V., Eshel, A., Vohr, J.H., and Wildman, M., *Fluid Film Lubrication*, John Wiley & Sons, Inc., NY, 1980.
31. Hardie, C.E., and Mc Ettles, C.M., "The Analysis of Self Acting Flexible Foil Slider Bearing," *Transactions of ASME, Journal of Tribology*, Vol. 110, pp. 134-138, 1988.
32. Hashemi, S.M., and Roylance, B.J., "Analysis of an Oscillatory Oil Squeeze Film Including Effects of Fluid Inertia," *Tribology Trans.*, Vol. 32, pp. 461-468, 1989.
33. Hashimoto, H., "Viscoelastic Squeeze Film Characteristics with Inertia Effects Between Two Parallel Circular Plates Under Sinusoidal Motion," *Trans. of ASME, Journal of Tribology*, Vol. 116, pp. 161-166, 1994.
34. Hashimoto, H., "Estimation of Air Film Thickness between Moving Webs and Guide Rollers", *Proceedings of the Fourth International Conference on Web Handling*, Web Handling Research Center, Stillwater, Oklahoma, June 1-4, 1997.
35. Heinrich, J.C., and Connolly, D., "Three-Dimensional Finite Element Analysis of Self-Acting Foil Bearing," *Computer Methods in Applied Mechanics and Engineering*, Vol. 100, pp. 31-43, 1992.
36. Heinrich, J.C., and Wadhwa, S.K., "Analysis of Self-Acting Foil Bearings: A Finite Element Approach," *Tribology and Mechanics of Magnetic Storage Systems*, Vol. III, editors, B. Bhushan and N.J. Eiss, Jr., pp. 152-159, 1986.

37. Jones, A.F., and Wilson S.D., "On the Failure of Lubrication Theory in Squeezing Flows," *Trans. of ASME, Journal of Lubrication. Tech.*, Vol. 97, pp. 101-104, 1975.
38. Knox, K.L., and Sweeney, T.L., "Fluid Effects Associated with Web Handling," *Ind. Eng. Chem. Process, Design, Dev.*, Vol. 10, pp. 201-205, 1971.
39. Kothari, S.K., "Computations of Air Films between Moving Webs and Support Rollers," *M.S Thesis*, School of Mechanical and Aerospace Engineering, Oklahoma State University, Stillwater, 1996.
40. Lilley, D.G., *Computational Fluid Dynamics*, Vol. 1, Lilley and Associates, Stillwater, OK., 1992.
41. Press, W.H., Teukolsky, S. A., Vetterling, W.T., and Flannery, B. P., *Numerical Recipes in Fortran*, Cambridge University Press, Second Edition, 1996.
42. Muftu, S., and Benson, R.C., "Modeling the Transport of Paper Webs Including the Paper Permeability Effects," *Advances in Information Storage and Processing Systems*, Vol. 1, pp. 247-258, 1995.
43. Randall, W., and Weinbaum, S., "On the Development of Fluid Trapping Beneath Deformable Fluid-Cell Membranes," *Journal of Fluid Mech.*, Vol. 121, pp. 315-343, 1982.
44. Riddiford, A.W., "Air Flow Between a Paper and a Dryer Surface," *TAPPI Journal*, Vol. 52, No. 5, pp. 939-942, 1969a.
45. Riddiford, A.W., "Air Entrainment Between an Impermeable Paper Web and Dryer Surface of Infinite Width," *Pulp and Paper Magazine of Canada*, pp. 53-57, February, 7, 1969b.
46. Rongen, P.M.J., "On Numerical Solution of the Instationary 2D Foil Bearing Problem," *Tribology and Mechanics of Magnetic Storage Systems*, ASLE Special Publication 26, pp. 130-138, 1989.
47. Satheesh, K., Kothari, S.K., Chambers, F.W., "Computations of Air Films and Pressures Between Moving Webs and Rollers for Steady and Unsteady Operating Conditions", *Proceedings of the Fourth International Conference on Web Handling*, Web Handling Research Center, Stillwater, Oklahoma, June 1-4, 1997.

48. Smith, D.P., and Von Behren, R.A., "Squeeze-Film Analysis of Tape Winding Effects in Data Cartridge," *Tribology and Magnetic Storage Systems*, Vol. VI, *STLE Special Publication SP-26*, editors, B. Bhushan and N.S. Eiss, Jr., pp. 88-92, 1989.
49. Stahl, K.J., White, J.W., and Deckert, K.L., "Dynamic Response of Self-Acting Foil Bearings," *IBM J. Res. Development*, Vol. 18, pp. 513-520, 1974.
50. Swain, R., Baugh, E., and Talke, F., "Two-Dimensional Algorithms for Determination of Head Tape Spacing from a Single Fringe Pattern," *Advances in Information Storage and Processing Systems*, Vol. 1, pp. 309-312, 1995.
51. Tanaka, K., "Analytical and Experimental Study of Tape Spacing for Magnetic Tape Unit - Effects of Tape Bending Rigidity, Gas Compressibility, and Molecular Mean Free Path," *Tribology and Mechanics of Magnetic Storage Systems*, *ASLE Special Publication 19*, pp. 72-79, 1985.
52. Tanaka, K., Oura, M., and Fujii, M., "Tape Spacing Characteristics of Cylindrical Heads with Flat Surfaces for Use in Magnetic Tape Units," *Tribology and Mechanics of Magnetic Storage Systems*, Vol. III, editors, B. Bhushan and N.J. Eiss, Jr., pp. 130-137, 1986.
53. Tichy, J.A., and Winer, W.O., "Inertial Considerations in Parallel Circular Squeeze Film Bearings," *Trans. of ASME, Journal of Lubrication. Tech.*, Vol. 92, pp. 588-592, 1970.
54. Von Behren, R.A., and Smith, D.P., "Squeeze-Film Analysis of Tape Winding Effects in Data Cartridge," *Tribology and Mechanics of Magnetic Storage Systems*, *ASLE Special Publication 26*, pp. 88-92, 1989.
55. Watanabe, Y., and Sueoka, Y., "Evaluation of Air Entrainment Between a Paper Web and a Roller," *Presented at Technical Association of the Graphic Arts, Kansas City, Mo.*, 1990.
56. Weinbaum, S., Lawrence, C.J., and Kuang, Y., "The Inertial Draining of a Fluid Layer Between Parallel Plates with a Constant Normal Force - Part I," *Journal of Fluid Mech.* Vol. 156, pp. 463-477, 1985.
57. Weinbaum, S., Lawrence, C.J., and Kuang, Y., "The Inertial Draining of a Fluid Layer Between Parallel Plates with a Constant Normal Force - Part II," *Journal of Fluid Mech.* Vol. 156, pp. 479-494, 1985.

58. Yamauchi, T., Murakami, K., and Inamura, R., "The Air Permeability of Paper Related to the Porous Structure," *Japan TAPPI Journal*, Vol. 30, No. 5, pp. 273-280, 1976.

APPENDIX A

DERIVATION OF GOVERNING EQUATIONS



The velocity profile of the air entrained between the web and the roller surface is

(given by eq. 3.6) -

$$V = \frac{1}{2\mu} \frac{\partial p}{\partial x} y^2 + C_1 y + C_2 \quad (1)$$

Thus.

$$\frac{\partial V}{\partial y} = \frac{1}{\mu} \frac{\partial p}{\partial x} y + C_1 \quad (2)$$

using the Boundary Conditions-

$$V \Big|_{y=0} = \lambda \frac{\partial V}{\partial y} \Big|_{y=0}$$

and,

$$V \Big|_{y=h} = V - \lambda \frac{\partial V}{\partial y} \Big|_{y=h}$$

Using the first boundary condition in equation (1) and (2) yields-

$$C_2 = \lambda C_1$$

The second boundary condition yields,

$$\frac{1}{2\mu} \frac{\partial p}{\partial x} h^2 + C_1 h + C_2 = V - \lambda \left( \frac{1}{\mu} \frac{\partial p}{\partial x} h + C_1 \right)$$

$$\Rightarrow \frac{1}{2\mu} \frac{\partial p}{\partial x} h^2 + C_1 h + \lambda C_1 = V - \left( \frac{\lambda}{\mu} \frac{\partial p}{\partial x} h + \lambda C_1 \right)$$

$$\Rightarrow C_1 (2\lambda + h) = V - \frac{\lambda}{\mu} \frac{\partial p}{\partial x} h - \frac{1}{2\mu} \frac{\partial p}{\partial x} h^2$$

$$\Rightarrow C_1 = \frac{V - \frac{h}{2\mu}(h+2\lambda)\frac{\partial p}{\partial x}}{(h+2\lambda)}$$

Thus,

$$C_2 = \lambda C_1$$

Now,

$$Q = \rho \int_{y=0}^{y=h} \left( \frac{1}{2\mu} \frac{\partial p}{\partial x} y^2 + C_1 y + C_2 \right) dy$$

$$Q = \rho \left( \frac{1}{6\mu} \frac{\partial p}{\partial x} h^3 + C_1 \frac{h^2}{2} + C_2 h \right)$$

Substituting  $C_2 = \lambda C_1$  yields,

$$Q = \rho \left( \frac{1}{6\mu} \frac{\partial p}{\partial x} h^3 + C_1 h(h+2\lambda) \right)$$

Substituting for  $C_1$  yields,

$$= \rho \left( \frac{1}{6\mu} \frac{\partial p}{\partial x} h^3 + \frac{h}{2} \left( V - \frac{h}{2\mu}(h+2\lambda)\frac{\partial p}{\partial x} \right) \right)$$

Simplifying the above equation yields,

$$Q = \rho \left( \frac{Vh}{2} - \frac{1}{12\mu} \frac{\partial p}{\partial x} h^3 - \frac{1}{2\mu} \frac{\partial p}{\partial x} h^2 \lambda \right)$$

Let us see how this equation would get modified when no slip assumption is made,

The velocity equation is given by

$$\Rightarrow C_1 = \frac{V - \frac{h}{2\mu}(h+2\lambda)\frac{\partial\phi}{\partial x}}{(h+2\lambda)}$$

Thus,

$$C_2 = \lambda C_1$$

Now,

$$Q = \rho \int_{y=0}^{y=h} \left( \frac{1}{2\mu} \frac{\partial\phi}{\partial x} y^2 + C_1 y + C_2 \right) dy$$

$$Q = \rho \left( \frac{1}{6\mu} \frac{\partial\phi}{\partial x} h^3 + C_1 \frac{h^2}{2} + C_2 h \right)$$

Substituting  $C_2 = \lambda C_1$  yields,

$$Q = \rho \left( \frac{1}{6\mu} \frac{\partial\phi}{\partial x} h^3 + C_1 h(h+2\lambda) \right)$$

Substituting for  $C_1$  yields,

$$= \rho \left( \frac{1}{6\mu} \frac{\partial\phi}{\partial x} h^3 + \frac{h}{2} \left( V - \frac{h}{2\mu}(h+2\lambda)\frac{\partial\phi}{\partial x} \right) \right)$$

Simplifying the above equation yields,

$$Q = \rho \left( \frac{Vh}{2} - \frac{1}{12\mu} \frac{\partial\phi}{\partial x} h^3 - \frac{1}{2\mu} \frac{\partial\phi}{\partial x} h^2 \lambda \right)$$

Let us see how this equation would get modified when no slip assumption is made,

The velocity equation is given by

$$V = \frac{1}{2\mu} \frac{\partial \mathcal{P}}{\partial x} y^2 + C_1 y + C_2 \quad (4)$$

for the case of rotating roller and moving web the boundary conditions would be,

$$V \Big|_{y=0} = V_R$$

and,

$$V \Big|_{y=h} = V_w$$

Where  $V_R$  is the roller surface velocity and  $V_w$  is the web velocity. Substituting the above two conditions in equation (4) yields,

$$V_R = C_2$$

and,

$$V_w = \frac{1}{2\mu} \frac{\partial \mathcal{P}}{\partial x} h^2 + C_1 h + C_2$$

$$\Rightarrow V_w = \frac{1}{2\mu} \frac{\partial \mathcal{P}}{\partial x} h^2 + C_1 h + V_R$$

Solving yields,

$$C_1 = \frac{\left( V_w - V_R - \frac{1}{2\mu} \frac{\partial \mathcal{P}}{\partial x} h^2 \right)}{h} \text{ and,}$$

$$C_2 = V_R$$

Now,

$$Q = \rho \int_{y=0}^{y=h} \left( \frac{1}{2\mu} \frac{\partial \mathcal{P}}{\partial x} y^2 + C_1 y + C_2 \right) dy$$

$$Q = \rho \left( \frac{1}{6\mu} \frac{\partial p}{\partial x} h^3 + C_1 \frac{h^2}{2} + C_2 h \right)$$

Substituting for  $C_1$  and  $C_2$  yields,

$$Q = \rho \left[ \frac{1}{6\mu} \frac{\partial p}{\partial x} h^3 + \left( \frac{V_w - V_R - \frac{1}{2\mu} \frac{\partial p}{\partial x} h^2}{h} \right) \frac{h^2}{2} + V_R h \right]$$

Simplifying yields,

$$Q = \rho \left[ \frac{h}{2} (V_R + V_w) - \frac{1}{12\mu} \frac{\partial p}{\partial x} h^3 \right]$$

For the permeable web we can say,

$$Q_{in} - Q_{out} = Q_{leakage} + \frac{\partial}{\partial t} (\rho h \Delta x)$$

$$Q_{in} - Q_{out} = \rho V_t (\Delta x) + \frac{\partial}{\partial t} (\rho h \Delta x)$$

where,

$V_t$  = Velocity of air through the permeable web, and

$\rho$  = air density.

This can be simplified as,

$$-\frac{\partial Q}{\partial x} = \frac{\partial}{\partial t} (\rho h) + \rho V_t$$

Substituting for  $Q$  and using the ideal gas relation at constant temperature and

bearing that  $\rho \propto p$  yields,

$$-\frac{\partial}{\partial x} \left\{ p \left( \frac{h}{2} (V_R + V_w) - \frac{1}{12\mu} \frac{\partial p}{\partial x} h^3 \right) \right\} = \frac{\partial}{\partial t} (ph) + pV_t$$

This can be simplified as the given differential equation,

$$(h^3 pp_x)_x = 6\mu(V_R + V_w)(ph)_x + 12\mu(ph)_t + 12\mu pV_t$$

Considering the slip flow case, the term  $6\lambda_a p_a (h^2 p_x)_x$  as in case derived for Impermeable web in the previous derivation will be included refining the equation to-

$$(h^3 pp_x)_x + 6\lambda_a p_a (h^2 p_x)_x = 6\mu(V_R + V_w)(ph)_x + 12\mu(ph)_t + 12\mu pV_t$$

**APPENDIX B**

**DERIVATION OF DIFFERENCE EQUATIONS**

Finite Difference operators used for Approximating the derivatives are-

$$y_{xx} = (y_{i+1}^{n+1} - 2y_i^{n+1} + y_{i-1}^{n+1}) / \Delta x^2$$

$$y_{tt} = (y_i^{n+1} - 2y_i^n + y_i^{n-1}) / \Delta t^2$$

$$y_{xt} = (y_{i+1}^{n+1} - y_{i+1}^{n-1} - y_{i-1}^{n+1} + y_{i-1}^{n-1}) / 4\Delta x\Delta t$$

$$p_x = (p_{i+1}^{n+1} - p_{i-1}^{n+1}) / 2\Delta x$$

$$p_t = (p_i^{n+1} - p_i^n) / \Delta t$$

$$p_{xx} = (p_{i+1}^{n+1} - 2p_i^{n+1} + p_{i-1}^{n+1}) / \Delta x^2$$

$$h_x = (h_{i+1}^{n+1} - h_{i-1}^{n+1}) / 2\Delta x$$

$$h_t = (h_i^{n+1} - h_i^n) / \Delta t$$

Substituting the above operators in the foil equation of motion yields,

1) Foil equation of motion-

$$\rho b \left( \frac{\partial^2 y}{\partial t^2} + 2V \frac{\partial^2 y}{\partial x \partial t} + V^2 \frac{\partial^2 y}{\partial x^2} \right) + \frac{EI}{w} \frac{\partial^4 y}{\partial x^4} - \frac{T}{w} \frac{\partial^2 y}{\partial x^2} = p - p_a$$

After substituting the finite difference operators yields an implicit formulation of equation of the type-

$$G_1 y_{i-2}^{n+1} + B_1 y_{i-1}^{n+1} + D_1 y_i^{n+1} + A_1 y_{i+1}^{n+1} + H_1 y_{i+2}^{n+1} = E_1$$

where,



$$G_1 = \frac{EI/w}{\Delta x^4}$$

$$B_1 = \left( \frac{V^2}{\Delta x^2} - \frac{2V}{4\Delta x\Delta t} - \frac{4EI/w}{\Delta x^4} - \frac{T/w}{\Delta x^2} \right)$$

$$D_1 = \left( \frac{\rho b}{\Delta t^2} - \frac{2V^2}{\Delta x^2} + \frac{2T/w}{\Delta x^2} + \frac{6EI/w}{\Delta x^4} \right)$$

$$A_1 = \left( \frac{2V}{4\Delta x\Delta t} - \frac{V^2}{\Delta x^2} - \frac{4EI/w}{\Delta x^4} - \frac{T/w}{\Delta x^2} \right)$$

$$E_1 = \left\{ (p_i^n - p_a) + \left[ \left( \frac{2\rho b}{\Delta t^2} \right) y_i^n - \left( \frac{\rho b}{\Delta t^2} \right) y_i^{n-1} + \left( \frac{\rho b V_w}{2\Delta x\Delta t} \right) y_{i+1}^{n-1} - \left( \frac{\rho b V_w}{2\Delta x\Delta t} \right) y_{i-1}^{n-1} \right] \right\}$$

2) Reynolds lubrication equation-

$$(h^3 pp_x)_x + 6\lambda_a p_a (h^2 p_x)_x = 6\mu(V_R + V_w)(ph)_x + 12\mu(ph)_t + 12\mu p V_t$$

After substituting the proper finite difference operators and rearranging collecting similar terms yields an implicit formulation of the type,

$$B_2 p_{i-1}^{n+1} + D_2 p_i^{n+1} + A_2 p_{i+1}^{n+1} = E_2$$

where,

$$B_2 = \left[ \frac{-6\mu(V_R + V_w)h_i^{n+1}}{2\Delta x} - \frac{(h_i^{n+1})^3 p_i^n}{\Delta x^2} + \frac{(h_i^{n+1})^3 (p_{i+1}^n - p_{i-1}^n)}{4\Delta x^2} + \frac{3(h_i^{n+1})^2 p_i^n (h_{i+1}^{n+1} - h_{i-1}^{n+1})}{4\Delta x^2} - \frac{6\lambda_a p_a (h_i^{n+1})^2}{\Delta x^2} + \frac{6\lambda_a p_a h_i^{n+1} (h_{i+1}^{n+1} - h_{i-1}^{n+1})}{2\Delta x^2} \right]$$

$$D_2 = \left[ \frac{12\mu(2h_i^{n+1} - h_i^n)}{\Delta t} + \frac{3\mu(V_R + V_w)(h_{i+1}^{n+1} - h_{i-1}^{n+1})}{\Delta x} + \frac{2(h_i^{n+1})^3 p_i^n}{\Delta x^2} + 6\lambda_a p_a \frac{2(h_i^{n+1})^2}{\Delta x^2} + 12\mu K(p_i^n - p_a) \right]$$

$$A_2 = \left[ \frac{6\mu(V_R + V_W)h_i^{n+1}}{2\Delta x} - \frac{(h_i^{n+1})^3 p_i^n}{\Delta x^2} - \frac{(h_i^{n+1})^3 (p_{i+1}^n - p_{i-1}^n)}{4\Delta x^2} - \frac{3(h_i^{n+1})^2 p_i^n (h_{i+1}^{n+1} - h_{i-1}^{n+1})}{4\Delta x^2} \right] \\ 6\lambda_a p_a \left( \frac{h_i^{n+1} (h_{i+1}^{n+1} - h_{i-1}^{n+1})}{2\Delta x^2} + \frac{(h_i^{n+1})^2}{\Delta x^2} \right)$$

and,

$$E_2 = \frac{12\mu p_i^n h_i^{n+1}}{\Delta t}$$

**APPENDIX C**

**COMPUTER PROGRAM FOR THE COMPUTATION OF AIR**

**FILMS AND PRESSURE DISTRIBUTIONS**

C\*\*\*\*\*

C MAE- THESIS

C OKLAHOMA STATE UNIVERSITY

C\*\*\*\*\*

C NUMERICAL MODEL TO PREDICT THE AIR-GAP AND THE PRESSURE  
C DISTRIBUTION BETWEEN MOVING WEBS AND SUPPORT ROLLERS  
C **(ZERO STIFFNESS MODEL-STEADY STATE CASE)**

C BY- KOTHARI, SATYANARAYAN & KANDASAMY SATHEESH

C\*\*\*\*\*

C DEFINING THE VARIABLES USED IN THIS PROGRAM.

C X - DISTANCE ALONG THE ROLLER(i.e. LONGITUDINAL DIRECTION).  
C Y - DISPLACEMENT OF THE FOIL OR WEB FROM THE EQUILLIBRIUM  
C POSITION W.R.T. X(i.e. ALONG LONGITUDINAL DIRECTION)  
C AND TIME T.  
C P - PRESSURE DISTRIBUTION BETWEEN THE FOIL AND THE ROLLER  
C W.R.T. X(i.e. ALONG LONGITUDINAL DIRECTION) AND TIME T.  
C PA - AMBIENT PRESSURE  
C PR - (P-PA)  
C H - AIR FILM GAP BETWEEN THE ROLLER AND THE FOIL.  
C HO - INITIAL AIR FILM THICKNESS.  
C PO - INITIAL PRESSURE DISTRIBUTION.  
C M - MASS PER UNIT WIDTH PER UNIT LENGTH OF THE FOIL(Kg/m<sup>2</sup>).  
C T - TENSION PER UNIT WIDTH APPLIED ON THE FOIL(N/m).  
C V - VELOCITY WITH WHICH THE FOIL IS MOVING(m/s).  
C AK - PERMEABILITY((m<sup>3</sup>/s)/(m<sup>2</sup>-Pa)).  
C R - ROLLER RADIUS(m).  
C VR - ROLLER SURFACE VELOCITY(m/s).  
C LE - LENGTH BETWEEN TWO END SUPPORTING ROLLERS(m).  
C MU - VISCOSITY OF AIR(N/(m<sup>2</sup>-s)).  
C LAM - MEAN FREE PATH OF AIR(m).  
C DEL - DESCRIBES THE ROLLER PROFILE.  
C DELX - MESH SIZE IN THE X DIRECTION.  
C DELT - TIME STEP (s)  
C A,AA,B,BB,C,CC,D,DD - ARE THE VARIABLES USED FOR STORING THE  
C ELEMENTS OF THE TRI-DIAGONAL MATRICES  
C FOR THE TWO GOVERNING EQUATIONS.

C\*\*\*\*\*

PROGRAM FOIL  
IMPLICIT DOUBLE PRECISION (A-Z)  
INTEGER I,J,ITER,NN,N,II,N1,N2,ITOTAL,IWRITE  
DIMENSION DEL(125),X(125),Y(125,5),H(125,5),P(125),PR(125)  
DIMENSION A(125),B(125),C(125),D(125)  
DIMENSION AA(125),BB(125),CC(125),DD(125)

```

DIMENSION FF1(0:150,0:150),FF2(0:150,0:150),FILM1(0:130,0:130)
CHARACTER FLNAME1 *15,FLNAME2 *15,FLNAME3 *15
C  CHOOSING AIR PROPERTY, TIME STEP
DATA MU,PA,DELT/1.81E-5,1.01325E5,5.0E-07/

C  CHOOSING SURFACE GEOMETRY,RADUIS OF THE ROLLER,LENGTH BETWEEN
C  GUIDE ROLLERS
DATA LE,X(1),XM,DELM,R/8.43E-1,3.465E-1,4.965E-1,0.635E-1,
#2.04E-1/
C  DATA LE,X(1),XM,DELM,R/12.645E-1,5.1975E-1,7.4475E-1,0.9525E-1,
C  #3.048E-1/

```

```

C*****
C                               INPUT PARAMETERS
C*****

```

```

WRITE(*,*) 'WHETHER TO CONSIDER SLIP FLOW OR NOT'
WRITE(*,*) 'IF YES 1,ELSE 0'
READ(*,*) LAM
WRITE(*,*) 'VELOCITY OF WEB IN FT/MIN'
READ(*,*) V_IN
WRITE(*,*) 'VELOCITY OF ROLLER IN FT/MIN'
READ(*,*) VR_IN
WRITE(*,*) 'TENSION APPLIED TO THE WEB IN LB/IN'
READ(*,*) T_IN
WRITE(*,*) 'IS THE WEB POROUS'
WRITE(*,*) 'IF POROUS USE EITHER 5E-5 ELAE 3.0E-5'
WRITE(*,*) 'ELSE USE A VALUE ZERO'
READ(*,*) AK
WRITE(*,*) 'MASS OF THE WEB PER UNIT WIDTH'
READ(*,*) M
WRITE(*,*) 'AFTER HOW MANY ITERATIONS OUTPUT SHOULD BE
* WRITTEN ON A FILE'
READ(*,*) IWRITE
ITOTAL=0
ISTATUS=0
V=(V_IN/196.8504)
VR=(VR_IN/196.8504)
T=(T_IN*175.3164556)
DELX=(XM-X(1))/124.
WRITE(*,*) 'GIVE NAMES FOR OUTPUT FILES(2 FILES) AND
*INPUT DATA FILE(1 FILE)(NOT MORE THAN 15 CHARACTERS)'
READ(*,11)FLNAME1,FLNAME2,FLNAME3
11  FORMAT(A15)
OPEN(7,FILE=FLNAME1,STATUS='UNKNOWN')
OPEN(5,FILE=FLNAME2,STATUS='UNKNOWN')
OPEN(9,FILE=FLNAME3,STATUS='UNKNOWN')
Q=(XM-X(1))/DELX
NN=INT(Q)

```

```

N=NN+1

C  CALCULATING THE HEAD PROFILE.

DO 2 I=1,N
2  DEL(I)=DELM-R+DSQRT(R**2-(X(1)+(I-1)*DELX-0.5*LE)**2)

C*****
C  INITIALIZING THE VALUES FOR FOIL DISPLACEMENT AND THE PRESSURE
C  ALONG THE ROLLER
C*****

HO=.643*R*(6.*MU*(V+VR)/T)**(2./3.)
PO=PA+T/R
THETA=0.
DO 10 I=1,5
YO=DELM+HO-(R+HO)*(1.-DCOS(THETA))
XO=.5*LE-(R+HO)*(DSIN(THETA))
10 THETA=DATAN(YO/XO)
AX=X(1)*YO/XO
DO 20 I=1,N
IF((X(1)+(I-1)*DELX) .GT. XO) GO TO 15
Y(I,2)=(X(1)+(I-1)*DELX)*YO/XO-AX
Y(I,1)=Y(I,2)
II=N-I+1
Y(II,2)=Y(I,2)
Y(II,1)=Y(I,2)
DEL(I)=DEL(I)-AX
P(I)=PA
H(I,2)=Y(I,2)-DEL(I)
H(I,1)=H(I,2)
FF1(I,KKK)=H(I,1)
DEL(II)=DEL(I)-AX
P(II)=PA
H(II,2)=H(I,2)
H(II,1)=H(II,2)
20 CONTINUE

15 II=N-I+1
DO 30 I=I,II
DEL(I)=DEL(I)-AX
Y(I,2)=DEL(I)+HO
Y(I,1)=Y(I,2)
P(I)=PO
H(I,2)=HO
H(I,1)=HO
30 CONTINUE

```

```

C*****
C SOLVING THE TRANSIENT REYNOLDS EQUATION FOR NEW PRESSURE PROFILE
C*****

```

```

WRITE(*,*)T
C CORRECTING WEB TENSION CONSIDERING THE MASS OF THE WEB

```

```

T=T-M*(V**2)
KKK=1
N2=N-2
N1=N-1
ITER=0
101 ITER=ITER+1
ITOTAL=ITOTAL+1
DO 40 I=1,N2
J=I+1

B(I)=(-6.*(V+VR)*MU*H(J,2)/(2.*DELX))-((H(J,2)**3)*P(J)/DELX**2)+
#(H(J,2)**3)*(P(J+1)-P(J-1))/(4.*DELX**2)+3.*(H(J,2)**2)*P(J)
#*(H(J+1,2)-H(J-1,2))/(4.*DELX**2)-6.*LAM*PA*H(J,2)**2/DELX**2+
#6.*LAM*PA*H(J,2)*(H(J+1,2)-H(J-1,2))/(2.*DELX**2)

D(I)=12.*MU*(2*H(J,2)-H(J,1))/DELT+2.*(H(J,2)**3)*P(J)/(DELX**2)
#+12.*LAM*PA*(H(J,2)**2)/(DELX**2)+3.*MU*(V+VR)*(H(J+1,2)-H(J-1,2))
#/DELX+(12*MU*AK*(P(J)-PA))

A(I)=(6.*(V+VR)*MU*H(J,2)/(2.*DELX))-((H(J,2)**3)*P(J)/DELX**2)-
#(H(J,2)**3)*(P(J+1)-P(J-1))/(4.*DELX**2)-3.*(H(J,2)**2)*P(J)
#*(H(J+1,2)-H(J-1,2))/(4.*DELX**2)-6.*LAM*PA*(H(J,2)**2)/DELX**2-
#6.*LAM*PA*H(J,2)*(H(J+1,2)-H(J-1,2))/(2.*DELX**2)

C(I)=12.*MU*H(J,2)*P(J)/DELT

```

```

40 CONTINUE

```

```

B(1)=0.0
A(N2)=0.0
C(1)=C(1)-
#((-6.*(V+VR)*MU*H(2,2)/(2.*DELX))-((H(2,2)**3)*P(2)/DELX**2)+
#(H(2,2)**3)*(P(3)-P(1))/(4.*DELX**2)+3.*(H(2,2)**2)*P(2)
#*(H(3,2)-H(1,2))/(4.*DELX**2)-6.*LAM*PA*H(2,2)**2/DELX**2+
#6.*LAM*PA*H(2,2)*(H(3,2)-H(1,2))/(2.*DELX**2))*PA

C(N2)=C(N2)-
#((6.*(V+VR)*MU*H(N1,2)/(2.*DELX))-((H(N1,2)**3)*P(N1)/DELX**2)-
#(H(N1,2)**3)*(P(N)-P(N2))/(4.*DELX**2)-3.*(H(N1,2)**2)*P(N1)
#*(H(N,2)-H(N2,2))/(4.*DELX**2)-6.*LAM*PA*(H(N1,2)**2)/DELX**2-
#6.*LAM*PA*H(N1,2)*(H(N,2)-H(N2,2))/(2.*DELX**2))*PA

```

C UPPER TRIANGULARIZATION

```
DO 49 I=2,N2
RR=B(I)/D(I-1)
D(I)=D(I)-RR*A(I-1)
49 C(I)=C(I)-RR*C(I-1)
```

C BACK SUBSTITUTION

```
C(N2)=C(N2)/D(N2)
DO 59 I=2,N2
J=N2-I+1
59 C(J)=(C(J)-A(J)*C(J+1))/D(J)
DO 69 I=1,N2
J=I+1
P(J)=C(I)
PR(J)=P(J)-PA
69 CONTINUE
```

```
PR(1)=P(1)-PA
PR(N)=P(N)-PA
```

C\*\*\*\*\*  
C SOLVING THE FOIL EQUATION USING THE UPDATED VALUES FOR PRESSURE  
C TO OBTAIN NEW VALUES FOR FOIL DISPLACEMENT AND AIR FILM GAP.  
C\*\*\*\*\*

```
DO 79 I=1,N2
J=I+1
BB(I)=-M*V/(2.*DELX*DELX)+M*(V**2)/(DELX**2)-T/(DELX**2)
DD(I)=M/(DELX**2)-(2.*M*(V**2))/(DELX**2)+(2.*T/(DELX**2))
AA(I)=M*V/(2.*DELX*DELX)+M*(V**2)/(DELX**2)-T/(DELX**2)
CC(I)=(P(J)-PA)+(2.*M/DELX**2)*Y(J,2)-(M/DELX**2)*Y(J,1)+
#(M*V/(2.*DELX*DELX)*Y(J+1,1)-(M*V/(2.*DELX*DELX)*Y(J-1,1))
79 CONTINUE
BB(1)=0.0
AA(N2)=0.0
CC(1)=CC(1)-M*V/(2.*DELX*DELX)+M*(V**2)/(DELX**2)-T/DELX**2*
#(Y(1,1))
CC(N2)=CC(N2)-(M*V/(2.*DELX*DELX)+(M*V**2/DELX**2)-T/DELX**2)*
#(Y(N,1))
```

C UPPER TRIANGULARIZATION

```
DO 89 I=2,N2
RRR=BB(I)/DD(I-1)
DD(I)=DD(I)-RRR*AA(I-1)
89 CC(I)=CC(I)-RRR*CC(I-1)
```



```

C   BACK SUBSTITUTION
CC(N2)=CC(N2)/DD(N2)
DO 99 I=2,N2
  J=N2-I+1
  CC(J)=(CC(J)-AA(J)*CC(J+1))/DD(J)
99  ENDDO
ERROR=0
DO I=1,N2
  J=I+1
  Y(J,3)=CC(I)
  H(J,3)=Y(J,3)-DEL(J)
  FILM1(J,ITER)=H(J,3)
ENDDO
DO 109 I=1,N2
  J=I+1

  ERROR=ERROR+ABS((Y(J,3)-Y(J,2)))/
  * ABS(Y(J,3)-DEL(J))

109 CONTINUE

  IF(ERROR .LE. 1E-4)THEN
    KKMAX=KKK
    DO I=2,N2
      FF1(I,KKMAX)=H(I,3)
      FF2(I,KKMAX)=PR(I)
    ENDDO
    GOTO 789
  ENDIF
  IF(ITER .EQ. 100) THEN
    ITER=0
  ENDIF

  Y(1,3)=Y(1,1)
  Y(N,3)=Y(N,1)
  H(1,3)=H(1,1)
  H(N,3)=H(N,1)

C*****
C   PRINTING THE SOLUTION i.e. THE AIR FILM THICKNESS AND THE
C   PRESSURE PROFILE ALONG THE ROLLER.
C*****

  IF (MOD(ITOTAL,IWRITE) .EQ. 10) THEN
    WRITE(*,*) ITOTAL,ERROR
    DO I=1,N
      FF1(I,KKK)=H(I,3)
      FF2(I,KKK)=PR(I)

```

```

ENDDO
KKK=KKK+1
ENDIF

C*****
DO 210 I=2,N2
Y(I,1)=Y(I,2)
H(I,1)=H(I,2)
Y(I,2)=Y(I,3)
H(I,2)=H(I,3)

210 CONTINUE

C*****

GOTO 101
789 CONTINUE
WRITE(9,*) 'VELOCITY OF THE WEB IS',V
WRITE(9,*) 'VELOCITY OF THE ROLLER IS',VR
WRITE(9,*) 'SLIP FLOW PARAMETER IS',LAM
WRITE(9,*) 'TENSION APPLIED IS',T
WRITE(9,*) 'POROSITY VALUE OF THE WEB IS',AK
WRITE(9,*) 'MASS OF THE WEB PER UNIT LENGTH IS',M
WRITE(9,*) 'TIME STEP IS',DELT
DO I=2,N2
WRITE(7,345) (FF1(I,JJ),JJ=1,KKMAX)
WRITE(5,345) (FF2(I,JJ),JJ=1,KKMAX)
345 FORMAT(100(E20.8,2X))
ENDDO
END

C*****
C      MECHANICAL AND AEROSPACE ENGINEERING, OSU.
C*****

```

```

C*****
C MAE- THESIS
C OKLAHOMA STATE UNIVERSITY

C NUMERICAL MODEL TO PREDICT THE AIR-GAP AND THE PRESSURE
C DISTRIBUTION BETWEEN MOVING WEBS AND SUPPORT ROLLERS
C ( ZERO STIFFNESS MODEL - FOR STEP CHANGE IN TENSION)
C BY- KANDASAMY SATHEESH

```

```

C*****
C DEFINING THE VARIABLES USED IN THIS PROGRAM.

C X - DISTANCE ALONG THE ROLLER(i.e. LONGITUDINAL DIRECTION).
C Y - DISPLACEMENT OF THE FOIL OR WEB FROM THE EQUILIBRM
C POSITION W.R.T. X(i.e. ALONG LONGITUDINAL DIRECTION)
C AND TIME T.
C P - PRESSURE DISTRIBUTION BETWEEN THE FOIL AND THE ROLLER
C W.R.T. X(i.e. ALONG LONGITUDINAL DIRECTION) AND TIME T.
C PA - AMBIENT PRESSURE
C PR - (P-PA)
C H - AIR FILM GAP BETWEEN THE ROLLER AND THE FOIL.
C HO - INITIAL AIR FILM THICKNESS.
C PO - INITIAL PRESSURE DISTRIBUTION.
C M - MASS PER UNIT WIDTH PER UNIT LENGTH OF THE FOIL(Kg/m^2).
C T - TENSION PER UNIT WIDTH APPLIED ON THE FOIL(N/m).
C V - VELOCITY WITH WHICH THE FOIL IS MOVING(m/s).
C AK - PERMEABILITY((m^3/s)/(m^2-Pa)).
C R - ROLLER RADIUS(m).
C VR - ROLLER SURFACE VELOCITY(m/s).
C LE - LENGTH BETWEEN TWO END SUPPORTING ROLLERS(m).
C MU - VISCOSITY OF AIR(N/(m^2-s)).
C LAM - MEAN FREE PATH OF AIR(m).
C DEL - DESCRIBES THE ROLLER PROFILE.
C DELX - MESH SIZE IN THE X DIRECTION.
C DELT - TIME STEP (s)
C A,AA,B,BB,C,CC,D,DD - ARE THE VARIABLES USED FOR STORING THE
C ELEMENTS OF THE TRI-DIAGONAL MATRICES
C FOR THE TWO GOVERNING EQUATIONS.

```

PROGRAM FOIL

```

IMPLICIT DOUBLE PRECISION (A-Z)
INTEGER I,J,ITER,NN,N,II,N1,N2,itotal,ITERA(50)
DIMENSION DEL(125),X(125),Y(125,5),H(125,5),P(125),PR(125)
DIMENSION A(125),B(125),C(125),D(125)
DIMENSION AA(125),BB(125),CC(125),DD(125)
DIMENSION FF1(0:150,0:150), FF2(0:150,0:150), FILM1(0:130,0:130)
CHARACTER FLNAME1 *15,FLNAME2 *15,FLNAME3 *15
DATA MU,PA,DELT/1.81E-5,1.01325E5,5.0E-07/
DATA LE,X(1),XM,DELM,R/8.43E-1,3.465E-1,4.965E-1,0.635E-1,

```

```

#2.04E-1/
C DATA LE,X(1),XM,DELM,R/12.645E-1,5.1975E-1,7.4475E-1,0.9525E-1,
C #3.048E-1/

KKK=1

```

```

C*****
C                               INPUT PARAMETERS
C*****

```

```

WRITE(*,*) 'WHETHER TO CONSIDER SLIP FLOW OR NOT'
WRITE(*,*) 'IF YES 1,ELSE 0'
READ(*,*) LAM
WRITE(*,*) 'VELOCITY OF WEB IN FT/MIN'
READ(*,*) V_IN
WRITE(*,*) 'VELOCITY OF ROLLER IN FT/MIN'
READ(*,*) VR_IN
WRITE(*,*) 'TENSION APPLIED TO THE WEB IN LB/IN'
READ(*,*) T_IN
WRITE(*,*) 'IS THE WEB POROUS'
WRITE(*,*) 'IF POROUS USE EITHER 5E-5 ELAE 3.0E-5'
WRITE(*,*) 'ELSE USE A VALUE ZERO'
READ(*,*) AK
WRITE(*,*) 'MASS OF THE WEB PER UNIT WIDTH'
READ(*,*) M
WRITE(*,*) 'STEP CHANGE'
READ(*,*) STEP
ITOTAL=0
ISTATUS=0
V=(V_IN/196.8504)
VR=(VR_IN/196.8504)
T=(T_IN*175.3164556)
C THE ENTIRE DOMAIN ALONG THE ROLLER IS DIVIDED INTO 123 NODES.
DELX=(XM-X(1))/(124)
WRITE(*,*) 'GIVE NAME FOR OUTPUT FILE AND A DATA FILE
* (NOT MORE THAN 15 CHARACTERS)'
READ(*,11) FLNAME1, FLNAME2, FLNAME3
11 FORMAT(A15)
OPEN(7, FILE=FLNAME1, STATUS='UNKNOWN')
OPEN(5, FILE=FLNAME2, STATUS='UNKNOWN')
OPEN(9, FILE=FLNAME3, STATUS='UNKNOWN')
Q=(XM-X(1))/DELX
NN=INT(Q)
N=NN+1
C CALCULATING THE HEAD PROFILE.
DO 2 I=1,N
2 DEL(I)=DELM-R+DSQRT(R**2-(X(1)+(I-1)*DELX-0.5*LE)**2)

```

```

C*****
C  INITIALIZING THE VALUES FOR FOIL DISPLACEMENT AND THE PRESSURE
C  ALONG THE ROLLER
C*****

```

```

      HO=.643*R*(6.*MU*(V+VR)/T)**(2./3.)
      WRITE(*,*)HO= ',HO
      PO=PA+T/R
      THETA=0.
      DO 10 I=1,5
      YO=DELM+HO-(R+HO)*(1.-DCOS(THETA))
      XO=.5*LE-(R+HO)*(DSIN(THETA))
10  THETA=DATAN(YO/XO)
      AX=X(1)*YO/XO
      DO 20 I=1,N
      IF((X(1)+(I-1)*DELX) .GT. XO) GO TO 15
      Y(I,2)=(X(1)+(I-1)*DELX)*YO/XO-AX
      Y(I,1)=Y(I,2)
      II=N-I+1
      Y(II,2)=Y(I,2)
      Y(II,1)=Y(I,2)
      DEL(I)=DEL(I)-AX
      P(I)=PA
      H(I,2)=Y(I,2)-DEL(I)
      H(I,1)=H(I,2)
      FF1(I,KKK)=H(I,1)
      DEL(II)=DEL(II)-AX
      P(II)=PA
      H(II,2)=H(I,2)
      H(II,1)=H(II,2)
20  CONTINUE
15  II=N-I+1
      DO 30 I=I,II
      DEL(I)=DEL(I)-AX
      Y(I,2)=DEL(I)+HO
      Y(I,1)=Y(I,2)
      P(I)=PO
      H(I,2)=HO
      H(I,1)=HO
30  CONTINUE

```

```

C*****
C  SOLVING THE TRANSIENT REYNOLDS EQUATION FOR NEW PRESSURE PROFILE
C*****

```

```

C  CORRECTING WEB TENSION CONSIDERING THE MASS OF THE WEB
      T=T-M*(V**2)

```

```

KKK=1
N2=N-2
N1=N-1
ITER=0

```

```

101 ITER=ITER+1

```

```

ITOTAL=ITOTAL+1
DO 40 I=1,N2
J=I+1

```

```

B(I)=(-6.*(V+VR)*MU*H(J,2)/(2.*DELX))-((H(J,2)**3)*P(J)/DELX**2)+
#(H(J,2)**3)*(P(J+1)-P(J-1))/(4.*DELX**2)+3.*(H(J,2)**2)*P(J)
#*(H(J+1,2)-H(J-1,2))/(4.*DELX**2)-6.*LAM*PA*H(J,2)**2/DELX**2+
#6.*LAM*PA*H(J,2)*(H(J+1,2)-H(J-1,2))/(2.*DELX**2)

```

```

D(I)=12.*MU*(2*H(J,2)-H(J,1))/DELT+2.*(H(J,2)**3)*P(J)/(DELX**2)
#+12.*LAM*PA*(H(J,2)**2)/(DELX**2)+3.*MU*(V+VR)*(H(J+1,2)-H(J-1,2))
#/DELX+(12*MU*AK*(P(J)-PA))

```

```

A(I)=(6.*(V+VR)*MU*H(J,2)/(2.*DELX))-((H(J,2)**3)*P(J)/DELX**2)-
#(H(J,2)**3)*(P(J+1)-P(J-1))/(4.*DELX**2)-3.*(H(J,2)**2)*P(J)
#*(H(J+1,2)-H(J-1,2))/(4.*DELX**2)-6.*LAM*PA*(H(J,2)**2)/DELX**2-
#6.*LAM*PA*H(J,2)*(H(J+1,2)-H(J-1,2))/(2.*DELX**2)

```

```

C(I)=12.*MU*H(J,2)*P(J)/DELT

```

```

40 CONTINUE

```

```

B(1)=0.0
A(N2)=0.0
C(1)=C(1)-
#((-6.*(V+VR)*MU*H(2,2)/(2.*DELX))-((H(2,2)**3)*P(2)/DELX**2)+
#(H(2,2)**3)*(P(3)-P(1))/(4.*DELX**2)+3.*(H(2,2)**2)*P(2)
#*(H(3,2)-H(1,2))/(4.*DELX**2)-6.*LAM*PA*H(2,2)**2/DELX**2+
#6.*LAM*PA*H(2,2)*(H(3,2)-H(1,2))/(2.*DELX**2))*PA

```

```

C(N2)=C(N2)-
#((6.*(V+VR)*MU*H(N1,2)/(2.*DELX))-((H(N1,2)**3)*P(N1)/DELX**2)-
#(H(N1,2)**3)*(P(N)-P(N2))/(4.*DELX**2)-3.*(H(N1,2)**2)*P(N1)
#*(H(N,2)-H(N2,2))/(4.*DELX**2)-6.*LAM*PA*(H(N1,2)**2)/DELX**2-
#6.*LAM*PA*H(N1,2)*(H(N,2)-H(N2,2))/(2.*DELX**2))*PA

```

```

C UPPER TRIANGULARIZATION

```

```

DO 49 I=2,N2
RR=B(I)/D(I-1)
D(I)=D(I)-RR*A(I-1)
49 C(I)=C(I)-RR*C(I-1)

```

```

C BACK SUBSTITUTION

```

```

C(N2)=C(N2)/D(N2)
DO 59 I=2,N2
  J=N2-I+1
59 C(I)=(C(J)-A(I)*C(J+1))/D(I)

```

```

DO 69 I=1,N2
  J=I+1
  P(I)=C(I)
  PR(I)=P(I)-PA
69 CONTINUE

```

```

PR(1)=P(1)-PA
PR(N)=P(N)-PA

```

```

C*****
C SOLVING THE FOIL EQUATION USING THE UPDATED VALUES FOR PRESSURE
C TO OBTAIN NEW VALUES FOR FOIL DISPLACEMENT AND AIR FILM GAP.
C*****

```

```

DO 79 I=1,N2
  J=I+1
  BB(I)=-M*V/(2.*DELX*DELX)+M*(V**2)/(DELX**2)-T/(DELX**2)

  DD(I)=M/(DELX**2)-(2.*M*(V**2))/(DELX**2)+(2.*T/(DELX**2))

  AA(I)=M*V/(2.*DELX*DELX)+M*(V**2)/(DELX**2)-T/(DELX**2)

  CC(I)=(P(J)-PA)+(2.*M/DELX**2)*Y(J,2)-(M/DELX**2)*Y(J,1)+
  #(M*V/(2*DELX*DELX))*Y(J+1,1)-(M*V/(2.*DELX*DELX))*Y(J-1,1)

```

```

79 CONTINUE

```

```

BB(1)=0.0
AA(N2)=0.0
CC(1)=CC(1)-(-M*V/(2.*DELX*DELX)+M*(V**2)/(DELX**2)-T/DELX**2)*
#(Y(1,1))
CC(N2)=CC(N2)-(M*V/(2.*DELX*DELX)+(M*V**2/DELX**2)-T/DELX**2)*
#(Y(N,1))

```

```

C UPPER TRIANGULARIZATION

```

```

DO 89 I=2,N2
  RRR=BB(I)/DD(I-1)
  DD(I)=DD(I)-RRR*AA(I-1)
89 CC(I)=CC(I)-RRR*CC(I-1)

```

C BACK SUBSTITUTION

```

CC(N2)=CC(N2)/DD(N2)
DO 99 I=2,N2
  J=N2-I+1
  CC(J)=(CC(J)-AA(J)*CC(J+1))/DD(J)
99 ENDDO
ERROR=0
DO 109 I=1,N2
  J=I+1
  Y(J,3)=CC(I)
  H(J,3)=Y(J,3)-DEL(J)
  FILM1(J,ITER)=H(J,3)
  IF(FILM1(J,ITER) .NE. 0) THEN
    ERROR=ERROR+ABS((Y(J,3)-Y(J,2)))/
    * ABS(Y(J,3)-DEL(J))
109 CONTINUE
    IF((ISTATUS .EQ. 0) .AND. (ERROR .LE. 1E-4)) THEN
      T(1.0+STEP)*T
    ENDIF
  IF(ERROR .LE. 1E-4) THEN
    ISTATUS=ISTATUS+1
  ENDIF
  IF(ITER .EQ. 100) THEN
    ITER=0
  ENDIF
  IF(ISTATUS .EQ. 2) THEN
    KKMAX=KKK
    ITERA(KKMAX)=ITOTAL
  DO I=1,N
    FF1(I,KKMAX)=H(I,3)
    FF2(I,KKMAX)=PR(I)
  ENDDO
  GOTO 789
  ENDI
  Y(1,3)=Y(1,1)
  Y(N,3)=Y(N,1)
  H(1,3)=H(1,1)
  H(N,3)=H(N,1)

```

C\*\*\*\*\*

C PRINTING THE SOLUTION i.e. THE AIR FILM THICKNESS AND THE  
C PRESSURE PROFILE ALONG THE ROLLER.

C\*\*\*\*\*

```

C OUTPUT WOULD BE WRITTEN AFTER EACH 2000 ITERATIONS
C AND AFTER CONVERGENCE
  IF(((ISTATUS .EQ. 1) .AND. (ERROR .LE. 1E-4))
  * .OR. ((ISTATUS .EQ. 1) .AND.
  * (MOD(ITOTAL,2000) .EQ. 10))) THEN
  WRITE(*,*) ITOTAL,ERROR
    ITERA(KKK)=ITOTAL
  DO I=1,N

```



```

FF1(I,KKK)=H(I,3)
FF2(I,KKK)=PR(I)
ENDDO
KKK=KKK+1
ENDIF

```

```

C*****
DO 210 I=1,N
Y(I,1)=Y(I,2)
H(I,1)=H(I,2)
Y(I,2)=Y(I,3)
H(I,2)=H(I,3)
210 CONTINUE

```

```

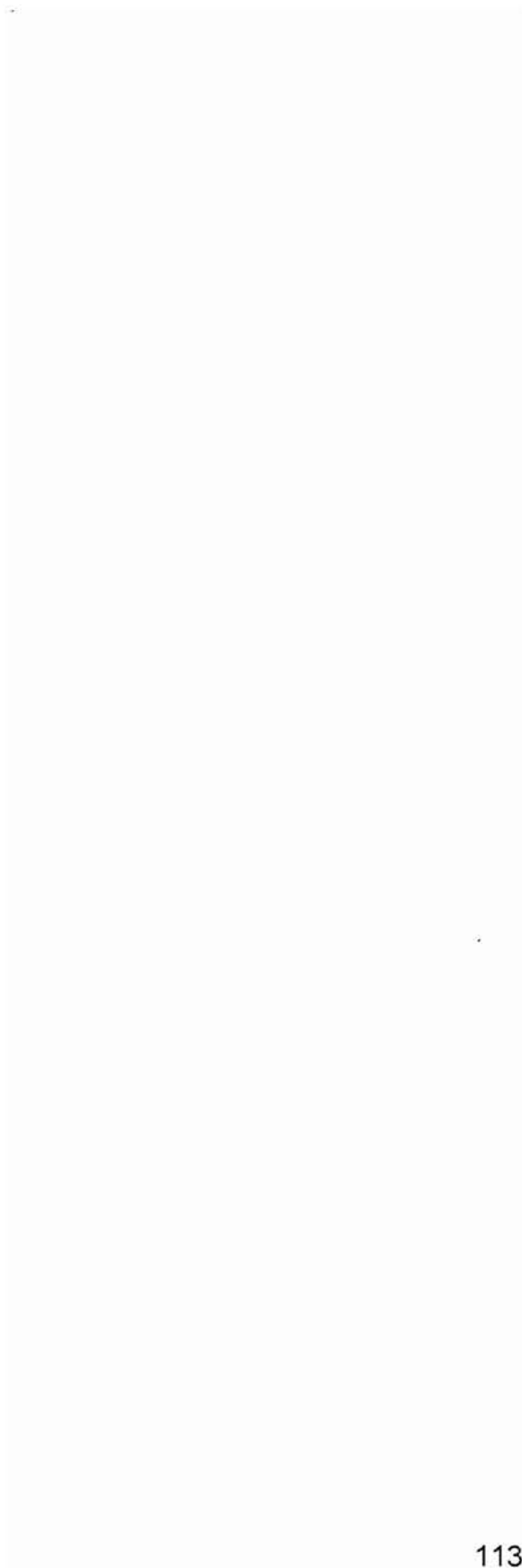
C*****
GOTO 101
789 CONTINUE
WRITE(9,*) 'VELOCITY OF THE WEB IS',V
WRITE(9,*) 'VELOCITY OF THE ROLLER IS',VR
WRITE(9,*) 'SLIP FLOW PARAMETER IS',LAM
WRITE(9,*) 'TENSION APPLIED IS',T
WRITE(9,*) 'POROSITY VALUE OF THE WEB IS',AK
WRITE(9,*) 'MASS OF THE WEB PER UNIT LENGTH IS',M
WRITE(9,*) 'TIME STEP IS',DELT
DO IJ=1,KKMAX
WRITE(9,*) ITERA(IJ)
ENDDO
DO LLL=2,N2
WRITE(7,345) (FF1(LLL,JJ),JJ=1,KKMAX)
WRITE(5,345) (FF2(LLL,JJ),JJ=1,KKMAX)
345 FORMAT(100(E20.8,2X))
ENDDO
CLOSE(9)
CLOSE(7)
CLOSE(5)
CLOSE(3)
END

```

```

C*****
C MECHANICAL AND AEROSPACE ENGINEERING, OSU.
C*****

```



```

C*****
C MAE- THESIS
C OKLAHOMA STATE UNIVERSITY
C NUMERICAL MODEL TO PREDICT THE AIR-GAP AND THE PRESSURE
C DISTRIBUTION BETWEEN MOVING WEBS AND SUPPORT ROLLERS
C ZERO STIFFNESS MODEL-SINUSOIDAL FLUCTUATION IN TENSION
C BY- KANDASAMY SATHEESH

```

```

C*****
C DEFINING THE VARIABLES USED IN THIS PROGRAM.
C X - DISTANCE ALONG THE ROLLER(i.e. LONGITUDINAL DIRECTION).
C Y - DISPLACEMENT OF THE FOIL OR WEB FROM THE EQUILLIBRIUM
C POSITION W.R.T. X(i.e. ALONG LONGITUDINAL DIRECTION)
C AND TIME T.
C P - PRESSURE DISTRIBUTION BETWEEN THE FOIL AND THE ROLLER
C W.R.T. X(i.e. ALONG LONGITUDINAL DIRECTION) AND TIME T.
C PA - AMBIENT PRESSURE
C PR - (P-PA)
C H - AIR FILM GAP BETWEEN THE ROLLER AND THE FOIL.
C HO - INITIAL AIR FILM THICKNESS.
C PO - INITIAL PRESSURE DISTRIBUTION.
C M - MASS PER UNIT WIDTH PER UNIT LENGTH OF THE FOIL(Kg/m^2).
C T - TENSION PER UNIT WIDTH APPLIED ON THE FOIL(N/m).
C V - VELOCITY WITH WHICH THE FOIL IS MOVING(m/s).
C AK - PERMEABILITY((m^3/s)/(m^2-Pa)).
C R - ROLLER RADIUS(m).
C VR - ROLLER SURFACE VELOCITY(m/s).
C LE - LENGTH BETWEEN TWO END SUPPORTING ROLLERS(m).
C MU - VISCOSITY OF AIR(N/(m^2-s)).
C LAM - MEAN FREE PATH OF AIR(m).
C DEL - DESCRIBES THE ROLLER PROFILE.
C DELX - MESH SIZE IN THE X DIRECTION.
C DELT - TIME STEP (s)
C A,AA,B,BB,C,CC,D,DD - ARE THE VARIABLESUSED FOR STORING THE
C ELEMENTS OF THE TRI-DIAGONAL MATRICES
C FOR THE TWO GOVERNING EQUATIONS.

```

```

C*****
PROGRAM FOIL
IMPLICIT DOUBLE PRECISION (A-Z)
INTEGER I,J,ITER,NN,N,II,N1,N2,ITOTAL,ISTATUS,ITERA(50)
DIMENSION DEL(125),X(125),Y(125,5),H(125,5),P(125),PR(125)
DIMENSION A(125),B(125),C(125),D(125),FF5(125)
DIMENSION AA(125),BB(125),CC(125),DD(125)
DIMENSION FF1(0:150,0:150),FF2(0:150,0:150),
* FILM1(0:130,0:130)
CHARACTER FLNAME1 *25,FLNAME2 *25,FLNAME3 *25
DATA MU,PA,DELT/1.81E-5,1.01325E5,5.0E-07/
DATA LE,X(1),XM,DELM,R/8.43E-1,3.465E-1,4.965E-1,0.635E-1,
#2.04E-1/
C DATA LE,X(1),XM,DELM,R/12.645E-1,5.1975E-1,7.4475E-1,0.9525E-1,
C #3.048E-1/

```

```

      KKK=1
      ISTATUS=0
C*****
C
      INPUT PARAMETERS
C*****
      WRITE(*,*) 'WHETHER TO CONSIDER SLIP FLOW OR NOT'
      WRITE(*,*) 'IF YES 1,ELSE 0'
      READ(*,*) LAM
      WRITE(*,*) 'VELOCITY OF WEB IN FT/MIN'
      READ(*,*) V_IN
      WRITE(*,*) 'VELOCITY OF ROLLER IN FT/MIN'
      READ(*,*) VR_IN
      WRITE(*,*) 'TENSION APPLIED TO THE WEB IN LB/IN'
      READ(*,*) T_IN
      WRITE(*,*) 'IS THE WEB POROUS'
      WRITE(*,*) 'IF POROUS USE EITHER 5E-5 ELAE 3.0E-5'
      WRITE(*,*) 'ELSE USE A VALUE ZERO'
      READ(*,*) AK
      WRITE(*,*) 'MASS OF THE WEB PER UNIT WIDTH'
      READ(*,*) M
      WRITE(*,*) 'AMPLITUDE OF FLUCTUATION'
      READ(*,*) AMPLITUDE
      WRITE(*,*) 'INTEGER MULTIPLE OF NATURAL FREQUENCY'
      READ(*,*) OMEGA

      ITOTAL=0
      ISTATUS=0
      V=(V_IN/196.8504)
      VR=(VR_IN/196.8504)
      T=(T_IN*175.3164556)
      DELX=(XM-X(1))/124.
      OPEN(7,FILE=FLNAME1,STATUS='UNKNOWN')
      OPEN(5,FILE=FLNAME2,STATUS='UNKNOWN')
      OPEN(9,FILE=FLNAME3,STATUS='UNKNOWN')
      Q=(XM-X(1))/DELX
      NN=INT(Q)
      N=NN+1
C   CALCULATING THE HEAD PROFILE.
      DO I=1,N
      DEL(I)=DELM-R+DSQRT(R**2-(X(1)+(I-1)*DELX-0.5*LE)**2)
      ENDDO
C*****
C   INITIALIZING THE VALUES FOR FOIL DISPLACEMENT AND THE PRESSURE
C   ALONG THE ROLLER
C*****

      HO=.643*R*(6.*MU*(V+VR)/T)**(2./3.)
      PO=PA+T/R
      THETA=0.
      DO 10 I=1,5
      YO=DELM+HO-(R+HO)*(1.-DCOS(THETA))
      XO=.5*LE-(R+HO)*(DSIN(THETA))
10  THETA=DATAN(YO/XO)

```

```

AX=X(1)*YO/XO
DO 20 I=1,N
IF((X(1)+(I-1)*DELX) .GT. XO) GO TO 15
Y(I,2)=(X(1)+(I-1)*DELX)*YO/XO-AX
Y(I,1)=Y(I,2)
II=N-I+1
Y(II,2)=Y(I,2)
Y(II,1)=Y(I,2)
DEL(I)=DEL(I)-AX
P(I)=PA
H(I,2)=Y(I,2)-DEL(I)
H(I,1)=H(I,2)
FF1(I,KKK)=H(I,1)
DEL(II)=DEL(II)-AX
P(II)=PA
H(II,2)=H(I,2)
H(II,1)=H(II,2)
20 CONTINUE

15 II=N-I+1
DO 30 I=I,II
DEL(I)=DEL(I)-AX
Y(I,2)=DEL(I)+HO
Y(I,1)=Y(I,2)
P(I)=PO
H(I,2)=HO
H(I,1)=HO

30 CONTINUE
C*****
C SOLVING THE TRANSIENT REYNOLDS EQUATION FOR NEW PRESSURE PROFILE
C*****

WRITE(*,*)T
C CORRECTING WEB TENSION CONSIDERING THE MASS OF THE WEB
T=T-M*(V**2)
TT1=T
WRITE(*,*)T
KKK=1
N2=N-2
N1=N-1
ITER=0
    TIME=0
    KKK=2
    ITER2=0
101 ITER=ITER+1
    IO=0
    ITOTAL=ITOTAL+1
    TIME=TIME+DELT
    IF(ISTATUS .EQ. 1) THEN
        ITER2=ITER2+1
        FACTOR=ATAN(1.0)/4.0

```

```

ANGLE1=(ATAN(1.0)/LE)*(TT1/M*(1+FACTOR))**0.5
ANGLE2=OMEGA*ANGLE1*TIME
ANGLE3=(180./ATAN(1.0))*ANGLE2
ANGLE4=MOD(ANGLE3,360.)
T=TT1+AMPLITUDE*TT1*SIN(ANGLE2)
ENDIF

```

```

DO 40 I=1,N2

```

```

J=I+1

```

```

B(I)=(-6.*(V+VR)*MU*H(J,2)/(2.*DELX))-((H(J,2)**3)*P(J)/DELX**2)+
#(H(J,2)**3)*(P(J+1)-P(J-1))/(4.*DELX**2)+3.*(H(J,2)**2)*P(J)
#*(H(J+1,2)-H(J-1,2))/(4.*DELX**2)-6.*LAM*PA*H(J,2)**2/DELX**2+
#6.*LAM*PA*H(J,2)*(H(J+1,2)-H(J-1,2))/(2.*DELX**2)

```

```

D(I)=12.*MU*(2*H(J,2)-H(J,1))/DELT+2.*(H(J,2)**3)*P(J)/(DELX**2)
#+12.*LAM*PA*(H(J,2)**2)/(DELX**2)+3.*MU*(V+VR)*(H(J+1,2)-H(J-1,2))
#/DELX+(12*MU*AK*(P(J)-PA))

```

```

A(I)=(6.*(V+VR)*MU*H(J,2)/(2.*DELX))-((H(J,2)**3)*P(J)/DELX**2)-
#(H(J,2)**3)*(P(J+1)-P(J-1))/(4.*DELX**2)-3.*(H(J,2)**2)*P(J)
#*(H(J+1,2)-H(J-1,2))/(4.*DELX**2)-6.*LAM*PA*(H(J,2)**2)/DELX**2-
#6.*LAM*PA*H(J,2)*(H(J+1,2)-H(J-1,2))/(2.*DELX**2)
C(I)=12.*MU*H(J,2)*P(J)/DELT

```

```

40 CONTINUE

```

```

B(1)=0.0

```

```

A(N2)=0.0

```

```

C(1)=C(1)-

```

```

#((-6.*(V+VR)*MU*H(2,2)/(2.*DELX))-((H(2,2)**3)*P(2)/
&DELX**2)+
#(H(2,2)**3)*(P(3)-P(1))/(4.*DELX**2)+3.*(H(2,2)**2)*P(2)
#*(H(3,2)-H(1,2))/(4.*DELX**2)-6.*LAM*PA*H(2,2)**2/
&DELX**2+
#6.*LAM*PA*H(2,2)*(H(3,2)-H(1,2))/(2.*DELX**2))*PA

```

```

C(N2)=C(N2)-

```

```

#((6.*(V+VR)*MU*H(N1,2)/(2.*DELX))-((H(N1,2)**3)*P(N1)/DELX**2)-
#(H(N1,2)**3)*(P(N)-P(N2))/(4.*DELX**2)-3.*(H(N1,2)**2)*P(N1)
#*(H(N,2)-H(N2,2))/(4.*DELX**2)-6.*LAM*PA*(H(N1,2)**2)/DELX**2-
#6.*LAM*PA*H(N1,2)*(H(N,2)-H(N2,2))/(2.*DELX**2))*PA

```

```

C UPPER TRIANGULARIZATION

```

```

DO 49 I=2,N2

```

```

RR=B(I)/D(I-1)

```

```

D(I)=D(I)-RR*A(I-1)

```

```

49 C(I)=C(I)-RR*C(I-1)

```

```

C BACK SUBSTITUTION

```

```

C(N2)=C(N2)/D(N2)

```

```

DO 59 I=2,N2
J=N2-I+1
59 C(J)=(C(J)-A(J)*C(J+1))/D(J)

```

```

DO 69 I=1,N2
J=I+1
P(J)=C(I)
PR(J)=P(J)-PA
69 CONTINUE

```

```

PR(1)=P(1)-PA
PR(N)=P(N)-PA

```

```

C*****
C SOLVING THE FOIL EQUATION USING THE UPDATED VALUES FOR PRESSURE
C TO OBTAIN NEW VALUES FOR FOIL DISPLACEMENT AND AIR FILM GAP.
C*****

```

```

DO 79 I=1,N2
J=I+1
BB(I)=-M*V/(2.*DELX*DELX)+M*(V**2)/(DELX**2)-T/(DELX**2)

```

```

DD(I)=M/(DELX**2)-(2.*M*(V**2))/(DELX**2)+(2.*T/(DELX**2))

```

```

AA(I)=M*V/(2.*DELX*DELX)+M*(V**2)/(DELX**2)-T/(DELX**2)
CC(I)=(P(J)-PA)+(2.*M/DELX**2)*Y(J,2)-(M/DELX**2)*Y(J,1)+
#(M*V/(2*DELX*DELX))*Y(J+1,1)-(M*V/(2.*DELX*DELX))*Y(J-1,1)

```

```

79 CONTINUE
BB(1)=0.0
AA(N2)=0.0
CC(1)=CC(1)-(-M*V/(2.*DELX*DELX)+M*(V**2)/(DELX**2)-T/DELX**2)*
#(Y(1,1))
CC(N2)=CC(N2)-(M*V/(2.*DELX*DELX)+(M*V**2/DELX**2)-T/DELX**2)*
#(Y(N,1))

```

```

C UPPER TRIANGULARIZATION

```

```

DO 89 I=2,N2
RRR=BB(I)/DD(I-1)
DD(I)=DD(I)-RRR*AA(I-1)
CC(I)=CC(I)-RRR*CC(I-1)
89 ENDDO

```

```

C BACK SUBSTITUTION
CC(N2)=CC(N2)/DD(N2)
DO 99 I=2,N2
J=N2-I+1
CC(J)=(CC(J)-AA(J)*CC(J+1))/DD(J)
99 ENDDO

```

```

ERROR=0

```

```

DO 109 I=1,N2

```

```

J=I+1
Y(J,3)=CC(I)
H(J,3)=Y(J,3)-DEL(J)
FILM1(J,ITER)=H(J,3)
FILM1(J,0)=h(j,1)

IF(FILM1(J,ITER) .GE. 1E-10) THEN
ERROR=ERROR+ABS((FILM1(J,ITER)-FILM1(J,ITER-1)))/
* ABS(FILM1(J,ITER)+1E-20)
ENDIF
109 CONTINUE
IF(ERROR .LE. 1E-4)THEN
  ISTATUS=ISTATUS+1
  IO=1
  TIMEMAX=TIME
  ITER2=0
ENDIF
IF(ITER2 .EQ. 2000) THEN
  ANGLE5=ANGLE4
  DO I=1,N2
  FF5(I)=FILM1(I,ITER)
  ENDDO
ENDIF
IF(ERROR .GT. 1E-1) GOTO 789
ERROR1=0.0
IF((ITER2 .GT. 2000) .AND. ((ANGLE5-ANGLE4) .LE. 5E-2)) THEN
  DO I=2,N2
  ERROR1=ERROR1+ABS(FILM1(I,ITER)-FILM1(I,ITER-1))/
  *FILM1(I,ITER)
  ENDDO
  ERROR=ERROR1
  IF(MOD(ITOTAL,500) .EQ. 0) THEN
  ENDIF
  IF(ERROR1 .LE. 5E-4) THEN
  KKMAX=KKK
  DO I=1,N2
  FF1(I,KKMAX)=H(I,3)
  FF2(I,KKMAX)=PR(I)
  ITERA(KKMAX)=ITOTAL
  ENDDO
  GOTO 789
  ENDIF
  ENDIF
  IF((MOD(ITOTAL,500) .EQ. 10) .AND. (ISTATUS .EQ. 0))THEN
  ENDIF
IF(ITER .EQ. 100) THEN
ITER=0
ENDIF

Y(1,3)=Y(1,1)
Y(N,3)=Y(N,1)
H(1,3)=H(1,1)

```



```

H(N,3)=H(N,1)
C*****
C PRINTING THE SOLUTION i.e. THE AIR FILM THICKNESS AND THE
C PRESSURE PROFILE ALONG THE ROLLER.
C*****

      IF(IO .EQ. 1)THEN
      DO I=1,N
      FF1(I,KKK)=H(I,3)
      FF2(I,KKK)=PR(I)
      ITERA(KKK)=ITOTAL
      ENDDO
      KKK=KKK+1
      ELSE
      IF((ITER2 .GT. 2000) .AND.(MOD(ITOTAL,500) .EQ. 10)) THEN
      DO I=1,N
      FF1(I,KKK)=H(I,3)
      FF2(I,KKK)=PR(I)
      ITERA(KKK)=ITOTAL
      ENDDO
      KKK=KKK+1
      ENDIF
      ENDIF
C*****
      DO 210 I=1,N
      Y(I,1)=Y(I,2)
      H(I,1)=H(I,2)
      Y(I,2)=Y(I,3)
      H(I,2)=H(I,3)
210 CONTINUE
C*****
      GOTO 101
789 CONTINUE
      WRITE(9,*) 'VELOCITY OF THE WEB IS',V
      WRITE(9,*) 'VELOCITY OF THE ROLLER IS',VR
      WRITE(9,*) 'SLIP FLOW PARAMETER IS',LAM
      WRITE(9,*) 'TENSION APPLIED IS',T
      WRITE(9,*) 'POROSITY VALUE OF THE WEB IS',AK
      WRITE(9,*) 'MASS OF THE WEB PER UNIT LENGTH IS',M
      WRITE(9,*) 'VELOCITY OF THE WEB IS',V
      WRITE(9,*) 'VELOCITY OF THE ROLLER IS',VR
      WRITE(9,*) 'SLIP FLOW PARAMETER IS',LAM
      WRITE(9,*) 'TENSION APPLIED IS',T
      WRITE(9,*) 'POROSITY VALUE OF THE WEB IS',AK
      WRITE(9,*) 'MASS OF THE WEB PER UNIT LENGTH IS',M
      WRITE(9,*) 'AMPLITUDE OF FLUCTUATION IS',AMPLITUDE
      DO IPP=1,KKMAX
      WRITE(9,*) ITERA(IPP)
      ENDDO
      DO I=2,N2
      WRITE(7,345) (FF1(I,JJ),JJ=1,KKMAX)
      WRITE(5,345)(FF2(I,JJ),JJ=1,KKMAX)

```

```
345 FORMAT(100(E20.8,2X))
ENDDO
ENDDO
END
```

```
C*****
C      MECHANICAL AND AEROSPACE ENGINEERING, OSU.
C*****
```

\*\*\*\*\*

C MAE- THESIS  
C OKLAHOMA STATE UNIVERSITY

C NUMERICAL MODEL TO PREDICT THE AIR-GAP AND THE PRESSURE  
C DISTRIBUTION BETWEEN MOVING WEBS AND SUPPORT ROLLERS  
C FINITE STIFFNESS MODEL-STEADY STATE CASE

C BY- KANDASAMY ,SATHEESH

C\*\*\*\*\*

C DEFINING THE VARIABLE USED IN THIS PROGRAM.

C X - DISTANCE ALONG THE ROLLER(i.e. LONGITUDINAL DIRECTION).  
C Y - DISPLACEMENT OF THE FOIL OR WEB FROM THE EQUILLIBRIUM  
C POSITION W.R.T. X(i.e. ALONG LONGITUDINAL DIRECTION)  
C AND TIME T.  
C P - PRESSURE DISTRIBUTION BETWEEN THE FOIL AND THE ROLLER  
C W.R.T. X(i.e. ALONG LONGITUDINAL DIRECTION) AND TIME T.  
C PA - AMBIENT PRESSURE  
C PR - (P-PA)  
C H - AIR FILM GAP BETWEEN THE ROLLER AND THE FOIL.  
C HO - INITIAL AIR FILM THICKNESS.  
C PO - INITIAL PRESSURE DISTRIBUTION.  
C M - MASS PER UNIT WIDTH PER UNIT LENGTH OF THE FOIL(Kg/m<sup>2</sup>).  
C T - TENSION PER UNIT WIDTH APPLIED ON THE FOIL(N/m).  
C V - VELOCITY WITH WHICH THE FOIL IS MOVING(m/s).  
C AK - PERMEABILITY((m<sup>3</sup>/s)/(m<sup>2</sup>-Pa)).  
C R - ROLLER RADIUS(m).  
C VR - ROLLER SURFACE VELOCITY(m/s).  
C LE - LENGTH BETWEEN TWO END SUPPORTING ROLLERS(m).  
C MU - VISCOSITY OF AIR(N/(m<sup>2</sup>-s)).  
C LAM - MEAN FREE PATH OF AIR(m).  
C DEL - DESCRIBES THE ROLLER PROFILE.  
C DELX - MESH SIZE IN THE X DIRECTION.  
C DELT - TIME STEP (s)  
C A,AA,B,BB,C,CC,D,DD - ARE THE VARIABLE USED FOR STORING THE  
C ELEMENTS OF THE TRI-DIAGONAL MATRICES  
C FOR THE TWO GOVERNING EQUATIONS.

C\*\*\*\*\*

PROGRAM FOIL  
IMPLICIT DOUBLE PRECISION (A-Z)  
INTEGER I,J,ITER,NN,N,II,N1,N2,ITOTAL,IWRITE  
DIMENSION DEL(125),X(125),Y(125,5),H(125,5),P(125),PR(125)  
DIMENSION A(125),B(125),C(125),D(125)  
DIMENSION AA(125,-1:127),CONST(125),BD(125)  
DIMENSION U(125,125),AL(125,125),ITERA(50)  
DIMENSION FF1(125,2),FILM(125,50),PRESSURE(125,50)  
CHARACTER FILNAME1 \*15,FILNAME2 \*15,FILNAME3 \*15  
DATA MU,PA,DELT/1.81E-5,1.01325E5,1.0E-7/

```

DATA LE,X(1),XM,DELM,R/8.43E-1,3.465E-1,4.965E-1,0.635E-1,
#2.04E-1/
C DATA LE,X(1),XM,DELM,R/12.645E-1,5.1975E-1,7.4475E-1,0.9525E-1,
C #3.048E-1/

```

```

C*****
C                               INPUT PARAMETERS
C*****

```

```

WRITE(*,*) 'WHETHER TO CONSIDER SLIP FLOW OR NOT'
WRITE(*,*) 'IF YES 1,ELSE 0'
READ(*,*) LAM
WRITE(*,*) 'VELOCITY OF WEB IN FT/MIN'
READ(*,*) V_IN
WRITE(*,*) 'VELOCITY OF ROLLER IN FT/MIN'
READ(*,*) VR_IN
WRITE(*,*) 'TENSION APPLIED TO THE WEB IN LB/IN'
READ(*,*) T_IN
WRITE(*,*) 'IS THE WEB POROUS'
WRITE(*,*) 'IF POROUS USE EITHER 5E-5 ELAE 3.0E-5'
WRITE(*,*) 'ELSE USE A VALUE ZERO'
READ(*,*) AK
WRITE(*,*) 'MASS OF THE WEB PER UNIT WIDTH'
READ(*,*) M
WRITE(*,*) 'FLEXURAL RIGIDITY OF THE WEB'
READ(*,*) EI
WRITE(*,*) 'ITERATION NUMBER AFTER WHICH THE VALUES BE
* STORED'
READ(*,*) IWRITE

```

```

C   INITIALIZING THE COUNT

```

```

ITOTAL=0

```

```

ISTATUS=0

```

```

C   CONVERTING THE VELOCITIES AND TENSIONS TO SI UNITS

```

```

V=(V_IN/196.8504)

```

```

VR=(VR_IN/196.8504)

```

```

T=(T_IN*175.3164556)

```

```

C   DETERMINING THE GRID SIZE

```

```

DELX=(XM-X(1))/124.

```

```

WRITE(*,*) 'GIVE NAME FOR OUTPUT FILE(NOT MORE THAN 15 CHARACTERS)'

```

```

READ(*,11)FLNAME1,FLNAME2,FLNAME3

```

```

11 FORMAT(A15)

```

```

OPEN(7,FILE=FILENAME1,STATUS='UNKNOWN')

```

```

OPEN(5,FILE=FILENAME2,STATUS='UNKNOWN')

```

```

OPEN(9,FILE=FILENAME3,STATUS='UNKNOWN')

```

```

Q=(XM-X(1))/DELX

```

```

      NN=INT(Q)
      N=NN+1
C      DETERMINING THE ROLLER PROFILE

      DO 2 I=1,N
2     DEL(I)=DELM-R+DSQRT(R**2-(X(1)+(I-1)*DELX-0.5*LE)**2)

C*****
C     INITIALIZING THE VALUES FOR FOIL DISPLACEMENT AND THE PRESSURE
C     ALONG THE ROLLER
C*****

      HO=.643*R*(6.*MU*(V+VR)/T)**(2./3.)
      PO=PA+T/R
      THETA=0.
      DO 10 I=1,5
      YO=DELM+HO-(R+HO)*(1.-DCOS(THETA))
      XO=.5*LE-(R+HO)*(DSIN(THETA))
10    THETA=DATAN(YO/XO)
      AX=X(1)*YO/XO
      DO 20 I=1,N
      IF((X(1)+(I-1)*DELX).GT.XO) GO TO 15
      Y(I,2)=(X(1)+(I-1)*DELX)*YO/XO-AX
      Y(I,1)=Y(I,2)
      II=N-I+1
      Y(II,2)=Y(I,2)
      Y(II,1)=Y(I,2)
      DEL(I)=DEL(I)-AX

      P(I)=PA
      H(I,2)=Y(I,2)-DEL(I)
      H(I,1)=H(I,2)
      DEL(II)=DEL(II)-AX
      P(II)=PA
      H(II,2)=H(I,2)
      H(II,1)=H(II,2)
20    CONTINUE

15    II=N-I+1
      DO 30 I=I,II
      DEL(I)=DEL(I)-AX
      Y(I,2)=DEL(I)+HO
      Y(I,1)=Y(I,2)
      P(I)=PO
      H(I,2)=HO
      H(I,1)=HO
30    CONTINUE

```

```

C*****
C SOLVING THE TRANSIENT REYNOLDS EQUATION FOR NEW PRESSURE PROFILE
C*****

```

```

T=T-M*(V**2)
KKK=1
N2=N-2
N1=N-1
ITER=0
COEFF1=EI/(DELX**4)
COEFF2=2.*M*V/(4.*DELX*DELX)+M*V**2/(DELX**2)-4.*EI/(DELX**4)-
* T/(DELX**2)
COEFF3=M/(DELX**2)-2.*M*V**2/(DELX**2)+6.*EI/(DELX**4)
COEFF3=COEFF3+2*T/(DELX**2)
COEFF4=M*V**2/(DELX**2)-2.*M*V/(4.*DELX*DELX)-4.*EI/(DELX**4)-
* T/(DELX**2)
COEFF5=COEFF1
101 ITER=ITER+1
ITOTAL=ITOTAL+1
DO 40 I=1,N2
J=I+1
B(I)=(-6.*(V+VR)*MU*H(J,2)/(2.*DELX))-((H(J,2)**3)*P(J)/DELX**2)+
#(H(J,2)**3)*(P(J+1)-P(J-1))/(4.*DELX**2)+3.*(H(J,2)**2)*P(J)
#*(H(J+1,2)-H(J-1,2))/(4.*DELX**2)-6.*LAM*PA*H(J,2)**2/DELX**2+
#6.*LAM*PA*H(J,2)*(H(J+1,2)-H(J-1,2))/(2.*DELX**2)

D(I)=12.*MU*(2*H(J,2)-H(J,1))/DELX+2.*(H(J,2)**3)*P(J)/(DELX**2)
#+12.*LAM*PA*(H(J,2)**2)/(DELX**2)+3.*MU*(V+VR)*(H(J+1,2)-H(J-1,2))
#/DELX+(12*MU*AK*(P(J)-PA))

A(I)=(6.*(V+VR)*MU*H(J,2)/(2.*DELX))-((H(J,2)**3)*P(J)/DELX**2)-
#(H(J,2)**3)*(P(J+1)-P(J-1))/(4.*DELX**2)-3.*(H(J,2)**2)*P(J)
#*(H(J+1,2)-H(J-1,2))/(4.*DELX**2)-6.*LAM*PA*(H(J,2)**2)/DELX**2-
#6.*LAM*PA*H(J,2)*(H(J+1,2)-H(J-1,2))/(2.*DELX**2)

C(I)=12.*MU*H(J,2)*P(J)/DELX
40 CONTINUE
B(1)=0.0
A(N2)=0.0
C(1)=C(1)-
#((-6.*(V+VR)*MU*H(2,2)/(2.*DELX))-((H(2,2)**3)*P(2)/DELX**2)+
#(H(2,2)**3)*(P(3)-P(1))/(4.*DELX**2)+3.*(H(2,2)**2)*P(2)
#*(H(3,2)-H(1,2))/(4.*DELX**2)-6.*LAM*PA*H(2,2)**2/DELX**2+
#6.*LAM*PA*H(2,2)*(H(3,2)-H(1,2))/(2.*DELX**2))*PA
C(N2)=C(N2)-
#((6.*(V+VR)*MU*H(N1,2)/(2.*DELX))-((H(N1,2)**3)*P(N1)/DELX**2)-
#(H(N1,2)**3)*(P(N)-P(N2))/(4.*DELX**2)-3.*(H(N1,2)**2)*P(N1)
#*(H(N,2)-H(N2,2))/(4.*DELX**2)-6.*LAM*PA*(H(N1,2)**2)/DELX**2-
#6.*LAM*PA*H(N1,2)*(H(N,2)-H(N2,2))/(2.*DELX**2))*PA
C UPPER TRIANGULARIZATION
DO 49 I=2,N2

```

```

RR=B(I)/D(I-1)
D(I)=D(I)-RR*A(I-1)
49 C(I)=C(I)-RR*C(I-1)
C BACK SUBSTITUTION
C(N2)=C(N2)/D(N2)
DO 59 I=2,N2
J=N2-I+1
59 C(J)=(C(J)-A(J)*C(J+1))/D(J)
DO 69 I=1,N2
J=I+1
P(J)=C(I)
PR(J)=P(J)-PA
69 CONTINUE
PR(1)=P(1)-PA
PR(N)=P(N)-PA

```

```

C*****
C SOLVING THE FOIL EQUATION USING THE UPDATED VALUES FOR PRESSURE
C TO OBTAIN NEW VALUES FOR FOIL DISPLACEMENT AND AIR FILM GAP.
C*****

```

```

DO I=1,N
DO J=1,N
AA(I,J)=0.0
ENDDO
CONST(I)=0.0
ENDDO
Y(N+1,1)=Y(N,1)
Y(N+2,1)=Y(N,1)
Y(N,2)=Y(N,1)
DO I=1,N
J=I+1
X1=(P(J)-PA)+(2.*M/DELX**2)*Y(J,2)
X2=(M/DELX**2)*Y(J,1)
X3=(M*V/(2*DELX*DELX))*Y(J+1,1)
X4=(M*V/(2*DELX*DELX))*Y(J-1,1)
CONST(I)=X1-X2+X3-X4
ENDDO
DO IL=1,N
AA(IL,IL+2)=COEFF1
AA(IL,IL+1)=COEFF2
AA(IL,IL)=COEFF3
AA(IL,IL-1)=COEFF4
AA(IL,IL-2)=COEFF5
ENDDO
CONST(1)=CONST(1)-2*(-M*V/(2*DELX*DELX)+M*(V**2)/(DELX**2)-
# T/DELX**2)*(Y(1,1))
CONST(2)=CONST(2)-2*(-M*V/(2*DELX*DELX)+M*(V**2)/(DELX**2)-

```

```

# T/DELX**2)*(Y(1,1))
CONST(N1)=CONST(N21)-(M*V/(2.*DELX*DELX)+(M*V**2/DELX**2)-
#   T/DELX**2)*(Y(N,1))
   CONST(N)=CONST(N)-(M*V/(2.*DELX*DELX)+(M*V**2/DELX**2)-
#   T/DELX**2)*(Y(N,1))
DO I=1,N
  AL(I,1)=AA(I,1)
  ENDDO
  DO J= 1,N
  U(1,J)=AA(1,J)/ AL(1,1)
  ENDDO
  DO J=2,N
  DO I=J,N
  SUM=0.0
  DO K=1,J-1
  SUM=SUM+AL(I,K)*U(K,J)
  ENDDO
  AL(I,J)=AA(I,J)-SUM
ENDDO
  U(J,J)=1.0
  DO I=J+1,N
  SUM=0.0
  DO K=1,J-1
  SUM=SUM+AL(J,K)*U(K,I)
  ENDDO
  U(J,I)=(AA(J,I)-SUM)/ AL(J,J)
ENDDO
  ENDDO
  BD(1)=CONST(1)/ AL(1,1)
DO I=2,N
  SUM=0.0
  DO K=1,I-1
  SUM=SUM+AL(I,K)*BD(K)
  ENDDO
  BD(I)=(CONST(I)-SUM)/ AL(I,I)
  ENDDO
Y(N,3)=BD(N)
DO JJ=N,1,-1
SUM2=0.0
DO K=JJ+1,N
SUM2=SUM2+U(JJ,K)*Y(K,3)
ENDDO
Y(JJ,3)=1.0*(BD(JJ-1)-SUM2)
ENDDO
DO J=1,N1
FF1(J,1)=0.0
FF1(J,2)=0.0
ENDDO
DO J=1,N
FF1(J,1)=Y(J,3)
FF1(J,2)=Y(J,2)
ENDDO

```



```

ERROR=0.0
DO I=3,N2
ERROR=ERROR+ABS(FF1(I,1)-FF1(I,2))/ ABS(FF1(I,1))
ENDDO
DO I=1,N
J=I+1
H(J,3)=Y(J,3)-DEL(J)
ENDDO
DO I=1,N
Y(I,1)=Y(I,2)
H(I,1)=H(I,2)
Y(I,2)=Y(I,3)
H(I,2)=H(I,3)
ENDDO
IF(MOD(ITOTAL,IWRITE) .EQ. 1)THEN
ENDIF
IF(MOD(ITOTAL,2000) .EQ. 10) THEN
DO J=2,N1
FILM(J,KKK)=H(J,3)
PRESSURE(J,KKK)=PR(J)
ENDDO
ITERA(KKK)=ITOTAL
KKK=KKK+1
ENDIF
IF((ITOTAL .GT. 1000) .AND. (ERROR .LE. 1E-4))THEN
KKMAX=KKK
ITERA(KKMAX)=ITOTAL
DO I=2,N2
FILM(I,KKMAX)=H(I,3)
PRESSURE(I,KKMAX)=PR(I)
ENDDO
GOTO 789
ENDIF

```

```

C*****
C PRINTING THE SOLUTION i.e. THE AIR FILM THICKNESS AND THE
C PRESSURE PROFILE ALONG THE ROLLER.
C*****

```

```

GOTO 101
789 CONTINUE
WRITE(9,*) 'VELOCITY OF THE WEB IS',V
WRITE(9,*) 'VELOCITY OF THE ROLLER IS',VR
WRITE(9,*) 'SLIP FLOW PARAMETER IS',LAM
WRITE(9,*) 'TENSION APPLIED IS',T
WRITE(9,*) 'POROSITY VALUE OF THE WEB IS',AK
WRITE(9,*) 'MASS OF THE WEB PER UNIT LENGTH IS',M
WRITE(9,*) 'TIME STEP IS',DELT

```

```
WRITE(9,*) 'ITERATION',IWRITE
WRITE(9,*) 'FLEXURAL RIGIDITY OF THE WEB'
DO KKK=1,KKMAX
WRITE(9,*) ITERA(KKK)
ENDDO
DO I=2,N2
WRITE(7,345) (FILM(I,JJ),JJ=1,KKMAX)
WRITE(5,345)(PRESSURE(I,JJ),JJ=1,KKMAX)
345 FORMAT(100(E20.8,2X))
ENDDO
CLOSE(7)
CLOSE(5)
CLOSE(9)
END
```

```
C*****
C      MECHANICAL AND AEROSPACE ENGINEERING, OSU.
C*****
```

VITA

Kandasamy Satheesh

Candidate for the Degree of

Master of Science

Thesis: COMPUTATIONS OF AIR FILMS BETWEEN MOVING WEBS AND SUPPORT ROLLERS FOR STEADY/UNSTEADY OPERATING CONDITIONS.

Major Field: Mechanical Engineering

Biographical:

Personal Data: Born in Anuradhapura, Srilanka, On February 08, 1973, the son of Dr. P. Kandasamy and Dr. (Mrs). G. Kandasamy

Education: Graduated from Royal College, Colombo, Srilanka, in December 1991; received Bachelor of Technology degree in Mechanical Engineering from Indian Institute of Technology, Bombay, India in July 1996. Completed the requirements for the Master of Science degree in Mechanical Engineering at Oklahoma State University in December, 1997.

Experience: Research Assistant, Department of Mechanical and Aerospace Engineering, Oklahoma State University, August 1996, to December 1997.

Professional Membership: American Society of Mechanical Engineers and American Society of Heating, Refrigerating and Air-conditioning Engineers.